

THE ROLE OF RAI2 PROTEIN IN THE MAINTENANCE OF GENOMIC STABILITY

Dissertation

With the aim of obtaining a doctoral degree (Dr. rer. nat.)
at the Department of Biology
Faculty of Mathematics, Informatics and Natural Sciences
University of Hamburg

Submitted by

Lena Böttcher

Born in Hamburg

Hamburg
May 2019

Reviewers of the dissertation:

Jun.-Prof. Wim Walter

Universität Hamburg
Fakultät für Mathematik, Informatik und Naturwissenschaften
Fachbereich Biologie
Institut für Pflanzenwissenschaften und Mikrobiologie
Molekulare Pflanzenphysiologie
Ohnhorststraße 18
22609 Hamburg

Prof. Harriet Wikman-Kocher

Institut für Tumorbilogie
Zentrum für Experimentelle Medizin
Universitätsklinikum Hamburg-Eppendorf
Campus Forschung N27 , 4. Etage
Martinistraße 52
20246 Hamburg

Date of diputation: 16.08.2019

TABLE OF CONTENTS

TABLE OF CONTENTS

Table of Contents.....	I
Summary	IV
Zusammenfassung	V
1 Introduction	1
1.1 Hallmarks of Cancer.....	1
1.1.1 Genomic Instability	2
1.1.2 Molecular Basis of Chromosomal Instability (CIN).....	4
1.2 CIN and Cancer Progression	10
1.2.1 Tumoural Heterogeneity and CIN.....	10
1.2.2 Metastasis Formation and CIN.....	11
1.3 Breast Cancer.....	11
1.3.1 Breast Cancer Metastasis.....	13
1.3.2 Breast Cancer Therapy.....	13
1.4 Retinoic Acid-Induced 2 Protein (RAI2)	14
1.4.1 RAI2 as Metastasis Suppressor Gene	14
1.4.2 Cell Cycle Association of RAI2.....	15
1.4.3 Interaction of RAI2 with C-terminal Binding Proteins (CtBPs).....	15
2 Aim of the Study	17
3 Material and Methods	18
3.1 Material.....	18
3.1.1 Cell lines	18
3.1.2 Laboratory Instruments.....	19
3.1.3 Consumables.....	20
3.1.4 Chemicals.....	20
3.1.5 Chemotherapeutics and Reagents	22
3.1.6 Buffer and Media.....	23
3.1.7 Vectors and Expression Plasmids.....	23
3.1.8 Antibodies	24
3.1.9 Secondary Antibodies.....	25
3.1.10 Kits.....	25
3.1.11 Oligonucleotides.....	26
3.1.12 Chemotherapeutics and Inhibitors	26
3.1.13 Software and Databases	27
3.2 Cell Culture Methods	28

TABLE OF CONTENTS

3.2.1	Standard Cultivation of Human Cell Lines.....	28
3.2.2	Cryopreservation of Human Cells Lines.....	28
3.2.3	Lentiviral Particle Production.....	28
3.2.4	shRNA-Mediated Knockdown of <i>RAI2</i> gene expression.....	28
3.2.5	Generation of Phosphor Histone 2B-GFP Cell Line.....	29
3.2.6	Live Cell Imaging.....	29
3.2.7	Cell Cycle Analysis Using Double Thymidine Block.....	30
3.2.8	Colony Formation Assay.....	30
3.3	Molecular Biological Technics.....	31
3.3.1	Gene Expression Analysis.....	31
3.3.2	Cell Cycle Analysis.....	32
3.3.3	Agarose Gel Electrophoresis.....	32
3.4	Protein Biochemical and Immunological Methods.....	33
3.4.1	Protein Isolation from Cultured Cells.....	33
3.4.2	Measurement of Protein Concentration.....	33
3.4.3	SDS-Polyacrylamide Gel Electrophoresis (SDS-PAGE).....	33
3.4.4	Western Blot Analysis.....	34
3.4.5	Immunofluorescence Staining.....	35
3.4.6	DNA Fiber Assay.....	36
3.4.7	Traffic Light Reporter Assay.....	36
4	Results.....	38
4.1	Analysis of Mitosis in <i>RAI2</i> -depleted Cells.....	38
4.1.1	Analysis of <i>RAI2</i> -depleted KPL-1 by Live Cell Imaging.....	38
4.1.2	Analysis of Mitotic Duration.....	39
4.1.3	Analysis of <i>de novo</i> Micronuclei Formation.....	40
4.1.4	Analysis of Mitotic Defects Underlying <i>RAI2</i> Depletion.....	41
4.2	Causes of Premitotic Defects in <i>RAI2</i> -depleted Cells.....	45
4.2.1	Analysis of DNA Double-Strand Breaks after <i>RAI2</i> Depletion.....	45
4.2.2	Impact of <i>RAI2</i> on DNA Replication.....	46
4.2.3	Impact of <i>RAI2</i> on DNA Damage Response.....	50
4.3	Analysis of <i>RAI2</i> Expression in Cell Cycle Phases.....	54
4.3.1	Analysis of <i>RAI2</i> Expression in Synchronised Breast Cancer Cells.....	54
4.3.2	Analysis of <i>RAI2</i> in Cells Treated with Chemotherapeutics.....	56
4.4	Clonogenic Capacity.....	59
4.4.1	Clonogenic Capacity in <i>RAI2</i> -depleted KPL-1 and MCF-7 Cell Line.....	59

TABLE OF CONTENTS

4.4.2	Clonogenic Capacity in Cells Treated with Cytotoxic Anti-Cancer Drugs.....	60
4.5	Localisation of RAI2 and CtBP1 in Cells Overexpressing RAI2 or CtBP-binding Mutant RAI2.	65
4.5.1	Localisation and Formation of RAI2/CtBP1 Speckle after Treatment with Etoposide.....	65
4.5.2	Quantification of Speckle Number after Treatment with Etoposide.....	66
4.6	Dependence of RAI2 Expression on the Clinical Outcome of Patients with CIN Tumours	68
5	Discussion	70
5.1	Mitosis in RAI2-depleted Cells	70
5.2	Premitotic Defects after RAI2 Depletion	71
5.3	Is the RAI2 Protein Cell Cycle-dependent Expressed?	74
5.4	Clonogenic Capacity after RAI2 Depletion	75
5.5	RAI2 Speckle Formation.....	76
5.6	Impact of RAI2 on Chromosomal Unstable Breast Cancer Patients.....	78
5.7	Conclusion and Outlook	79
6	Literature	82
	List of Abbreviations	95
	Danksagung	97
	Eidesstattliche Versicherung.....	99
	English Certificate	100

SUMMARY

A variety of checkpoint mechanisms and DNA repair pathways are active during cell division in order to avoid loss of genetic information. Disruption of these mechanisms results in loss of genetic information in the form of chromosomes/chromosome fragments or due to mutations and is known as genomic instability. Genomic instability is part of the Hallmarks of Cancer which describe the characteristics of a cell leading to cancer progression and is an enabling characteristic of tumours. Genome instability especially on the chromosome level, which is described as chromosomal instability (CIN), can create high levels of intratumoural heterogeneity, which is the main reason for ineffective therapeutic response and drug resistance in cancer treatment. The current study investigated the role of the putative tumour suppressor RAI2 in maintenance of genetic stability. In luminal breast cancer cell lines, depletion of RAI2 results in a prolonged mitosis and increased incidence of chromosomal fragments that are lost during mitosis. It was shown that these fragments are incorporated into micronuclei after mitosis. Moreover, RAI2 depletion leads to an accumulation of double-strand breaks due to the fact that the capacity to repair DNA damage by non-homogenous end-joining is decreased in the absence of RAI2. Experiments applying chemotherapeutics to breast cancer cells revealed that RAI2 gene and protein expression is elevated upon treatment and correlates with an increased expression of DNA damage markers. It has been shown before that RAI2 is localised in form of speckles in the nucleus together with its main binding partner CtBP. The current study demonstrated that the number of RAI2/CtBP1 speckles was increased under chemotherapeutic conditions and the formation of the speckles was dependent on the binding of RAI2 to CtBP1. Finally, survival analysis, using a clinical breast cancer patient dataset, showed that patients with low *RAI2* expression and a high CIN score had the lowest five-year overall survival with 63.8% compared to <79.4% in the other three groups. Taken together, the results indicate a so far unknown function of the RAI2 protein as a guardian of genome stability by maintaining DNA damage response.

ZUSAMMENFASSUNG

Eine Vielzahl von Überwachungsmechanismen und DNA-Schadensreparaturwegen wird während der Zellteilung aktiviert um das Verlorengelassen von genetischer Information zu vermeiden. Eine Dysfunktion dieser Mechanismen führt zu einem Verlust genetischer Informationen in Form von Chromosomen/Chromosomfragmenten oder aufgrund von Mutationen und ist bekannt als genomische Instabilität. Genomische Instabilität, insbesondere auf Instabilität auf chromosomaler Ebene, ist eine der Gründe für die Entstehung intratumoraler Heterogenität, die wiederum eine der Hauptursachen für die Entstehung von Resistenzen gegenüber Krebstherapien ist. Die vorliegende Arbeit untersucht die Rolle des putativen Tumorsuppressor-Gens *RAI2* in der Aufrechterhaltung von genetischer Stabilität. In luminalen Brustkrebszelllinien führt der Verlust von *RAI2* zu einer zeitlichen Verlängerung der Mitose sowie zu einem erhöhten Auftreten von chromosomalen Fragmenten, die während der Mitose verloren gehen. Es konnte gezeigt werden, dass diese Fragmente nach der Mitose in Mikrokerne eingeschlossen werden. Darüber hinaus demonstriert die Arbeit, dass der Verlust von *RAI2* eine Anhäufung von Doppelstrangbrüchen zur Folge hat, was darauf zurück zu führen ist, dass Zellen mit *RAI2*-Verlust eine verringerte Fähigkeit zur Reparatur von Doppelstrangbrüchen über den NHEJ-Signalweg aufweisen. Weitere Experimente mit Wildtyp-Brustkrebszellen konnten eine erhöhte Expression der *RAI2*-Gens und -Proteins nach chemotherapeutischer Behandlung zeigen, welche mit einer ansteigenden Expression von DNA-Schädigung-Markern korreliert. Vorherige Arbeiten zeigten eine Lokalisierung des *RAI2*-Proteins zusammen mit dem *RAI2*-Bindungspartner CtBP im Nucleus in Form von Sprenkeln. Die vorliegende Arbeit konnte darlegen, dass die Anzahl der *RAI2*/CtBP-Sprenkel unter chemotherapeutischen Bedingungen zunimmt und beweisen, dass die Bildung der Sprenkel abhängig von der Bindung von *RAI2* zu CtBP ist. Abschließende Überlebensanalysen unter der Verwendung eines klinischen Brustkrebs-Datensatzes ergaben, dass Patienten mit einer niedrigen *RAI2* Expression und hoher chromosomaler Instabilität die schlechteste Prognose mit einem Fünf-Jahres-Überleben von 63,8% im Vergleich zu den anderen drei Gruppen mit <79,4% hatten. Zusammenfassend weisen die Daten auf eine bislang unbekannt Funktion des *RAI2* Proteins in der Antwort auf DNA-Schäden und in der Aufrechterhaltung der genomischer Stabilität hin.

1 INTRODUCTION

In 1890, abnormal cell divisions in histological sections of different carcinomas were described for the first time by the German pathologist David Hanseemann (Hanseemann, 1890). He postulated that asymmetric cell divisions and nuclei alteration such as small and large nuclei were characteristics of tumour tissue (Hanseemann, 1892). Based on this research, Theodor Boveri described the connection between an aneuploidic karyotype in cancer cells and the development of malignant carcinoma (Boveri, 1914). The first link between carcinogenesis and mutation was drawn by Brookes and Lawley (Brookes and Lawley, 1964), after Watson and Crick had decoded the biological structure of the DNA (Watson and Crick, 1953) and following the finding that genes could get mutated (Burdette, 1955). Nowadays, the connection between genomic instability and the development of human tumours are manifested in the tumour field, however the understanding of the molecular basis behind these connection is still under investigation.

1.1 HALLMARKS OF CANCER

Today, cancer is known as a complex and variable disease and the basic concept of tumour development were described in an influential review as the “Hallmarks of Cancer” by Hanahan and Weinberg (Hanahan and Weinberg, 2000). It comprises six biological characteristics leading to cancer progression including sustaining of proliferative signaling, evading of growth suppressors, resisting cell death as well as enabling replicative immortality, inducing angiogenesis and activating invasion and metastasis (Figure 1) (Hanahan and Weinberg, 2011). In 2011, the hallmarks were expended by the emerging characteristics of tumour progression – avoiding immune destruction and deregulation of the cellular energetics – as well as by two enabling characteristics – the tumour-promoting inflammation and genomic instability and mutations (Hanahan and Weinberg, 2011). These hallmarks are well accepted in the cancer research field and help to understand the core traits in cancer initiation and progression.

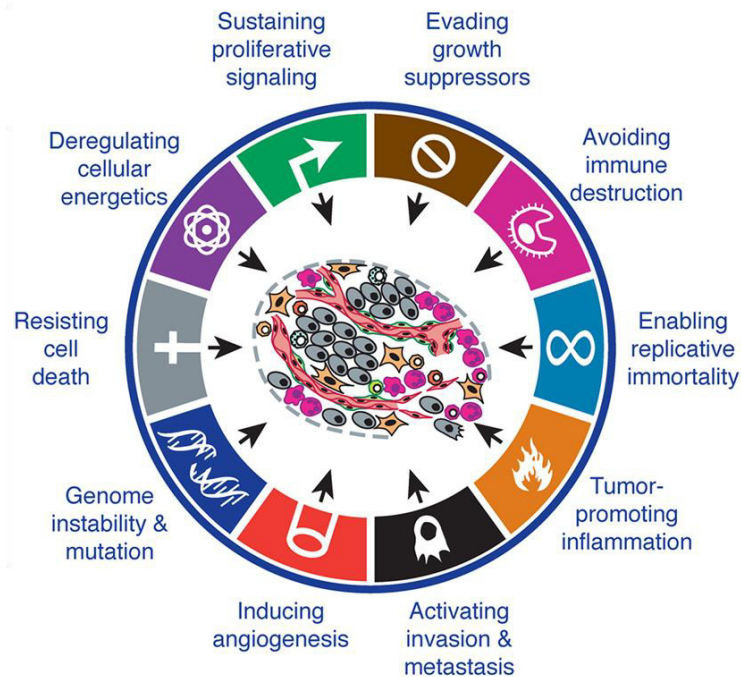


Figure 1: Hallmarks of Cancer including the emerging and enabling characteristics describing the main capabilities in tumour progression. Taken and adapted from (Hanahan and Weinberg, 2011).

1.1.1 GENOMIC INSTABILITY

Genomic instability is a characteristic of the majority of human tumours and describes the increased tendency to stepwise accumulate mutations (Lee et al., 2016). Genomic instability can be divided into two forms: nucleotide-level genomic instability and instabilities manifested on the chromosome level (Lee et al., 2016; Lengauer et al., 1998). The nucleotide-level genomic instability includes subtle sequence changes like point mutations and nucleotide substitutions, deletions and insertions (Lee et al., 2016). This types of defects are connected to DNA mismatch repair (MMR), which is a repair pathway that maintains DNA replication fidelity after replication errors (Preston et al., 2010). Defects in MMR lead to a high mutation rate in short nucleotide repeats, the so-called microsatellite instability. This type of instability is associated with a hypermutation phenotype and can be used as therapeutic target (Lee et al., 2016). Moreover, it has been shown that increased mutational burden correlates with a generation of neo-antigens and a response to anti-PD 1 therapy in lung cancer patients (McGranahan et al., 2016; Rizvi et al., 2015) pointing out the therapeutic relevance of nucleotide-level genomic instability.

Another form of genomic instability is chromosomal instability (CIN) which is characterised by large-scale chromosomal aberrations within the genome. Common chromosomal rearrangements resulting from CIN include loss or gain of whole chromosomes or chromosomal fragments as well as translocation and amplification of chromosomal fragments (Lengauer et al., 1998; van Gent et al., 2001). It should be mentioned that aneuploidy is the state of abnormal karyotype whereas CIN describes an increased rate of gains and losses of whole chromosomes or chromosome fragments during cell divisions (Lengauer et al., 1998).

CIN is common in human cancer and loss of chromosomal fragments can result in a loss of tumour suppressor genes (Gordon et al., 2012). For instance, deletion of the major tumour suppressor gene *TP53* is present in about 50% of all human tumours (Olivier et al., 2010; Robles and Harris, 2010; Vogelstein et al., 2000). As “the guardian of the genome” p53, encoded by *TP53*, triggers checkpoint activation of the cell cycle to pause proliferation in cells with damaged DNA and thereby preventing tumourgenesis (Lane, 1992). On the other side, amplification of genome regions can lead to an activation of oncogene (Lengauer et al., 1998). In breast cancer, the *Human epidermal growth factor 2 (HER2)* gene locus is commonly amplified and this correlates with bad patient’s outcome (Cameron et al., 2017; Ross and Fletcher, 1998). HER2 can activate downstream signalling pathways that regulate processes like cell survival, proliferation and differentiation (Yarden and Sliwkowski, 2001). Moreover, *HER2* amplification status is used as prognostic factor and acts as therapeutic target for treatment with anti-HER2 or tyrosine inhibitors antibodies in breast cancer patients (Cameron et al., 2017; Geyer et al., 2006). By using gene expression signatures including genes that are deregulated in cancer cells with aneuploidy, it was shown that a CIN signature based on gene expression data predicts clinical outcome in numerous cancer types (Carter et al., 2006). This points out the importance of CIN in tumour progression and as potential therapeutic target for drug development. The molecular basis underlying CIN and its impact on tumour diversity and metastasis is further explained in detail in the following chapters.

1.1.2 MOLECULAR BASIS OF CHROMOSOMAL INSTABILITY (CIN)

Mechanisms and defects contributing to CIN are related to processes whose malfunction can lead to double-strand breaks (DSBs) or structurally instable chromosomes. These include DNA damage repair pathways, replication and the coordination of the cell cycles by checkpoint mechanism. Moreover, failure in the coordination or dynamics during chromosome separation can result in a CIN phenotype.

1.1.2.1 DNA DAMAGE PATHWAYS IN CANCER

Alterations in DNA damage response genes are prevalent in many cancer types and mutations accompanied with loss of heterozygosity were observed in approximately 1/3 of DNA damage response genes as shown by the analysis of 33 cancer types from TCGA data set (Knijnenburg et al., 2018). The most frequent types of DNA damage in cancer are single strand breaks (SSBs) and DSBs. Pathways repairing DNA damage are key cell survival pathways (Gordon et al., 2012). SSBs can arise either indirectly during base excision repair or directly as a result of oxidative stress and are repaired by different factors including PARP and XRCC1 (Caldecott, 2008). The two main DSB repair pathways are the homologous recombination (HR) and non-homologous end-joining (NHEJ). HR needs a homologous DNA sequence for repair and is therefore active during S and G2 phase of the cell cycle. NHEJ represents a more error-prone pathway, which is active during the entire cell cycle and acts template-independent (Pilie et al., 2019). Incomplete repair of DSBs can result in acentric chromosomes (chromosome lacking a centromere) and can lead to a loss of genomic integrity and cancer progression (Gordon et al., 2012). The basics of the DSB repair pathways mechanisms are illustrated in Figure 2 and their impact on maintaining genome integrity is described in the following chapters.

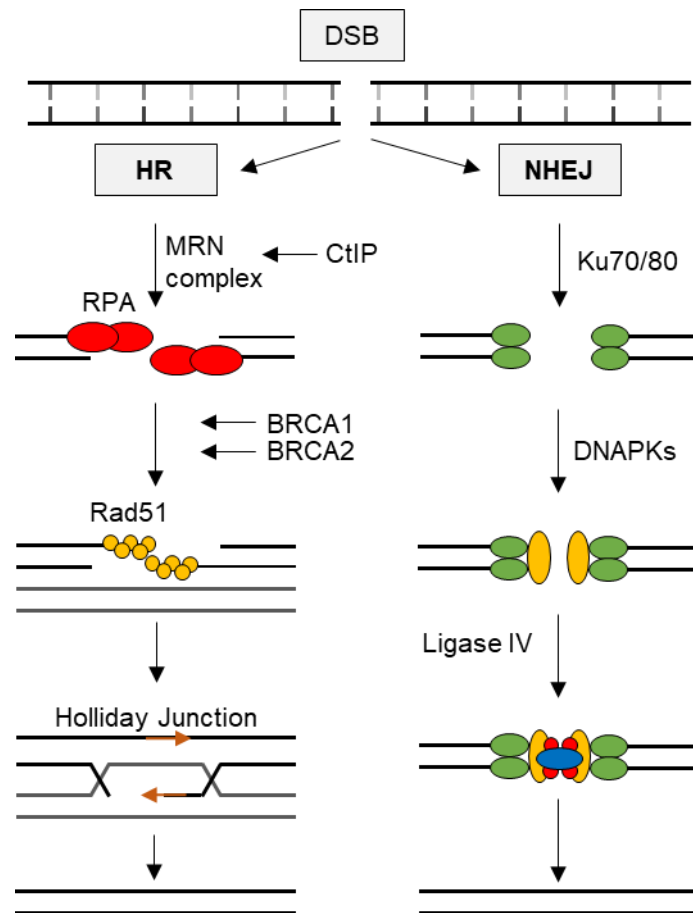


Figure 2: DNA double-strand break (DSB) pathways. In response to DSB two predominant pathways can be activated to maintain genomic integrity: the error-free homologous recombination (HR) and the error-prone non-homologous end-joining (NHEJ). HR can be divided into three phases. Initially, a 5' to 3' end resection is facilitated by the MRN complex and CtIP. The second step includes the coating of the single-strand DNA ends with RPA filaments. As a third step, RPA is replaced by Rad51 mediated by a BRCA1- and BRCA2-dependent process. Next, Rad51 catalyses the homology search and invasion of the homologous strand. Finally, the DNA strand is synthesised and the resulting intermediate structure known as Holliday junction is resolved resulting in an error-free repair of the DSB (Li and Heyer, 2008). During NHEJ, DSBs are repaired by a blunt end resection independently of a sequence homology. At first, the Ku hetero dimer ring complex binds to the DNA ends building a scaffold for the recruitment of the NHEJ machinery. Ku70/80 recruits DNAPK which is required for NHEJ, but its function is not yet completely known. Different factors are active to ensure that the DNA ends are prepared for blunt end resection, before the DNA Ligase IV proceeds with ligation being stabilised by the XRCC4 (Sishc and Davis, 2017). BRCA: Breast cancer type susceptibility protein, CtIP: C-terminal binding protein 1 interacting protein, XRCC4: X-ray repair cross-complementing protein 4, DNAPK: DNA-dependent protein kinase catalytic subunit, MRN: Mre11-Rad50-Nbs1 complex, RPA: replication protein A.

1.1.2.1.1 HOMOLOGOUS RECOMBINATION

DSBs that occur during S and G₂ phase are mainly repaired by homologous recombination (Pilie et al., 2019). One of the coordinators in response to DSBs is the Ataxia telangiectasia mutated (ATM) protein as it interacts with the MRN complex. Humans with mutations in ATM (Ataxia telangiectasia patients) are predisposed to lymphoid cancer in childhood and cells of Ataxia telangiectasia patients show higher spontaneous incidence of chromosome breaks, acentric

fragments and aneuploidy (Bishop and Schiestl, 2001; McKinnon, 2004). In addition, ATM mutations are also found in 8% of metastatic breast cancer patients (Lefebvre et al., 2016). Moreover, germline mutations in *BRCA1* and *2* genes that are involved in HR, are associated with a high risk to develop breast and/or ovarian cancer and are a typical feature of sporadic triple-negative breast cancer. Selective inactivation of *BRCA1* in mice results in CIN further showing the importance of HR to maintain chromosomal integrity (Bishop and Schiestl, 2001).

1.1.2.1.2 NON-HOMOLOGOUS END-JOINING

In mouse studies it was demonstrated that deficiency of Ku80, a protein that is part of a complex in the first steps of NHEJ, leads to CIN marked by chromosomal aberrations including breakage, translocations and aneuploidy (Difilippantonio et al., 2000). Moreover, defects occurring directly during the end-joining process can lead to a joining of ends from different DSBs resulting in chromosomal rearrangements (Rothkamm et al., 2001). Leukemia patients with inherited hypomorphic mutations in the NHEJ gene *Ligase IV* show an impaired DNA damage repair, increased radiosensitivity and significantly elevated chromosomal breaks upon irradiation (Riballo et al., 1999). Beyond that, germline polymorphisms of the NHEJ genes *Ku70*, *Ku80*, *DNA-PKs*, *Ligase IV* and *XRCC4* correlate with an increased risk to develop breast cancer (Someya et al., 2006) and delayed DNA-PK activation in cancer stem cells induces aneuploidy (Wang et al., 2018). Taken together, NHEJ functions as a caretaker that prevent tumourigenesis and maintains chromosomal stability.

1.1.2.2 REPLICATION STRESS

Replication is the basic process to duplicate DNA during cell cycle progression. To ensure that DNA replication is completed before mitosis, checkpoint mechanisms exist to maintain genomic stability. Malfunction of replication, which results in replication fork stalling or a collapse of the replication fork, is referred to as replication stress (Zeman and Cimprich, 2014). Replication stress is linked to structural as well as numerical CIN in cancer and can be induced by activation of oncogenes or inactivation of tumour suppressor genes (Burrell et al., 2013a; Dereli-Oz et al., 2011). This triggers cell proliferation and can lead to hyper-replication in the cells. In turn, this can result in stalled replication forks or, if not fixed in time, in replication fork collapse and consequently in DSBs (Di Micco et al., 2006; Hanahan and Weinberg, 2011; Petermann et al., 2010).

Both, transcription and replication operate on DNA which can cause collision between replication and transcriptional machinery leading to DSBs. The “early replicating fragile sites” are highly transcribed during early S phase and are a prominent genomic site for the formation of DSBs (Barlow et al., 2013). Moreover, failure in RNA processing can slow down the transcription and hybrids from nascent RNA and DNA can be formed. These DNA/RNA-hybrids (R-loops) cause DNA damage leading to instable DNA (Aguilera and Garcia-Muse, 2012). Beside the fragile sites mentioned above, “common fragile sites” exist that are prevalently showing genomic rearrangement, deletion and copy number variations (Glover et al., 2017). These regions seemed to be the last that are replicated during S phase and contain large genes. Taken into account that the transcription of these regions takes at least the full cell cycle, a collision of replication and transcription machinery is unavoidable consequently resulting in CIN (Ozer and Hickson, 2018).

1.1.2.3 MITOTIC DEFECTS

Mitosis is part of the cell cycle and includes the separation of the earlier replicated chromosomes to daughter cells. Mitosis can be further divided into prophase, prometaphase, metaphase, anaphase and telophase. The process is shown in Figure 3.

Defects in mitotic processes are a widespread phenomenon in solid tumours and frequent reasons for CIN. Malfunctions that affect mitotic fidelity and thus causing CIN are occurring in the regulation of chromosome cohesion, mitotic checkpoint, centromere formation as well as kinetochore-microtubule attachment (Thompson et al., 2010). For instance, genes encoding for sister chromatid cohesion were described to be mutated in different cancer types (Barber et al., 2008; Rocquain et al., 2010; Solomon et al., 2011). In glioblastoma cell lines, Solomon et al. describe an inactivation of *STAG2*, a gene encoding for the subunit protein of the cohesion complex, leading to cohesion defects, thereby resulting in aneuploidy and a CIN phenotype (Solomon et al., 2011). For an accurate sister chromatid separation, a centrosome positioning and timing needs to be ensured (Nam et al., 2015). Both, accelerated and delayed centrosome timing can cause spindle geometry defects in metaphase leading to mitotic errors (Nam et al., 2015; Silkworth et al., 2012). Moreover, it was shown that 80% of breast tumours have amplified centrosomes. This amplification correlates with CIN (Lingle et al., 2002) further demonstrating the relevance of mitotic fidelity to avoid the occurrence of CIN.

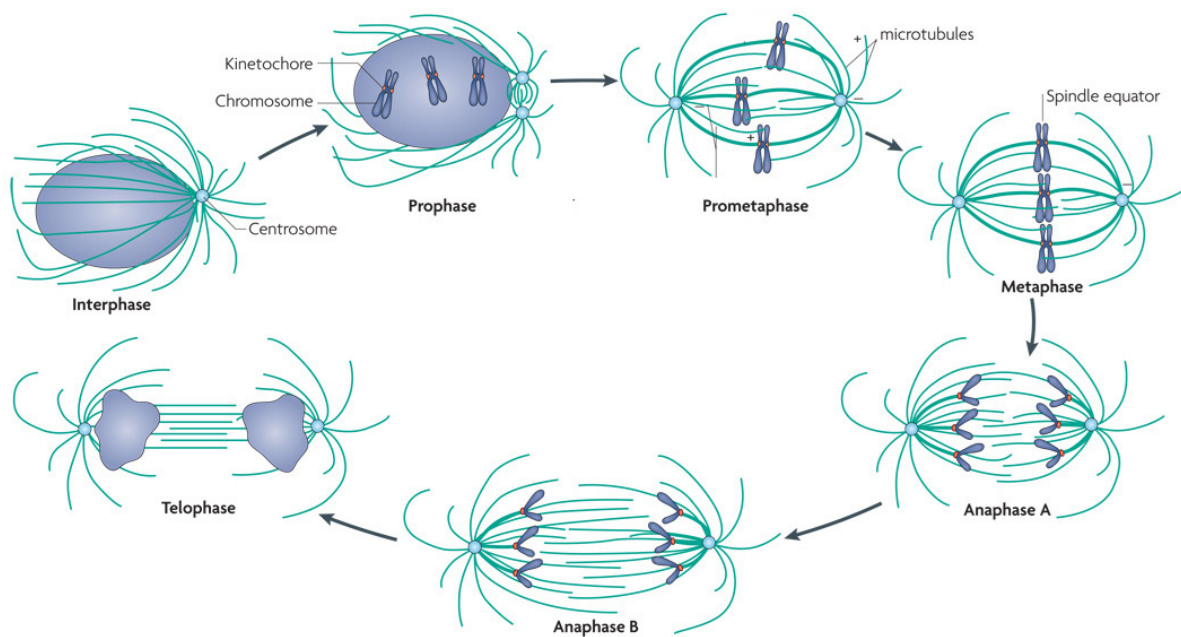


Figure 3: Process of mitosis showing the different phases. During interphase, the chromosomes are decondensated. In prophase, the condensation process of the chromosomes starts and the cohesion protein complex, which keeps the sister chromosomes together, is removed. During prometaphase, the breakdown of the nuclear membrane (nuclear envelope) begins and that the spindle apparatus gains access to the chromosomes. In parallel, chromosome kinetochores are established at the centromeric site of the chromosome. Microtubules grow out of the two spindle poles and connect to the centromeres (Prometaphase). In the following metaphase, the centromeric sites of the chromosomes line up at the equator of the spindle. Checkpoint mechanisms ensure that the chromosomes are properly arranged in the equator area and that the spindle is correctly assembled. In anaphase, sister chromatids separate to the opposite spindle poles by shortening of the microtubules. The telophase finalises the mitosis: the nuclear membrane rebuilds and chromosomes start to decondensate again. As a very last step, the cytoplasm is divided and allocated to the two daughter cells (Boettcher and Barral, 2013; Walczak et al., 2010). Adapted from (Walczak et al., 2010).

1.1.2.4 DEFECTS IN CHECKPOINT MECHANISMS

Checkpoints in all phases of the cell cycle, especially during the transition from G_2 to M phase, and checkpoints during mitosis, are essential to monitor DNA damage before entering mitosis as well as to ensure proper segregation of the chromosomes during mitosis (Musacchio and Salmon, 2007; Zhou and Elledge, 2000).

1.1.2.4.1 DEFECTS IN THE G_2/M CHECKPOINT

The G_2/M checkpoint is activated upon DNA damage in G_2 phase and allows the cell to repair DNA damage before entering mitosis. Studying yeast using a single site-specific DSB revealed that even a single DSB could induce the G_2/M arrest leading to lethality (Bennett et al., 1997).

However, others have shown in primary fibroblast containing irradiation induced-DSBs that cells have a defined threshold of 10-20 DSBs preventing mitotic entry. The majority of fibroblasts arrested at the G₂/M checkpoint give rise to one or two chromosome breaks upon release (Deckbar et al., 2007).

1.1.2.4.2 DEFECTS IN THE MITOTIC CHECKPOINT

The mitotic checkpoint or spindle-assembly checkpoint is important for the prevention of chromosome mis-segregation in mitosis. To ensure that all chromosomes are separated during anaphase, the mitotic checkpoint arrests cell division at metaphase until all kinetochores are attached to the microtubules of the spindles (Musacchio and Salmon, 2007). Mutations of genes involved in mitotic checkpoint were considered as an obvious candidate to promote CIN. However, they are rarely observed in aneuploidic human tumours (Perez de Castro et al., 2007). Hyperactivation of mitotic checkpoint genes is more frequent and can contribute to CIN *in vivo* and *in vitro* (Schvartzman et al., 2010). For instance, overexpression of MAD2, a checkpoint protein blocking the dissolution of sister chromatids, leads to aneuploidy and tumourigenesis in mouse models (Sotillo et al., 2007). Moreover, overactivation of mitotic checkpoint proteins can result in prolonged mitosis and lagging chromosomes. However, as key regulators of the mitotic checkpoint are mostly under control of transcription factors acting downstream of the retino blastoma protein, a tumour suppressor which is frequently mutated in human cancer, it is challenging to investigate the mitotic checkpoint in a tumoural background (Schvartzman et al., 2010).

1.1.2.5 TELOMERE DYSFUNCTION

Telomeres are DNA sequences located at the end of chromosomes consisting of non-coding tandem 5'-TTAGGG-3' sequences and telomere-associated proteins. Together, they build a cap structure that prevents the termini of the chromosomes from replication-associated sequence loss. They function as a barrier for DSB repair to avoid continuously repair of the chromosome termini that would otherwise be recognised as DSB (de Lange, 2009). During ongoing cell division telomeres are shortened in every round of replication and consequently lose their protection activity. If the protective activity is lost, normal cells trigger DNA-damaged like signaling and go into senescence or apoptosis due to p53 and p16 activation (d'Adda di Fagagna et al., 2003; de

Lange, 2009; Jacobs and de Lange, 2004; O'Sullivan and Karlseder, 2010). Dysfunction in telomeres is one of the mechanisms leading to genomic instability in cancer (Artandi and DePinho, 2010; Maser and DePinho, 2002). When chromosome ends are unprotected because of telomere dysfunction, DNA repair activities can generate end-to-end fusion of unprotected chromosomes. During mitotic anaphase, these fused chromosomes randomly break due to the tension of the spindle fiber. This can initiate a cascade termed as “breakage-fusion-bridge cycles” leading to an accumulation of chromosome rearrangements (Murnane, 2012). The main reasons of these telomere alterations are replication-mediated shortening of the tandem repeats together with a loss of p53 activity, defective telomere-associated proteins or direct damage of the telomere (Bailey and Murnane, 2006).

1.2 CIN AND CANCER PROGRESSION

CIN is known to be associated with drug resistance and poor prognosis in several cancer types and recent studies also demonstrated that CIN has effects on tumour heterogeneity and clonal evolution upon metastasis formation (Bakhoun et al., 2018; Turajlic and Swanton, 2016; Turajlic et al., 2018).

1.2.1 TUMOURAL HETEROGENEITY AND CIN

Genetic diversity exists between individuals with the same tumour type (intertumoural heterogeneity) as well as within a tumour of one patient (intratumoural heterogeneity) (Burrell et al., 2013b). For both, genome instability represents a prominent source for diversity apart from transcriptomic, epigenetic, and/or phenotypic changes (Burrell et al., 2013b; Dagogo-Jack and Shaw, 2018). Genetically, a tumour consists of heterogeneous subpopulations of cells (subclones) arising originally from one single cell during tumour evolution. These subclones may contain different mutations important for progression and survival, and react different in response to treatment. In patients, intratumoural heterogeneity is one of the key factors leading to ineffective therapeutic response and drug resistance (Greaves). Recently, results from the TRACERx study showed that intratumoural heterogeneity in non-small-cell lung cancer is a direct result of genome doubling and massive dynamic CIN (Jamal-Hanjani et al., 2017).

1.2.2 METASTASIS FORMATION AND CIN

Activation of invasion and metastases is a Hallmark of Cancer (Hanahan and Weinberg, 2000). The formation of metastasis is the final result of a multistep process including the shedding of the primary tumour to the circulation, survival of the circulating tumour cell (CTC) in the hematogenous and/or lymphatic circulation, arresting and extravasation into the new organ and consequently growth and vascularization of the metastatic tumour (Joosse et al., 2015). As metastasis is the cause of death in 90% of the cancer patients, this process is intensively in cancer research (Chaffer and Weinberg, 2011). In breast cancer and other cancer types it was shown that increased CIN is associated with increased metastatic progression (Turajlic and Swanton, 2016). Recently, results from the TRACERx study revealed that CIN directly drives disease recurrence in both renal cell and lung cancer (Turajlic et al., 2018). Moreover, ongoing chromosome segregation errors in primary cell lines activate the cGAS-STING cytosolic DNA-sensing pathway mediating immune response and maintains cells into a pro-metastatic state compared to cell lines in which CIN was suppressed but which were still aneuploidic (Bakhoum et al., 2018).

1.3 BREAST CANCER

With worldwide two million new cases in 2018, breast cancer is the most frequently occurring cancer entity in females (Bray et al., 2018). In Europe, 28.2% of the new female cancer cases reported are breast cancer (522,200) followed by colorectal (122,000, 12.3%) and lung cancer (158,000, 8.5%, Figure 4) (Bray et al., 2018). Because of improved screening and treatment options, the five-year overall survival rate is relatively high (81.8%) compared to other cancer entities like colorectal (57.0%) or lung cancer (13.0%) (De Angelis et al., 2014). However, 20-30% of the breast cancer patients will develop distant recurrence and median survival in metastatic patients ranges between two to three years (Cardoso et al., 2012). Due to that, female breast cancer is the leading cause of death in women with cancer in Europe (138,000, 16.2%) (Ferlay et al., 2018).

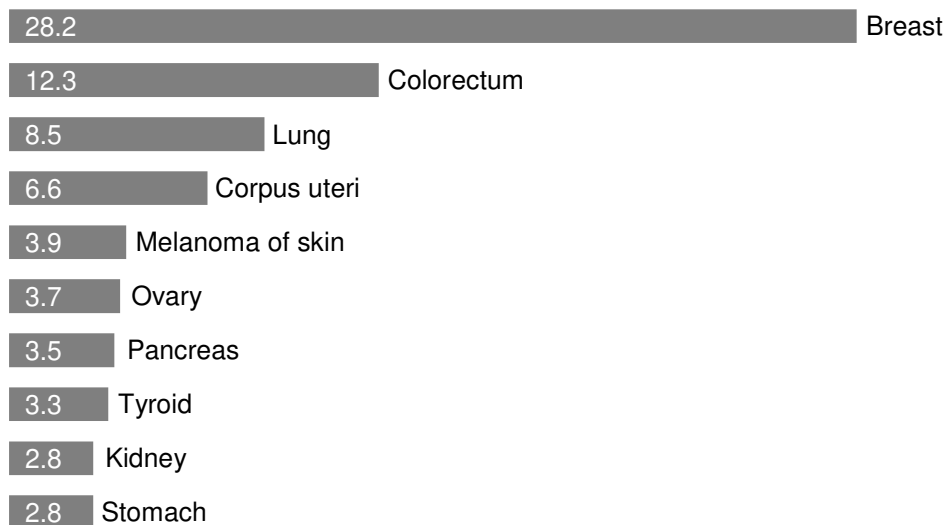


Figure 4: Incidence of the leading female cancer in Europe. The percentage of new tumour cases is related to the total number of new tumour cases in women in Europe in 2018 (Ferlay et al., 2018).

Breast cancer is a heterogeneous disease and therefore a classification of the individual patient is necessary to determine prognosis and personalised therapy. Tumours are characterised by the primary tumour site (pT0-4), lymph node involvement (pN1-3), distant metastasis spread (pM0-1) and the occurrence of micrometastasis at the time of diagnosis. The pT-status is categorised according to the size, whereas for pN-status, the number and localisation of affected lymph nodes is counted. The stage of differentiation can range from a well differentiated tumours (grade 1) to a poorly differentiated ones (grade 3) (Bloom and Richardson, 1957). Consideration of all TNM factors and the grading results in an overall stage ranged from stage I-IV (Cserni et al., 2018). For breast cancer, five-year relative survival rate varies between 99% for stage I patients and 15% for stage IV at time of diagnosis (England, 2002-2006). Histologically, breast tumours are distinguished as non-invasive (*in situ*) and invasive carcinoma (invasive ductal or lobular) (Li et al., 2005). On molecular basis, breast cancer can be classified immunohistochemically according to the expression status of receptors. Of therapeutic relevance is the status of the oestrogen receptor (ER), progesterone receptor (PR) as well as human epidermal growth factor receptor 2 (HER2) (Fisher et al., 1996; Romond et al., 2005). Distinction is drawn between *basal like* tumours, which are positive for keratin 5/6 and 17 on breast basal cells, *triple-negative tumours*, which are classified as ER-negative, PR-negative and HER2-negative, and *Luminal A* (ER-positive, low

grade), *Luminal B* (ER-positive, high grade) and *HER2-positive* tumours (amplification of *ERBB2* gene) (Perou et al., 2000; Sotiriou and Pusztai, 2009). *Basal like* and *HER2-positive* tumours have a worse recurrence rate compared to the luminal subtypes (Langlands et al., 2013). Staging, grading and the receptor status of the breast tumour are included in the choice of treatment.

1.3.1 BREAST CANCER METASTASIS

Breast cancer primarily metastasizes to regional lymph node and to distant secondary organs like lung, liver and brain with the bone as most common metastatic site (Berman et al., 2013). The median survival of early breast cancer patients differs between 2.2 years for patients with *luminal A* subtype and just 0.5 years for patients with *basal like* breast cancer (Kennecke et al., 2010). Overall, approximately 40% of the breast cancer patients with metastatic relapse ultimately die of metastatic breast cancer (Weigelt et al., 2005). Thus, the understanding metastatic traits and the development of new prognostic markers is needed to identify patients that have a metastatic potential to adjust therapeutic strategies.

1.3.2 BREAST CANCER THERAPY

Treatment of breast cancer patients depends on the stage, grade and receptor status. The main types of treatment are surgery, radiotherapy, chemotherapy, endocrine therapy and targeted therapy as well as a combination of those in some cases. Localised breast cancer is usually removed surgically followed by an adjuvant therapy including radio- and chemotherapy (NCCN, 2018). Most chemotherapeutics used for treatment of early breast cancer patients are anthracyclines and taxane. Anthracyclines are antibiotics with cytostatic activity that inhibit topoisomerase activity or intercalate with the DNA leading to a block of DNA replication or transcription. Taxanes avoid the disaggregation of the spindle apparatus and block the cells in mitosis (Schneeweiss et al., 2015).

Patients with a *luminal* subtype are ER-positive and endocrine therapy targeting against ER (tamoxifen) is offered to the majority of these patients (NCCN, 2018). However, 5-20 years after treatment with endocrine therapy the risk of distant recurrence is still about 13% for T1N-negative patients and even higher for T2N-positive patients (41%) (Pan et al., 2017). *Her2-positive* patients benefit from a combination of chemotherapy and anti-*HER2*-targeted therapy with the aim to

arrest the cell cycle and DNA repair in the cancer cells (Callahan and Hurvitz, 2011). For *basal like/triple-negative* tumours surgery combined with chemotherapy is the standard treatment option (NCCN, 2018).

Already approved cancer therapies that are successfully exploit the concept of synthetic lethality are based on the reliance of cancer cells on DNA repair to maintain cell division. Patients with hereditary breast cancer caused by a germline mutation of *BRCA1* or *BRCA2* can be treated with poly(ADP-ribose) polymerase (PARP)-inhibitors based on synthetic lethality concept (Mavaddat et al., 2012). Both *BRCA1* and *2* play a role in HR in response to DNA damage (Scully and Livingston, 2000). By inhibition of PARP SSBs occur, which are usually repaired by HR including *BRCA*. In *BRCA*-deficient patients the unrepaired SSBs cause stalling of replication forks and consequently result in an accumulation of DSBs leading to cell death (Faraoni and Graziani, 2018). In germline *BRCA*-deficient patients, inhibition of PARP using specific inhibitor like Olaparib leads to an increased response rate of 59.9% compared to standard chemotherapy (28.8%) (Robson et al., 2017). This points out the importance of new therapeutic approaches to increase the response and reduce the numbers of patients with recurrence.

1.4 RETINOIC ACID-INDUCED 2 PROTEIN (RAI2)

RAI2 is a putative metastasis-associated gene, which is located in the Xp22.2 region of the X chromosome (Walpole et al., 1999; Werner et al., 2015). The *RAI2* gene – as the name already proposed– is inducible by retinoic acid and is described to be involved in neural development in normal cells (Jonk et al., 1994).

1.4.1 RAI2 AS METASTASIS SUPPRESSOR GENE

In 2015, the *RAI2* gene was described at the Institute of Tumor Biology (ITB) to play a role in metastasis. More precisely, *RAI2* was identified as a metastasis suppressor gene for early dissemination from primary tumours to the bone marrow in breast cancer patients (Werner et al., 2015). In several published large breast cancer datasets it was shown that low *RAI2* transcript expression is an independent prognostic factor for overall survival and is associated with less differentiated and more aggressive breast tumours. This prognostic impact is particularly

significant in ER-positive breast cancer patients. Functional analysis demonstrated that RAI2 protein sustains epithelial traits and luminal differentiation in ER-positive breast cancer cells. Moreover, loss of RAI2 leads to a more invasive phenotype and contributes to epithelial-to-mesenchymal plasticity (Werner et al., 2015). Following work at the ITB showed that RAI2 acts as a corepressor of the hormone response in breast and prostate cancer and that loss of RAI2 contributes to hormone-independent proliferation in both tumour entities (Besler et al., 2018). Moreover, a tumour-suppressive function of RAI2 was also identified in colorectal cancer and promoter methylation of RAI2 was described as an independent prognostic factor in colorectal cancer (Yan et al., 2018).

1.4.2 CELL CYCLE ASSOCIATION OF RAI2

Recent analysis using global gene expression profiling in luminal breast cancer cell lines depleted for RAI2 showed a deregulation of genes involved in maintaining mitotic fidelity (Werner et al., 2016). Moreover, a deregulation of cell cycle-associated genes was observed in RAI2-depleted cells, with most of the genes and corresponding proteins orchestrating the G₂/M transition. In patients, low *RAI2* expression correlates with a mutant *TP53* gene status (Werner et al., 2015). This data strongly indicates that function of RAI2 may contribute to cell cycle or cell cycle-dependent processes.

1.4.3 INTERACTION OF RAI2 WITH C-TERMINAL BINDING PROTEINS (CTBPs)

Examining the binding partner of the RAI2 protein revealed that it interacted with the C-terminal binding protein 2 (CtBP2) (Werner et al., 2015). The two highly homologous *CtBP1* and *CtBP2* genes encode for co-repressors which are recruited by different sequence-specific transcription factors and acting as scaffolds for multi-protein transcriptional complexes. They are involved in many processes of tumorigenesis including activation of metastasis, cell differentiation, sustaining proliferation (Blevins et al., 2017). In breast cancer, CtBPs function together with p130 and HDAC as a corepressor complex on the *BRCA1* promoter, linking CtBP to the DNA damage response (Di et al., 2010). Genome-wide profiling analysing the association of CtBP with the genome of breast cancer cells demonstrated that CtBP targeted three main types of genes. These genes are involved in genome stability, epithelial to mesenchymal transition and stem cell pathways (Di et al., 2013). Loss of CtBP1 leads to upregulation of pro-oncogenic genes like *p21*,

Noxa and *Bax* (Grooteclaes et al., 2003). Moreover, CTBPs regulate the SAC proteins which play an important role in proper spindle attachment and by this they maintain mitotic fidelity (Bergman et al., 2009).

Proteins that bind to CtBP are reported to contain a highly conserved “PDXLS” interaction domain (Byun and Gardner, 2013). The binding of RAI2 to CtBP2 depends on the two ADLS binding motives on the RAI2 protein as the binding is disrupted in CtBP-binding mutant cells (Werner et al., 2015). Moreover, in luminal breast cancer cells RAI2 colocalises with CtBP and forms speckles in the nucleus (Werner et al., 2015). However, the function of these speckles is still unknown. As depletion of RAI2 deregulates genes that are important to maintain mitotic fidelity (Werner et al., 2016), and CtBP2 as the main binding partner of RAI2 regulates genes involved in genome stability and DNA damage response (Bergman et al., 2009; Di et al., 2013; Di et al., 2010) the question arises, if RAI2 might play a role in the maintenance of genomic integrity.

2 AIM OF THE STUDY

RAI2 was identified as metastasis suppressor gene for early hematogenous dissemination in luminal breast cancer patients and *RAI2*-depleted luminal breast cancer cell lines show a more aggressive phenotype and elevated invasiveness (Werner et al., 2015). Further clinical and functional analyses performed at the ITB provided evidence that *RAI2* might also function in maintaining genomic integrity. The main purpose of this study was to investigate the role of *RAI2* protein during cell cycle progression and the impact on maintaining genome stability. Therefore, mitotic progression in *RAI2*-depleted luminal breast cancer cell lines was analysed using live cell imaging and immunofluorescence staining. Two of the main mechanism that avoid the onset of a chromosomal instable phenotype are functionality in DNA damage and replication. Thus, the influence of *RAI2* on both processes was studied in cell culture experiments. Besides, analysis of *RAI2* gene and protein expression levels in different cell cycle phases should reveal, in which phase *RAI2* may function. Moreover, the influence of *RAI2* loss on the response to chemotherapeutics, which effects different steps in the cell cycle, was investigated. As CtBPs are the main binding partner of *RAI2* and both might associated with chromosomal stability, *RAI2*/CtBP speckle formation was analysed in the presence of chemotherapeutics. Finally, the impact of *RAI2* gene expression on patients' survival was investigated in breast cancer patients with chromosomal instable tumours.

3 MATERIAL AND METHODS

3.1 MATERIAL

3.1.1 CELL LINES

Supplements for cell culture media are described in chapter 3.1.6.

Table 1: Human cell lines used in this study.

Description	Tissue type	Culture Medium	Source
MCF-7	Breast adeno carcinoma, pleura effusion	DMEM	ITB, UKE
KPL-1	Recurrent breast adeno carcinoma, pleura effusion	DMEM	ITB, UKE
HEK293T	Embryonic kidney cells	DMEM	Volker Assmann, ITB, UKE
KPL-1 eYFP-Histone 2B	Recurrent breast adeno carcinoma, pleura effusion	DMEM	Stefan Werner, ITB, UKE
KPL-1 RAI2 OE	Recurrent breast adeno carcinoma, pleura effusion	DMEM	Stefan Werner, ITB, UKE
KPL-1 vec	Recurrent breast adeno carcinoma, pleura effusion	DMEM	Stefan Werner, ITB, UKE
MCF-7 RAI2 OE	Breast adeno carcinoma, pleura effusion	DMEM	Stefan Werner, ITB, UKE
MCF-7 vec	Breast adeno carcinoma, pleura effusion	DMEM	Stefan Werner, ITB, UKE

ITB: Institute of Tumor Biology

UKE: University Medical Center Hamburg-Eppendorf

OE: Overexpression

Vec: vector control

3.1.2 LABORATORY INSTRUMENTS

Table 2: Laboratory instruments used in this study.

Instrument name	Company	Office
Analysis scale CP224S-OCE	Sartorius	Göttingen, DE
Analysis scale BP610	Sartorius	Göttingen, DE
Analysis scale BP6100	Sartorius	Göttingen, DE
Axioplan2 imaging with AxioCam MRm and light source HXP120V	Carl Zeiss	Jena, DE
BioPhotometer with thermal printer DPU-414	Eppendorf	Hamburg, DE
Centrifuge 5417R	Eppendorf	Hamburg, DE
Developer Curix 60	AGFA HealthCare	Bonn, DE
Electrophoresis power source 250 V	VWR International	Radnor, PA, US
FACS AriaIIIu	BD Bioscience	Franklin Lakes NJ, US
FACS Canto II	BD Bioscience	Franklin Lakes NJ, US
FACS LSR Fortessa	BD Bioscience	Franklin Lakes NJ, US
Hoefer Dual Gel Caster	GE Healthcare	Chalfont St Giles, GB
Hoefer SE250	GE Healthcare	Chalfont St Giles, GB
Incubator Hera cell 150	Thermo Fisher Scientific	Waltham, MA, US
Magnetic stirrer MR 3001	Heidolph Instruments	Schwabach, DE
Multipette M4	Eppendorf	Hamburg, DE
Nanodrop ND100 spectrometer	PeqLab	Erlangen, DE
pH Meter inoLab	WTW	Heidelberg, DE
Realplex mastercycler ep gradient S	Eppendorf	Hamburg, DE
SpinningDisk microscope	Visitron Systems	Puchheim, DE
Titramex 100	VWR International	Radnor, PA, US
Transblot DS semidry transfer cell	Bio-Rad Laboratories	Hercules, CA, US
Ultrasound homogenisator	Hielscher Ultrasonics GmbH	Teltow, DE

3.1.3 CONSUMABLES

Table 3: Consumables used in this study.

Consumable	Company	Office
6-well plate	Sarstedt	Nümbrecht, DE
96-well microtiter plate	eppendorf	Hamburg, DE
Cell scraper	bioswisstec	Schaffhasuen, CH
Culture slides 80426	ibidi	Planegg, DE
Falcon chambered cell culture slides	Thermo Fisher Scientific	Waltham, MA, US
Protran BA 85, pore size 0.45 µm	GE Healthcare	Chalfont St Giles, GB
Serological pipettes	Sarstedt	Nümbrecht, DE
Super RX films	Fujifilm	Minato, JP
T25 cell culture flask	Sarstedt	Nümbrecht, DE
T75 cell culture flask	Sarstedt	Nümbrecht, DE
Pipettes tips	Sarstedt	Nümbrecht, DE

3.1.4 CHEMICALS

Table 4: Chemicals used in this study.

Chemical	Company	Office
Acetic acid	J.T. Baker	Deventer, NL
Acetone	J.T. Baker	Deventer NL
Agarose LE	Genaxxon Bioscience	Ulm, DE
Ammonium persulfate	AppliChem	Darmstadt, DE
Aqua	B. Braun Melsungen	Melsungen, DE
Bromphenol blue	Merck	Darmstadt, DE
BSA Fraction V (Bovines Serum Albumin)	Biomol	Hamburg, DE
Complete Protease Inhibitor	Roche Applied Science AG	Penzberg, DE
Crystal violette	Sigma-Aldrich	St. Louis, MO, US
DAPI (4',6-Diamidine-2-phenylindole)	Carl Roth	Karlsruhe, DE
DMEM High Glucose-Medium (Dulbecco's Modified Eagle's Medium)	PAN Biotech	Aidenbach, DE

MATERIAL AND METHODS

DMSO (dimethyle sulfoxide)	Serva	Heidelberg, DE
DNA-Marker GeneRuler 1 kb DNA Ladder	Thermo Fisher Scientific	Waltham, MA, US
dNTPs (desoxyribonucleoside triphosphate set)	Roche Diagnostics	Mannheim, DE
DTT (dithiothreitol)	Sigma-Aldrich	St. Louis, MO, US
Ethanol absolute	Merck	Darmstadt, DE
Ethanol denaturated	Chemsolute/TH Geyer	Renningen, DE
FCS (fetal calf serum)	PAA Laboratories	Pasching, A
Glycine pufferan	Carl Roth	Karlsruhe, DE
Hydrochloride acid 1 N (HCl)	Carl Roth	Karlsruhe, DE
Isopropyl alcohol	Carl Roth	Karlsruhe, DE
L-glutamine	PAA Laboratories	Pasching, A
Lipofectamine2000 Transfection Reagent	Thermo Fisher Scientific	Waltham, MA, US
Luminol	Sigma-Aldrich	St. Louis, MO, US
Methanol	J.T. Baker	Deventer, NL
Milk Powder	Carl Roth	Karlsruhe, DE
Mounting Medium Immuno-Fluore	Thermo Fisher Scientific	Waltham, MA, US
Mowiol	Merck (Calbiochem)	Darmstadt, DE
Nuclease-free Water	Qiagen	Hilden, DE
OptiMEM medium	Gibco	Eggenstein, DE
p-Coumaric acid	Sigma-Aldrich	St. Louis, MO, US
PFA (Paraformaldehyde)	Merck	Darmstadt, DE
PhosSTOP	Roche Applied Science AG	Penzberg, DE
Polybrene (Hexadimethrinbromide)	Fluka (Thermo Fisher)	Waltham, MA, US
Propodium iodide	Sigma-Aldrich	St. Louis, MO, US
ProteinLadderr Page Ruler Prestained Protein Ladder 10 – 180 kDa	Thermo Fisher Scientific	Waltham, MA, US
Rnase A	Thermo Fisher Scientific	Waltham, MA, US
Rotiphorese Gel 40%	Sigma-Aldrich	St. Louis, MO, US
SDS-solution 20% (sodium dodecyl sulfat)	AppliChem	Darmstadt, DE

MATERIAL AND METHODS

Sodium chlorid (NaCl)	Carl Roth	Karlsruhe, DE
Sodium hydroxide (NaOH)	Merck	Darmstadt, DE
TEMED (Tetramethylethylenediamine)	Sigma-Aldrich	St. Louis, MO, US
Tris-acetate	Sigma-Aldrich	St. Louis, MO, US
Tris-EDTA (TE) buffer; pH 8.0	Sigma-Aldrich	St. Louis, MO, US
Triton X-100	Sigma-Aldrich	St. Louis, MO, US
Trizma base	Sigma-Aldrich	St. Louis, MO, US
Trypanblau	Sigma-Aldrich	St. Louis, MO, US
Trypsin-EDTA solution 0.25% (w/v)	Gibco	Eggenstein, DE
Tween-20	Fluka (Thermo Fisher)	Waltham, MA, US
Vectashield Mounting Medium with DAPI	Vector Laboratories	Burlingame, CA, US
Wester nova 2.0	Cyanagen	Bologna, IT

3.1.5 CHEMOTHERAPEUTICS AND REAGENTS

Table 5: Chemicals and reagents used in this study.

Description	Function	Company	Office
5-Chloro-20-deoxyuridine (CldU)	Thymidine analogue	Sigma-Aldrich	St. Louis, MO, US
5-Iodo-20-deoxyuridine (IdU)	Thymidine analogue	Sigma-Aldrich	St. Louis, MO, US
Camptothecin	Topoisomerase I inhibitor	Sigma-Aldrich	St. Louis, MO, US
Doxorubicin	DNA intercalation	Sigma-Aldrich	St. Louis, MO, US
Etoposide	Topoisomerase II inhibitor	Sigma-Aldrich	St. Louis, MO, US
Hydroxy Urea	Replication fork inhibitor	Sigma-Aldrich	St. Louis, MO, US
Olaparib	PARP inhibitor	Selleckchem	Houston, TX, US
Paclitaxel	Inhibitor of mitotic spindle degradation	New England Biolabs	Ipswich, MA, US
Peroxide (H ₂ O ₂)	Induced of oxidative stress	Merck	Darmstadt, DE
RO-3306	Cdk1 inhibitor	Sigma-Aldrich	St. Louis, MO, US
Thymidine	DNA synthesis inhibitor	Sigma-Aldrich	St. Louis, MO, US

3.1.6 BUFFER AND MEDIA

Table 6: Composition of buffer and media used in this study.

Description	Composition
3x SDS sample buffer	30% Glycerol 6% SDS 187.5 mM Tris/HCl, pH 6.8 0.01% Bromophenol blue
Cell culture medium Dulbecco's Modified Eagle Medium (DMEM)	500 mL DMEM 10% FCS 2 mM L-Glutamine
Dulbecco's Phosphate Buffered Saline (DPBS) no calcium, no magnesium	2.7 mM KCl 1.5 mM KH ₂ PO ₄ 137.9 mM NaCl 8.1 mM Na ₂ HPO ₄ 7 H ₂ O
Electrochemoluminescence (ECL) solution 1	0.1 M Tris-HCl (pH 8.5) 2.5 mM Luminol 0.396 mM p-Coumarine acid
Electrochemoluminescence (ECL) solution 2	0.1 M Tris-HCl (pH 8.5) 0.018% (v/v) H ₂ O ₂
Laemmli buffer	19.2 mM Glycine 0.01% SDS 2.5 mM Tris base
50 x TAE buffer, pH 8.0	40 mM Tris base 20 mM Acetic acid 50 mM EDTA, pH 8.0
TBS-T, pH 7.6	150 mM NaCl 50 mM Tris base 0.05% Tween 20
Transfer buffer	39 mM Glycine 20% Methanol 0.037% SDS 48 mM Tris base

3.1.7 VECTORS AND EXPRESSION PLASMIDS

Table 7 shows all plasmids that were used in this study with composition, vector backbone and addgene ID number if available. Vectors with no depicted addgene ID number were prepared and kindly provided by Dr. Stefan Werner (Institute of Tumor Biology, UKE).

MATERIAL AND METHODS

Table 7: Plasmid vectors used for lentiviral transduction and transfection for Traffic Light Reporter Assay.

Plasmid	Vector Backbone	Addgene#	Source
pH2B-EYFP	pEYFP-N1	51002	Addgene, Cambridge, MA, US
empty	phCMV3		Stefan Werner, ITB, UKE
RAI2 OE (Werner et al., 2015)	phCMV3		Stefan Werner, ITB, UKE
SFFV d14GFP Donor	pCVL	31475	Addgene, Cambridge, MA, US
Traffic Light Reporter 1.1 (Sce target) Ef1a BFP	pCVL	31481	Addgene, Cambridge, MA, US
pLKO.1 non-target	pCVL		Stefan Werner, ITB, UKE
pLKO.1 shRNA1	pCVL		Stefan Werner, ITB, UKE
Lentiviral packaging plasmid	psPAX2	12260	Addgene, Cambridge, MA, US
VSV-6 envelope expression plasmid	pMD2.G	12259	Addgene, Cambridge, MA, US

3.1.8 ANTIBODIES

Table 8: Antibodies used for Western Blot analysis, immunofluorescence staining and DNA fiber assay.

Antigen	Clone	Species	Company	Office
RAI2	D4W9P	rabbit	Cell Signalling Technologies	Danvers, MA, US
Cyclin B1	D5C10	rabbit	Cell Signalling Technologies	Danvers, MA, US
Cyclin E2	4132P	rabbit	Cell Signalling Technologies	Danvers, MA, US
Survivin	71G4B7	rabbit	Cell Signalling Technologies	Danvers, MA, US
p53	DO-7	rabbit	Dako	Glostrup, DK
P-H3 (Ser10)	D2C8	rabbit	Cell Signalling Technologies	Danvers, MA, US
H2A.X	20E3	rabbit	Cell Signalling Technologies	Danvers, MA, US
cleaved PARP1	D64E10	rabbit	Cell Signalling Technologies	Danvers, MA, US
HSC-70	clone B-6	mouse	Santa Cruz	Dallas, TX, US

MATERIAL AND METHODS

GFP	polyclonal	rabbit	Abcam	Cambridge, UK
CtBP1	3/CtBP1	mouse	BD Bioscience	Franklin Lakes NJ, US
BrDU	BU1/75	rat	Bio-Rad Laboratories	Hercules, CA, US
BrDU	B44	mouse	BD Bioscience	Franklin Lakes NJ, US

3.1.9 SECONDARY ANTIBODIES

Table 9: Secondary antibodies used in this study for Western Blot analysis, immunofluorescence staining and DNA fiber assay.

Antigen	Clone	Species	Conjugate	Company	Office
rabbit-IgG	polyclonal	goat	HRP	CST	Danvers, MA, US
mouse-IgG	polyclonal	horse	HRP	CST	Danvers, MA, US
rabbit-IgG (H+L)	polyclonal	goat	Alexa Fluor 546	Thermo Fisher Scientific	Waltham, MA, US
rat-IgG (H+L)	polyclonal	mouse	Alexa Fluor 555	Thermo Fisher Scientific	Waltham, MA, US
mouse-IgG (H+L)	polyclonal	goat	Alexa Fluor 488	Thermo Fisher Scientific	Waltham, MA, US

3.1.10 KITS

Table 10: Kits used in this study.

Kit	Application	Company	Office
NucleoSpin® RNA kit	total RNA purification	Macherey Nagel	Düren, DE
First strand cDNA Synthesis Kit	cDNA synthesis	Thermo Fisher Scientific	Waltham, MA, US
Maxima SYBR Green/Fluorescein qPCR Master Mix	qRT-PCR	Thermo Fisher Scientific	Waltham, MA, US
NucleoSpin® Gel and PCR Clean-up	clean-up for DNA	Macherey Nagel	Düren, DE

3.1.11 OLIGONUCLEOTIDES

Table 11: Synthetic oligonucleotides for qRT-PCR. Sequence and melting temperature (T_m) are specified.

Declaration	Target gene	Sequence (5'-3')	T _m
RAI2 for	<i>RAI2</i>	GGCGAAGTCAAGGCTGAAAA	59°C
RAI2 rev	<i>RAI2</i>	TCCCCTTGGCTGTTGATGTC	59°C
CCNB1 for	<i>CCNB1</i>	TTGGGGACATTGGTAACAAAGTC	60°C
CCNB1 rev	<i>CCNB1</i>	ATAGGCTCAGGCGAAAGTTTT	60°C
CCNE2 for	<i>CCNE2</i>	CTATTTGGCTATGCTGGAGG	63°C
CCNE2 rev	<i>CCNE2</i>	TCTTCGGTGGTGCATAATG	63°C
RPLP0 for	<i>RPLP0</i>	TGAGGTCCTCCTTGGTGAACA	60°C
RPLP0 rev	<i>RPLP0</i>	CCAGCTCTGGAGAAACTGC	60°C

3.1.12 CHEMOTHERAPEUTICS AND INHIBITORS

Table 12: Chemotherapeutics and inhibitors used for cell culture experiments. The corresponding function of the inhibitors is specified.

Description	Function	Company	Office
5-Chloro-20-deoxyuridine (CldU)	Thymidine analogue	Sigma-Aldrich	St. Louis, MO, US
5-Iodo-20-deoxyuridine (IdU)	Thymidine analogue	Sigma-Aldrich	St. Louis, MO, US
Camptothecin	Topoisomerase I inhibitor	Sigma-Aldrich	St. Louis, MO, US
Doxorubicin	DNA intercalation reagent	Sigma-Aldrich	St. Louis, MO, US
Etoposide	Topoisomerase II inhibitor	Sigma-Aldrich	St. Louis, MO, US
Hydroxy Urea	Replication fork inhibitor	Sigma-Aldrich	St. Louis, MO, US
Olaparib	PARP inhibitor	Selleckchem	Houston, TX, US
Paclitaxel	Inhibitor of mitotic spindle degradation	New England Biolabs	Ipswich, MA, USA
Peroxide (H ₂ O ₂)	Induction of oxidative stress	Merck	Darmstadt, DE
RO-3306	Cdk1 inhibitor	Sigma-Aldrich	St. Louis, MO, US
Thymidine	DNA synthesis inhibitor	Sigma-Aldrich	St. Louis, MO, US

3.1.13 SOFTWARE AND DATABASES

Table 13: Software for analysis and databases used in this study.

Software/Database	Application	Source
GIMP (2.8)	Image processing	www.gimp.org
Axiovision	Image processing	www.zeiss.de
BoxPlotR	Generation of boxplots	http://shiny.chemgrid.org/boxplotr/
FACSdiva	Analysis of FACS data	BD Bioscience, Franklin Lakes, NJ, US
ImageJ (1.52a)	Image processing	https://imagej.nih.gov/ij/
METABRIC dataset	Data set for survival analysis	http://www.cbioportal.org/
NCBI	Database for literature (PubMed), proteins, DNA and RNA	www.ncbi.nlm.nih.gov

3.2 CELL CULTURE METHODS

3.2.1 STANDARD CULTIVATION OF HUMAN CELL LINES

Cells were grown as monolayers on plastic cell culture dishes in DMEM supplemented with 10% fetal calf serum and 2 mM L-glutamine (see 3.1.6) at 37°C in a humidified atmosphere containing 10% CO₂. According to their growth rates, cells were constantly splitted by washing them with PBS, adding trypsin and incubating them at 37°C for 5 min. When cells were detached, trypsin was quenched with medium containing serum and cells were centrifuged. The cell pellet was resuspended in medium and cells were seeded into new cell culture dishes.

3.2.2 CRYOPRESERVATION OF HUMAN CELLS LINES

To store the cells cryopreservation tubes were filled with 1 mL cell suspension containing 100 µL DMSO and tubes were stored at -20°C. For longer storage duration, tubes were moved to a nitrogen container. To reculture cells, tubes were thawed at 37°C and the cell suspension was carefully mixed with 5 mL medium. Cells were centrifuged and cultured in fresh cell culture dishes.

3.2.3 LENTIVIRAL PARTICLE PRODUCTION

Lentiviral supernatant was produced by transfecting HEK293T cells using a three plasmid packing system. Cells containing 70% confluency were transfected with either pLKO.1 shRNA 1 or pLKO.1 non-target (harboring a scrambled non-targeting shRNA sequence) in a pCVL plasmid (5000 ng) and additionally with psPAX2 packing plasmid (3750 ng) and pMD2.G envelope plasmid (1250 ng) using Lipofectamine2000 reagent (see 3.1.7). Cells were incubated with transfection cocktail overnight. The next day, medium was replaced and the supernatant was harvested 48h and 72h after infection and sterile filtered with Millex Filters (pore size 0.45 µm). Supernatants were stored in reaction tubes at -20°C.

3.2.4 SHRNA-MEDIATED KNOCKDOWN OF *RAI2* GENE EXPRESSION

Target cells were infected with in 1:10 ratio with lentiviral particles (see 3.2.3) in presence 1:1000 polybrene overnight. The pLKO.1 non-target vector was used as negative control. Medium was changed and another round of transfection was performed 32h after the first change of medium

for 8 h. Because of the recovery of RAI2 expression 14 days after the first transduction, assays were performed within seven to twelve days after first infection.

3.2.5 GENERATION OF PHOSPHOR HISTONE 2B-GFP CELL LINE

To establish KPL-1 cells with a constitutive expression of eYFP-H2B fusion protein cells were transfected with the pH2B-EYFP plasmid (see 3.1.7) using Lipofectamine2000 transfection reagent according to manufacturer's protocol. After 72h, eYFP-positive cells were enriched using fluorescence activated cell sorting ("FACS AriaIIIu" equipped with "FACSDiva software"). This procedure was repeated after 10 days to enrich cells with stable expression of the eYFP-H2B fusion protein.

3.2.6 LIVE CELL IMAGING

Live cell imaging was done in cooperation with Bernd Zobiak from the UKE imaging facility, who handled the spinning disk microscope and processed the images. KPL-1 cells stably expressing eYFP-H2B (see 3.2.5) were transduced with RAI2-specific and non-target control shRNAs (see 3.2.4) and transferred into chambered culture slides 7 days after transduction (ibidi). To maintain cell viability cells were kept in a humidified environmental chamber supplied with 5% CO₂ at 37°C. Cell divisions were recorded with a Visitron SpinningDisk microscope and low power 488 nm laser excitation using a 40x/NA1.3 Plan Fluor oil objective and a high sensitive EM-CCD camera for detection. 20 µm z-stacks with a spacing of 5 µm were acquired as time-lapse series at 1 min intervals. This acquisition setup allowed to obtain high-resolution data and to critically reduce phototoxic effects that would have otherwise interfered with cell cycle progression. As an additional control, cells were cultured in an external incubator for 24h and images were taken at time point 0h and 24h to assess frequency of micronuclei formation and thus impact of continuously absorbed radiation on mitotic fidelity. Images were further processed in FIJI (Schindelin et al., 2012) by applying maximum intensity projection, background correction and noise reduction. In two independent experiments, mitotic cells were analysed by scanning 5 to 10 positions in the chamber culture slide over 24h. At least 100 cell divisions per cell line were recorded and used for evaluation. Total duration of mitosis (min) and of individual mitotic stages as well as *de novo* micronuclei formation was analysed.

3.2.7 CELL CYCLE ANALYSIS USING DOUBLE THYMIDINE BLOCK

MCF-7 cells were synchronised by a double treatment with 2 mM thymidine in DMEM for 16h each with 8h pause between the blocks. Protein, RNA and FACS (see 3.4.1, 3.3.1.1, 3.3.2) samples were taken before treatment, after the first block and 0h, 2h, 4h, 6h, 8h, 10h and 12h after the second block with thymidine to analyse samples with Western Blot (0), qRT-PCR (3.3.1.3) and to investigate the cell cycle distribution (3.3.2).

3.2.8 COLONY FORMATION ASSAY

For the analysis of clonogenic capacity cell solutions of 1000 cells for MCF-7 or 2000 cells of KPL-1 were prepared and seeded into 6-well plates. After 24h cells were continuously grown in presence of the chemotherapeutic reagent for 12 days or were pulse treated. Table 14 summarises how KPL-1 and MCF-7 cells were treated with the indicated reagent.

Table 14: Reagents used for colony formation assay in this study. Type of treatment and concentration are indicated.

Reagent	Type of Treatment	Concentration
Camptothecin	4h pulse treatment, renew medium after 7 days	10 nM
Doxorubicin	4h pulse treatment, renew medium after 7 days	100 nM
Etoposide	4h pulse treatment, renew medium after 7 days	10 μ M
Olaparib	continuous treatment, renew medium containing reagent after 7 days	100 nM
H ₂ O ₂	4h pulse treatment, renew medium after 7 days	30 μ M

For analysis, medium was removed and colonies were washed with PBS. Afterward, colonies were fixed with 5% (w/v) PFA/PBS for 10 min and stained with 0.5% (w/v) crystal violet/H₂O solution for 30 min. Excessive staining solution was washed away with desH₂O. Subsequently, plates were scanned and colonies were evaluated using the ColonyArea plugin for ImageJ (Guzman et al., 2014).

3.3 MOLECULAR BIOLOGICAL TECHNIQS

3.3.1 GENE EXPRESSION ANALYSIS

3.3.1.1 ISOLATION OF TOTAL RNA FROM CULTURED CELLS

Total RNA of cells was isolated using the “NucleoSpin® RNA” kit and diluted in nuclease-free water. Measurement of RNA concentration was performed using the Nanodrop® ND-1000 system.

3.3.1.2 cDNA SYNTHESIS

In order to analyse gene expression, RNA has first to be transcribed into cDNA for quantitative real-time PCR (qRT-PCR). For this, 500 ng of isolated total RNA of each sample (3.3.1.1) was transcribed into cDNA using random hexamer primers and M-MuLV reverse transcriptase in a total volume of 10 µl according to the manufacturer`s protocol (First Strand cDNA Synthesis). “Titramex 100” cyclor machine was used for transcription and cDNA was diluted 1:10 for further experiments and stored at -20°C.

Table 15: Program for cDNA synthesis used in this study.

Step	Temperature	Time
Annealing	25°C	5 min
Reverse transcription	37°C	60 min
Inactivation of transcriptase	70°C	5 min

3.3.1.3 QUANTITATIVE REAL-TIME POLYMERASE CHAIN REACTION (qRT-PCR)

In order to analyse gene expression of specific target genes a qRT-PCR was applied, where before generated cDNA is relatively quantified based on a PCR reaction. qRT-PCR was performed using “Maxima SYBR Green/Fluorescein qPCR Master Mix” kit and experiments were performed in triplicate on 96-well microtiter plate. 2 µL of diluted cDNA (see 3.3.1.2) was used in a total volume of 10 µL and PCR reaction program was applied as depicted below (Table 16) and executed on a “Mastercycler epGradientS”. Primer sequences and corresponding annealing temperatures are described in chapter 3.1.11.

Table 16: Program of qRT-PCRs.

Step	Temperature	Time	Cycles
Initial denaturation	95°C	5 s	1
Denaturation	95°C	15 s	35x
Annealing	59-63°C	30 s	
Extension	68°C	30 s	
Annealing	95°C	15 s	1
Extension	60°C	55 s	1
Melting gradient	60°C to 95°C	20 min	1

Raw data was analysed with the so called comparative c_t method. As a first step the reference gene was normalised: $\Delta c_t = c_t$ (target gene) - c_t (reference gene). In this study, large ribosomal protein gene (*RPLP0*) was used as reference gene. Next, the difference between gene of interest and control gene was calculated, for example by calculating the difference between unsynchronised and blocked cells for the analysis of gene expression during cell cycle: $\Delta\Delta c_t = \Delta c_t$ (blocked) - Δc_t (synchronised). The determined ratio indicates the relative expression difference: ratio = $2^{-\Delta\Delta c_t}$. A ratio below 1 indicates a downregulation and a ratio above 1 indicates an upregulation of the gene of interest.

3.3.2 CELL CYCLE ANALYSIS

For determination of cellular DNA content as a surrogate for different cell cycle stages cells were trypsinised and single cell solution was quenched with DMEM. Cell solution was centrifuged at 850g at 4°C and medium was carefully aspirated from the cells. The pellet was resuspended in 300 μ l cold PBS and 700 μ l ice-cold absolute EtOH was added dropwise. Fixed cells were stored at 4°C until FACS analysis. For analysis, cells were spun down at 850g at 4°C and stained in freshly prepared propidium iodide buffer (20 μ g/mL propidium iodide, 0.2 mg/mL RNase A, 0.1% (v/v) Triton X-100 in PBS). Flow cytometry was performed using a “FACS Canto II” equipped with “FACSDiva software”.

3.3.3 AGAROSE GEL ELECTROPHORESIS

Agarose gel electrophoresis was performed for preparative purpose in horizontal agarose gel chambers (“EasyPhor Gelchamber”). A 1% (w/v) TAE agarose gel was prepared containing

ethidium bromide (1:10000). DNA samples were mixed with 6 x DNA loading-dye, loaded on the gel and were separated according to their molecular weight with an electric tension of 80 V. As a marker for molecular weight “DNA-Marker GeneRuler 1 kb DNA Ladder” was applied in parallel. DNA was visualised by the ethidium bromide that intercalated with the DNA, and recorded using a trans-illuminator (wavelength of 234 nm). Documentations was done with the gel documentation system “Gene Genius 2”.

3.4 PROTEIN BIOCHEMICAL AND IMMUNOLOGICAL METHODS

3.4.1 PROTEIN ISOLATION FROM CULTURED CELLS

To isolate total cell extract from cultured cells, nearly confluent cells were washed with PBS before 1 mL PBS was added. The cell layer was removed from the surface using a cell scraper and suspension was spun down in a 1.5 µL reaction tube (750g) for 3 min at 4°C. Next, the supernatant was removed and the cell pellet was resuspended in an appropriate amount of 1x SDS sample buffer (40-200 µL, depending on the size of the pellet) containing “PhosSTOP™ phosphatase inhibitor” and “cOmplete™ mini proteinase inhibitor”. Samples were homogenised by sonification (“Ultrasound homogenisator”) and supplemented with 1 µL bromophenol blue solution. Afterwards, cell extracts were denaturated at 95°C for 5 min, placed on ice and stored at -20°C.

3.4.2 MEASUREMENT OF PROTEIN CONCENTRATION

Protein concentration of total cell extract was measured using “Pierce BCA Protein Assay” kit according to the manufacturer`s protocol before supplementation of bromophenol blue solution (see 3.4.1). Initially, a calibration series was prepared from 0 µg to 30 µg bovine serum albumin (BSA) solution. 1 µL of total cell extract was mixed with reagent A reagent B (1:50) and after color change, the extinction of each sample was measured at a wave length of 540 nm. Protein concentration was calculated using linear regression of the calibration series.

3.4.3 SDS-POLYACRYLAMIDE GEL ELECTROPHORESIS (SDS-PAGE)

To perform Western Blot analyses, proteins of total cell extracts had to be separated according to their molecular weight by SDS-Polyacrylamide Gel Electrophoresis (SDS-PAGE). Using Hoefer

SE250 system, total protein extracts (see 3.4.1) were applied on a SDS polyacrylamide gel, consisting of a stacking gel and a separation gel. The chosen acrylamide concentration of the separation gel depended on the molecular weight of the analysed protein. For proteins with a molecular weight between 40-120 kDa an 8% gel was used, for proteins below 40 kDa a 14% gel was applied. Electrophoresis was performed using Laemmli buffer at 25 mA per gel at room temperature for 1h. To estimate the protein size in the Western Blot afterwards, “PageRuler™ Prestained Protein Ladder” was used as size control.

Table 17: Components of Tris/Glycine SDS-Polyacrylamide Gels

Component	6% stacking gel	8% separation gel	14% separation gel
desH ₂ O	1.46 mL	2.1 mL	1.4 mL
Rotiphorese Gel 40%	0.3 mL	0.8 mL	1.5 mL
1.0 M Tris (pH 6.8)	0.3 mL	-	-
1.0 M Tris (pH 8.8)	-	1.0 mL	1.0 mL
10% SDS	20 µL	40 µL	40 µL
10% ammonium persulfate	20 µL	40 µL	40 µL
TEMED	2 µL	4 µL	4 µL

3.4.4 WESTERN BLOT ANALYSIS

Proteins, which were previously separated in a SDS-PAGE (see 3.4.3), were blotted on a membrane and protein amount was analysed based on antibodies specific for the protein of interest. Blotting from the SDS-PAGE to a nitrocellulose membrane (“Protran BA 85”) was performed by semi-dry electrophoretic transfer (Trans-Blot SD semi-dry transfer cell) in transfer buffer at room temperature at 40 mA per gel for 2h. The membrane was washed in TBS-T buffer for 5 min and incubated with 5% (w/v) milk/TBS-T for 30 min to block unspecific antibody binding on the membrane. This was followed by incubation under continuous shaking with 5% (w/v) milk/TBS-T or 5% (w/v) BSA/TBS-T containing primary antibody against the protein of interest over night at 4°C. The next day, the membrane was washed three times with TBS-T for 5 min and incubated with HRP-conjugated secondary antibody in 5% (w/v) milk/TBS-T for 2h. Again, the membrane was washed three times with TBS-T for 5 min and proteins were detected based on a peroxidase

reaction using x-ray films. For this, ECL solution 1 and 2 were mixed in a 1:1 ratio and the membrane was coated for 1 min with the solution. Afterwards, the membrane was put together with an x-ray film (“Super RX films”) into a cassette and the film was developed in the “Curix 60 Processor”.

3.4.5 IMMUNOFLUORESCENCE STAINING

Staining cells with fluorescence-labeled antibodies is a method to visualise proteins and to estimate localisation of proteins within the cells. Cells were grown on chamber slides and initially washed with PBS and fixed with 4% (w/v) PFA/PBS for 10 min. Cells were washed with PBS before they were permeabilised with 0.2% Triton X-100/PBS for 10 min. After three times washing with PBS, cells were incubated with primary antibodies overnight (1:500 for RAI2 and CtBP1) or for 4h (Histone H3 (Ser10) (1:500), ACA (1:100) and γ H2AX (1:500) in 1% (v/w) milk/PBS at 4°C. Cells were washed three times with PBS and secondary antibodies labeled with Alexa Fluor 488 (goat anti-mouse) and Alexa Fluor 546 (goat anti-rabbit) in 1% (v/w) milk/PBS were applied at room temperature for 2h. Cells were stained with DAPI/PBS (1:10,000) at room temperature for 7 min and covered with mowiol. Stainings were analysed using fluorescence microscopy Axioplan2 imaging with AxioCam MRm and light source HXP120V.

For the analysis of γ H2AX foci, KPL-1 cells stained 10 days after shRNA-mediated knock-down of RAI2. Cells with a high frequency of small foci were counted and analysed in three experiments. Total γ H2AX intensity of at least 100 cells per experiment were measured. For quantification of the γ H2AX-signal corrected total cell fluorescence was measured using ImageJ software (Corrected total cell Fluorescence=Integrated Density-(Area of selected cell x Mean Fluorescence of Background readings)).

In order to analyse speckle formation, KPL-1 and MCF-7 control cells as well as KPL-1 and MCF-7 overexpressing RAI2 and the CtBP-binding mutant RAI2 (see 3.1.1) were seeded to chamber slides one day before they were continuously treated with DMSO as control or with 10 μ M etoposide for 48h. Speckles were counted in at least 100 cells in three experiments and results were blotted as violin plot.

3.4.6 DNA FIBER ASSAY

Exponentially growing cells were pulse-labelled with 25 μM CldU and 250 μM IdU for 20 min and in one experiment also treated with 2 mM hydroxyurea (HU) for 4h in between. After labelling, cells were harvested and a cell solution of 5×10^5 cells/ml was prepared. A spot of 2 μl cell solution was spotted on a slide and dried partial. Lysis buffer (200 mM Tris-HCl pH 7.4, 50 mM EDTA, 0.5% (v/v) SDS) was added and slides are tilt slightly that the drops can run down the slide slowly and chromatin fibers can build. Fibers were air-dried, fixed with MeOH/AcOH (v/v 3:1) for 10 min and denaturated in 2.5 M HCl for 75 min. Fibers were blocked with 2% (w/v) BSA/PBS with 0.1% (v/v) Tween for 1h and afterwards stained with monoclonal rat anti-BrdU antibody (1:1000 in blocking buffer) to detect CldU, and with monoclonal mouse anti-BrdU antibody (1:1000 in blocking buffer) to detect IdU at 37°C for 1h. Slides were washed with PBS, fixed with 4% PFA and washed three times with blocking solution for 5 min. For secondary staining, goat anti-rat Alexa Fluor 555 and goat anti-mouse Alexa Fluor 488 (1:500 in blocking buffer) were used and incubated for 2h. Slides were washed with PBS and mounted in Immuno-Fluor mounting medium. Fiber tracts were examined using fluorescence microscopy (“Axioplan2 imaging with AxioCam MRm and light source HXP120V”). Images were taken from randomly selected fields with untangled fibers and analysed using the ImageJ software. Replication fork speeds was measured by converting the micrometer values of CldU and IdU into kilobases (kb). A conversion factor for the length of a labelled track of 1 μm =2.59 kb was used. A minimum of 100 individual fibers was analysed for each experiment.

3.4.7 TRAFFIC LIGHT REPORTER ASSAY

In order to analyse capacity of cells to repair double-strand breaks (DSBs) by either non-homologous end-joining (NHEJ) or homologous recombination (HR) the Traffic Light Reporter (TLR) assay was applied (Certo et al., 2011). The BFP-TLR-SceI plasmid (see 3.1.7), which contains a BFP sequence and a SceI restriction site, was digested with SceI (NEB) in 10 x CutSmart Buffer (NEB) for 4h. An agarose gel electrophoresis (3.3.3) was performed, the band with the digested plasmid was cut out and DNA was cleaned-up using „NucleoSpin Gel and PCR Clean-up“ kit according to manufacturer’s protocol. DNA was eluted with TE buffer and concentration was measured using Nanodrop® ND-1000 system. HEK293T cells were seeded and shRNA-mediated

RAI2 knockdown was produced as describes in 3.2.4. 24h after induction of the RAI2 knockdown, cells were transfected with 500 ng cut BFP-TLR-SceI and with 500 ng GFP donor plasmid (see 3.1.7) using OPTIMEM and Lipofectamin2000 transfection reagent. 48h post transfection, cells were trypsinised and quenched with media. mCherry, eGFP and BFP fluorescence signals were analysed by flow cytometry (LSR Fortessa) using a 561 nm, a 488 nm and a 405 nm laser. For analysis the percentage of mCherry-positive cells (for NHEJ events) and eGFP-positive cells (for HR events) of the BFP-positive cell fraction were used.

4 RESULTS

4.1 ANALYSIS OF MITOSIS IN RAI2-DEPLETED CELLS

RAI2 was first identified as a putative tumour suppressor gene in breast cancer associated with early dissemination to the bone marrow. Depletion of *RAI2* leads to dedifferentiation of luminal breast cancer cells and to increased invasiveness (Werner et al., 2015). Moreover, previous analysis of published gene expression data from breast cancer patients revealed that low *RAI2* gene expression significantly correlates with mutation of the *TP53* gene in breast cancer patients (Werner et al., 2015). Gene expression analysis demonstrated that *RAI2* depletion in luminal breast cancer cell lines leads to a deregulation of genes important for G₂/M transition of the cell cycle (Werner et al., 2016). Therefore, the effect of *RAI2* depletion on mitosis was further investigated in this study.

4.1.1 ANALYSIS OF RAI2-DEPLETED KPL-1 BY LIVE CELL IMAGING

As the luminal breast cancer cell line KPL-1 showed the strongest effect in deregulation of the G₂/M genes in previous studies, this cell line was chosen to further analyse the consequences of *RAI2* depletion on cell cycle progression. In order to test whether *RAI2* depletion impairs mitotic fidelity of KPL-1 cells, individual cells were analysed using live cell imaging. For this purpose, KPL-1 cells with stable expression of eYFP-Histone 2B fusion protein were generated. Histone H2B is a core protein in the nucleosome structure of the chromatin that can be used as an indicator for DNA in a cell. Here, KPL-1 eYFP-Histone 2B-expressing cells were used for lentiviral transduction either with shRNA1 against *RAI2* or with a control non-target shRNA. Overexpression of eYFP-Histone H2 fusion protein and *RAI2* depletion were verified by Western Blot analysis, indicating a stable expression of eYFP-Histone 2B and depletion of *RAI2* (Figure 5a). Seven days after induction of *RAI2* depletion, cell divisions were monitored by time-lapse series at 1 min intervals over 24h. Figure 5b shows fixed images of a control and a *RAI2*-depleted cell undergoing mitosis. The control cells mostly showed normal mitotic processes with accumulation of DNA (prophase), arrangement of chromosomes in the metaphase plate (metaphase), separation of the chromosomes (anaphase) and telophase. Contrarily, *RAI2* depletion results in alterations of the mitotic process in the cells (Figure 5b). More precisely, not all chromosomal material was

properly arranged in metaphases and was, therefore, not separated during the following anaphase to one of the poles (marked by arrows). Beside this, the lost chromosomal material was incorporated into micronuclei after telophase (marked by arrows, see also 4.1.3).

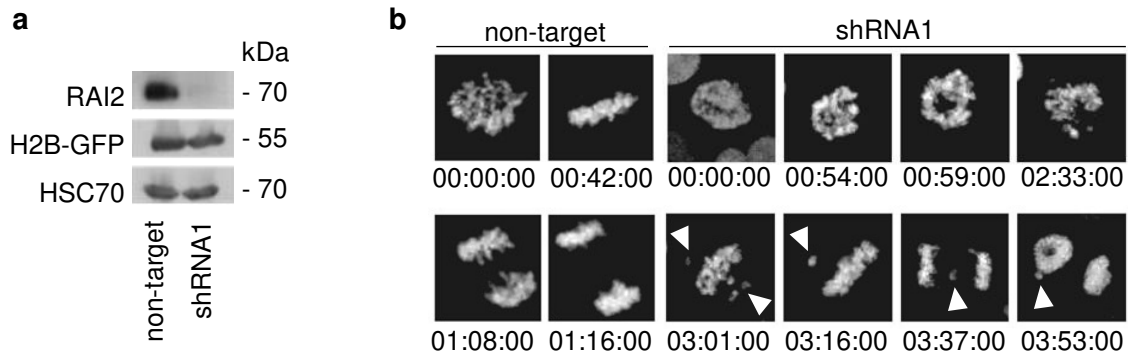


Figure 5: Analysis of mitosis in RAI2-depleted KPL-1 by live cell imaging. **a**, Stable expression of eYFP-Histone 2B fusion protein and RAI2 depletion in KPL-1 cells were tested by Western Blot analysis. HSC70 was used as loading control. **b**, RAI2-depleted KPL-1 cells were monitored by live cell imaging. Images show one mitosis of control and RAI2-depleted KPL-1 cells as examples. Time in mitosis is indicated in hour:min:sec and unaligned chromosome/chromosomal fragments and micronuclei are marked by arrows.

4.1.2 ANALYSIS OF MITOTIC DURATION

Duration of mitosis was measured in at least 90 cells using the time lapse series. Analysis showed that the duration of mitosis was significantly longer in RAI2-depleted cells compared to control cells (Figure 6a). In order to investigate which mitotic phase mostly caused this altered duration, the individual phases were studied in detail. Analysis of RAI2-depleted cells showed no significant difference between time of prophase (Figure 6b) and anaphase (Figure 6d) compared to non-target control cells. However, the time of metaphase was significantly prolonged ($p < 0.05$, Figure 6c). Thus, extended mitosis in RAI2-depleted KPL-1 eYFP-Histone 2B cells results mainly from increased time in metaphase.

RESULTS

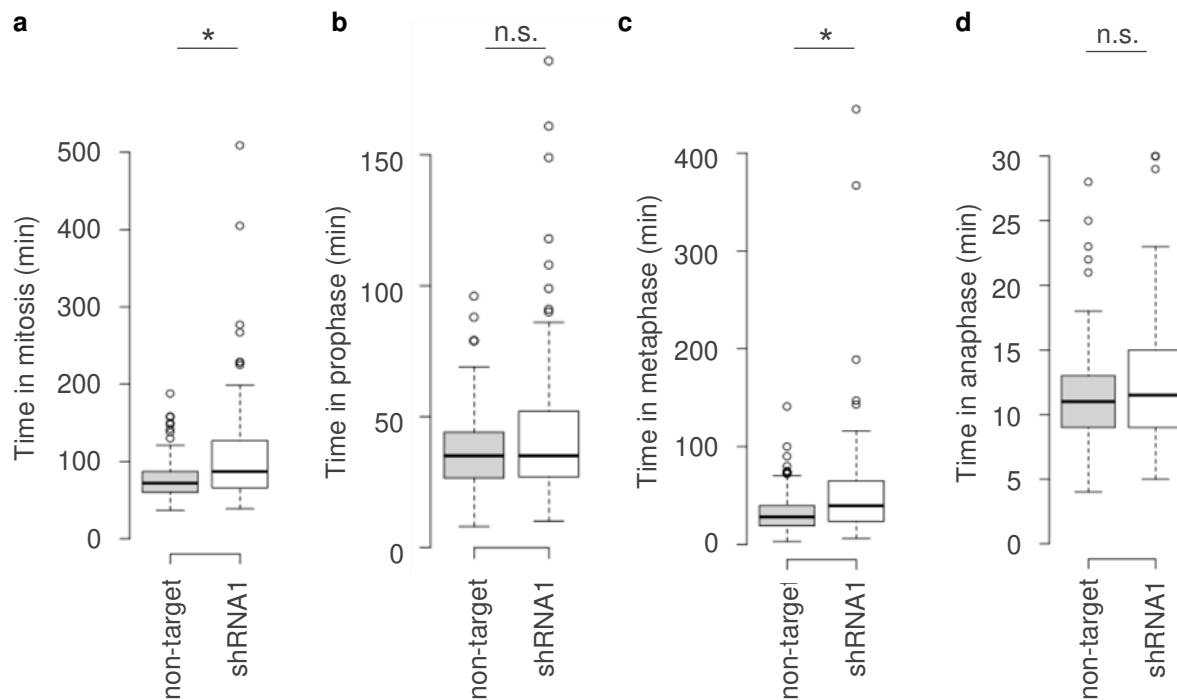


Figure 6: Analysis of duration of mitosis in RAI2-depleted KPL-1 cells. Total time of mitosis (a), duration of prophase (b), metaphase (c) as well as anaphase (d) were measured using live cell images of RAI2-depleted and non-target control KPL-1 eYFP-Histone 2B cells. Analysis was performed with at least 90 cells from two independent experiments. P-values were calculated by Student's *t*-test (* $p < 0.05$).

4.1.3 ANALYSIS OF *DE NOVO* MICRONUCLEI FORMATION

Moreover, formation of micronuclei was analysed using live cell images of RAI2-depleted KPL-1 and non-target control cells that had completed the nuclear division. Morphologically, micronuclei are similar to nuclei, but smaller, located next to the nuclei and can be observed using conventional nuclear staining. They can contain acentric chromosome fragments or whole chromosomes that have not been correctly separated to the daughter nuclei in anaphase (Fenech et al., 2011). Analysing *de novo* micronuclei formation in RAI2-depleted KPL-1 cells revealed a significantly increased frequency of micronuclei formation of 34% vs 11% compared to non-target control cells ($p < 0.0001$, Figure 7). Taken together, the results obtained by time-lapse microscopy showed that RAI2 depletion in KPL-1 cells leads to prolonged mitosis and micronuclei formation.

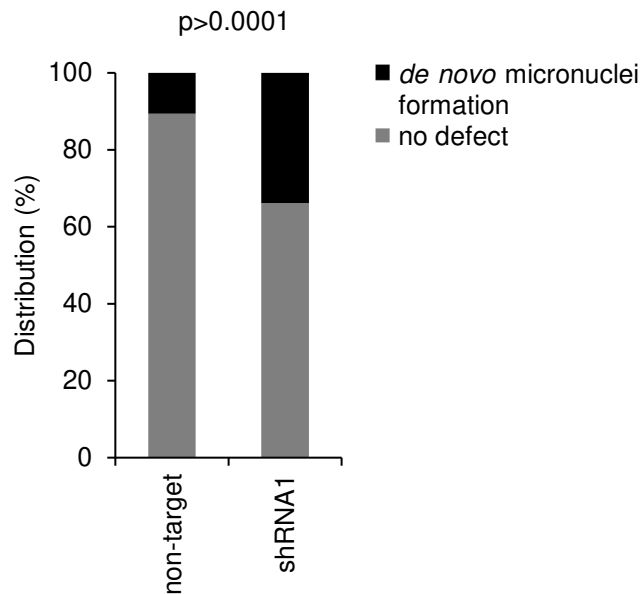


Figure 7: Analysis of micronuclei formation in RAI2-depleted KPL-1 cells. *De novo* micronuclei formation was measured in live cell images of eYFP-Histone 2B KPL-1 non-target and RAI2-depleted cells; at least 100 cells from two independent experiments were assessed. P-value was calculated by Student's *t*-test.

4.1.4 ANALYSIS OF MITOTIC DEFECTS UNDERLYING RAI2 DEPLETION

Analysis of the live cell imaging data demonstrated that RAI2-depleted KPL-1 cells show defects in mitosis marked by prolonged duration of metaphase and increased *de novo* micronuclei formation. In order to investigate the nature behind these defects, fixed cells were stained with an anti-histone H3 antibody (H3 Ser10) and with an anti-centromere antibody (ACA) to detect possible abnormalities in the chromosomes during mitosis. For this analysis, additionally to the KPL-1 cells, the luminal breast cancer cell line MCF-7 was used. Figure 8 shows different types of chromosomal defects that were observed in metaphases and anaphases by combined immunofluorescence analysis of histones and centromeres: (1) unaligned whole chromosomes containing centromere; (2) acentric chromosomes that lost their centromeres and (3) anaphase bridges that still show a connection of the chromatin during anaphase.

RESULTS

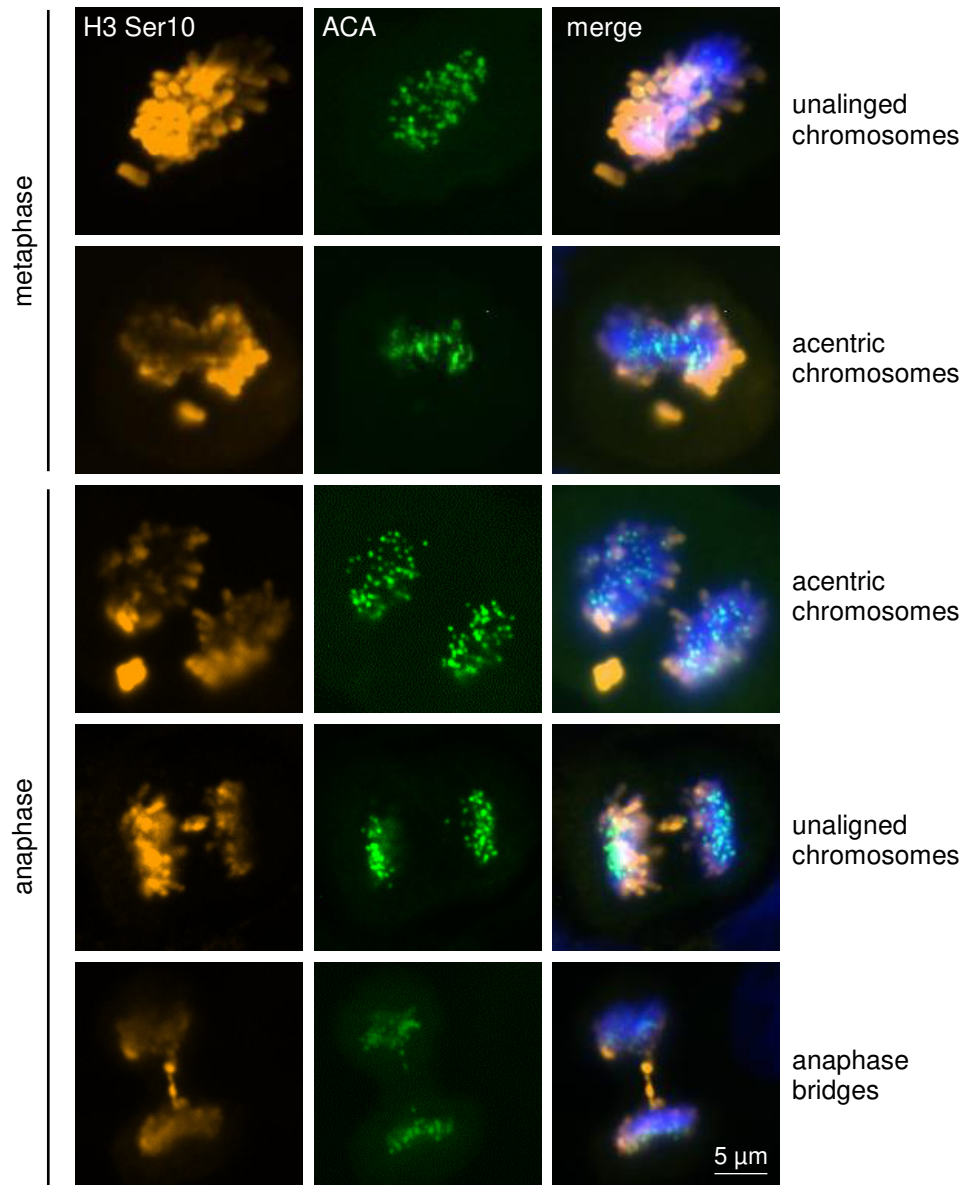


Figure 8: Immunofluorescence images showing defects in mitosis in RAI2-depleted MCF-7 cells. Fixed cells were stained for phospho-Histone 3 Serin 10 (H3 Ser10) to visualise mitotic chromatin and anti-centromeric antibody (ACA). Microscope images were taken with a 40x magnification.

Both RAI2-depleted KPL-1 and MCF-7 cells were stained with above mentioned antibodies, analysed under the microscope and events of acentric chromosomes, unaligned chromosomes and anaphase bridges were counted.

4.1.4.1 ANALYSIS OF DEFECTS IN METAPHASE

Analysing KPL-1 and MCF-7 cells that undergo metaphase demonstrated no significant difference in the frequency of unaligned chromosomes between RAI2-depleted and non-target control cells (Figure 9a and b). Interestingly, frequency of acentric fragments during metaphase was significantly increased in both cells lines after RAI2-depletion ($p < 0.05$, Figure 9a and b).

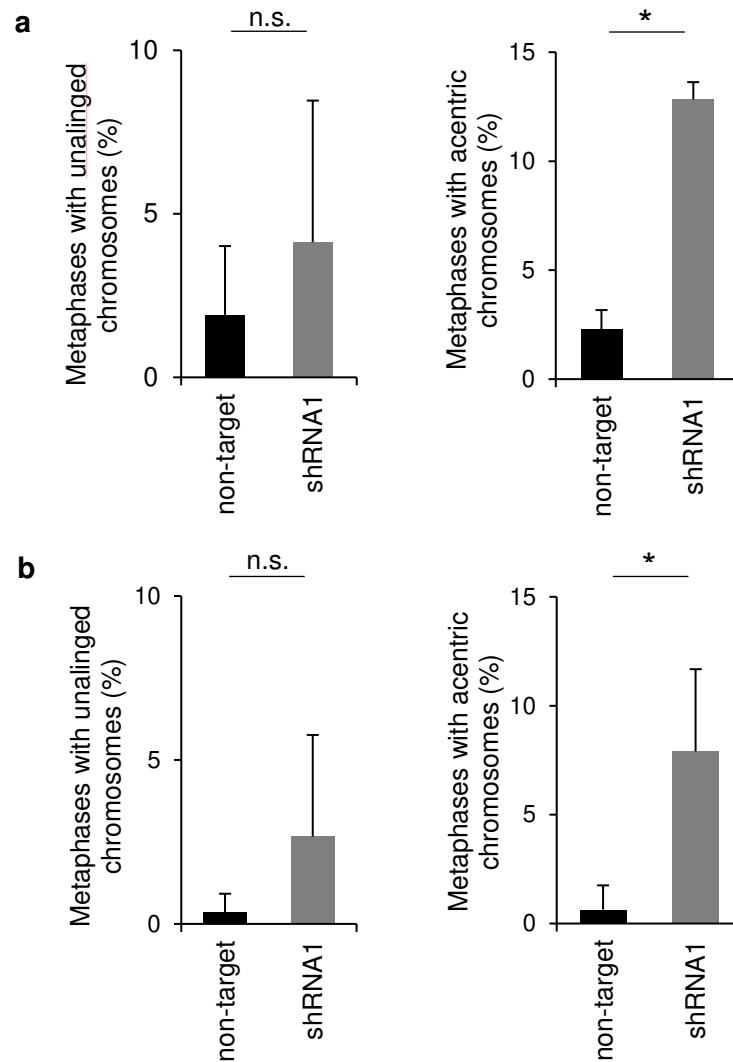


Figure 9: Analysis of metaphase defects in RAI2-depleted cells. Frequency of unaligned and acentric chromosomes were analysed in KPL-1 (a) and MCF-7 cells (b) cells undergoing metaphase. Indicated values are the mean of four replicates. For p-values (student's *t*-test) a cut-off of 0.05 was applied.

4.1.4.2 ANALYSIS OF DEFECTS IN ANAPHASE

In anaphase, RAI2 depletion does not affect frequency of unaligned chromosomes and also the incidence of anaphase bridges was not different to control cells in both cell lines. Here, also frequency of acentric chromosomes is elevated after RAI2 depletion in both cell lines ($p < 0.05$, Figure 10a and b).

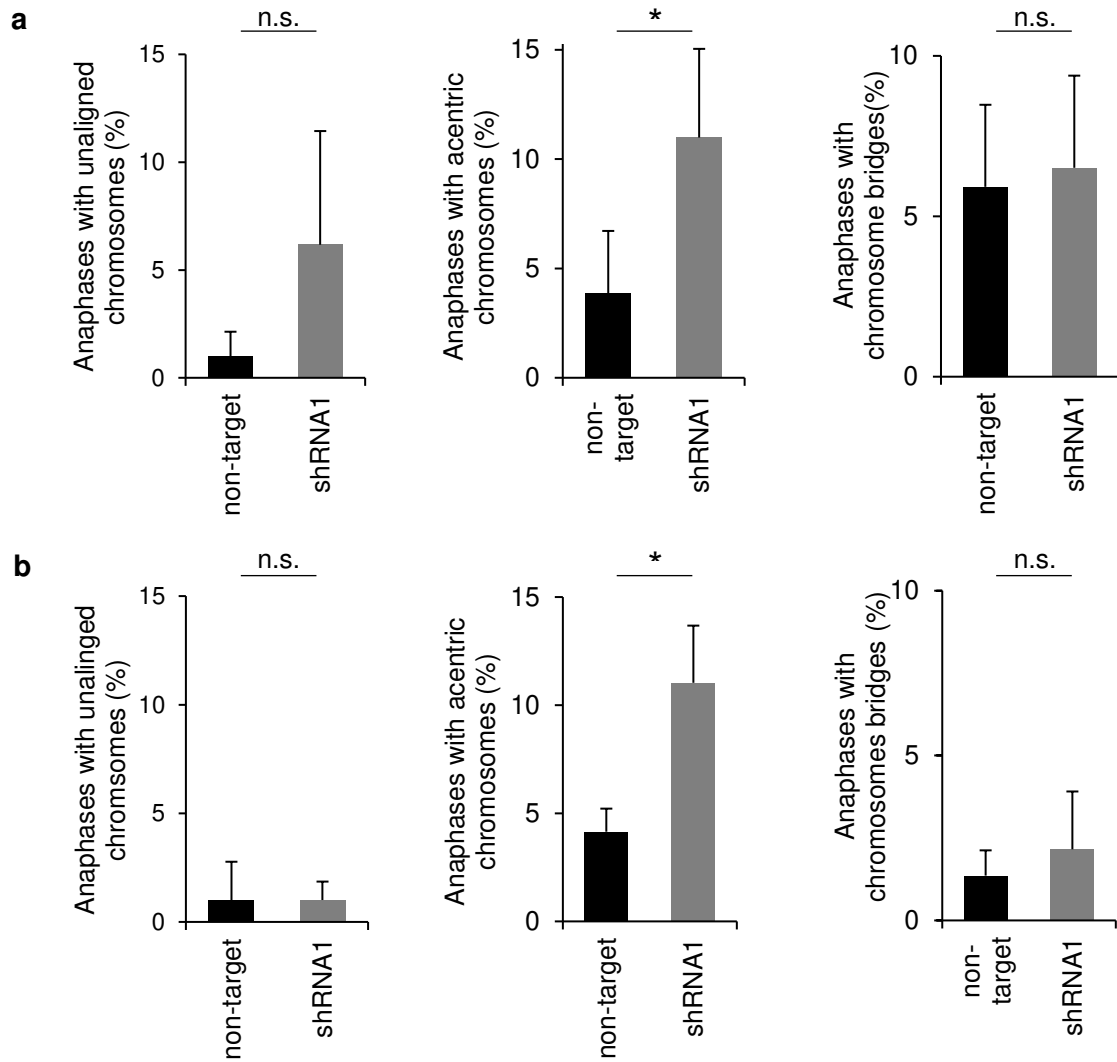


Figure 10: Analysis of anaphase defects in RAI2-depleted cells. Frequency of unaligned and acentric chromosomes as well as anaphase bridges were analysed in KPL-1 (a) and MCF-7 (b) cells undergoing anaphase. Indicated values are the mean of four replicates. For p-values (student's *t*-test) a cut-off of 0.05 was applied.

Acentric chromosomes arise from defects occurring before mitosis as a result of unrepaired or misrepaired DSBs (Fenech, 2007; Mateuca et al., 2006; Savage, 1988). Here, RAI2 depletion leads to increased frequency of acentric chromosomes in meta- as well as anaphase, thus loss of RAI2 might result in premitotic defects that may arise from unrepaired DSBs.

4.2 CAUSES OF PREMITOTIC DEFECTS IN RAI2-DEPLETED CELLS

As described above, the main cause of acentric chromosomes during mitosis are mis- or unrepaired DSBs (Fenech, 2007; Ichijima et al., 2010; Mateuca et al., 2006; Savage, 1988). In this chapter, the influence of RAI2 on DSB formation and events that can cause them are examined. Incorrect replication or defects in DNA damage response are considered as the main reason for the occurrence of DSBs. A continuous repair of DSBs is important to avoid chromosomal instability (CIN), otherwise damaged DNA results in chromosomal aberration and mutated genes that could cause malfunction of genes or cell death (van Gent et al., 2001).

4.2.1 ANALYSIS OF DNA DOUBLE-STRAND BREAKS AFTER RAI2 DEPLETION

The main mechanism in cells to mark DSBs for subsequent repair is the phosphorylation of Histone H2AX on Ser139 (γ H2AX), referred to as formation of γ H2AX foci (Rogakou et al., 1999). This phosphorylation status can be used to analyse DSBs in fixed cells that are stained with antibody against γ H2AX. Foci formation was investigated in KPL-1 cells 7 days after RAI2 depletion. Interestingly, an association of γ H2AX signal with micronuclei was detected in RAI2-depleted cells, which supports the general assumption that broken chromosomes are transferred into micronuclei after mitosis (Figure 7 and Figure 11a left). Moreover, the number of cells with small γ H2AX foci (Figure 11a, right image) was significantly increased after RAI2 depletion ($p=0.004$, Figure 11a). Measuring total intensity of γ H2AX signal in the whole cell population showed an elevated signal intensity in RAI2-depleted KPL-1 cells compared to control cells. In conclusion, this indicates an overall increase of DNA DSBs in RAI2-depleted KPL-1 cells. ($p=0.025$, Figure 11b).

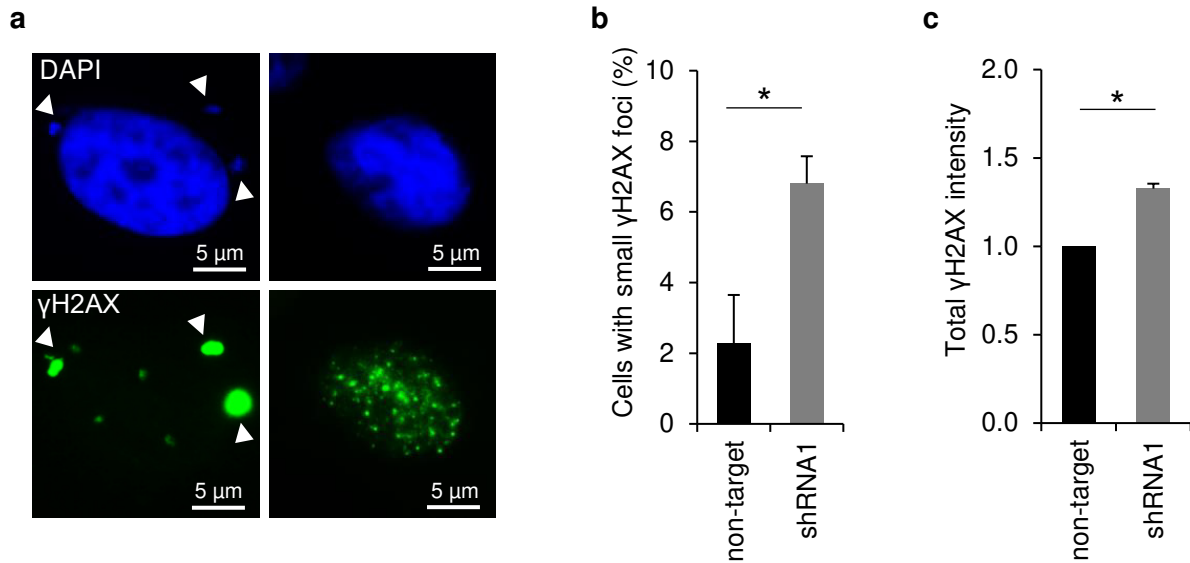


Figure 11: DNA damage analysis measuring γ H2AX foci in RAI2-depleted KPL-1 cells. **a**, Images showing cells stained for γ H2AX and DAPI. Micronuclei are marked by white arrows. **b**, Cells were stained for γ H2AX and cells with a high frequency of small foci were counted in three experiments. For p-values (two sided *t*-test) a cut-off of 0.05 was applied. **c**, Total γ H2AX intensity of at least 100 cells per experiment were measured using ImageJ. For p-values (one sample *t*-test) a cut-off of 0.05 was applied.

4.2.2 IMPACT OF RAI2 ON DNA REPLICATION

Before cell division, DNA has to be replicated during S phase of the cell cycle to enable the transfer of identical genomic DNA to daughter cells. When replication is perturbed due to stalled or collapsed replication forks, cells can activate checkpoint mechanisms to regulate DNA replication machinery. This avoids the accumulation of DNA lesions and DSB induced by replication stress and, consequently, reduces the formation of CIN (Branzei and Foiani, 2010; Burrell et al., 2013a; Ichijima et al., 2010; van Gent et al., 2001). Therefore, *in vitro* analysis of replication provides insights into possible reasons of DSB formation observed in RAI2-depleted cells.

4.2.2.1 DNA FIBER ASSAY

A standard method to analyse DNA replication in cell culture is the DNA fiber assay (Figure 12). This assay is based on incorporation of nucleotide analogues during replication, which are supplied in the cell medium. These analogues can be visualised on chromatin level using antibody-based fluorescence staining. Figure 12 shows the workflow of the DNA fiber assay. As a first step, exponentially growing cells are incubated with medium containing CldU (5-Chloro-20-deoxyuridine) and subsequently with another containing IdU (5-Iodo-20-deoxyuridine). Both

RESULTS

nucleotide analogues are incorporated into newly synthesised DNA instead of thymidine and can be visualised after chromatin fibers are spread onto slides and stained with fluorescence antibodies against the CldU and IdU (Figure 12). This approach provides information about replication speed by analysing the fiber length, and about restart capacity of the replication forks when stalling the replication forks using treatment with hydroxyurea (HU) (Nieminuszczy et al., 2016).

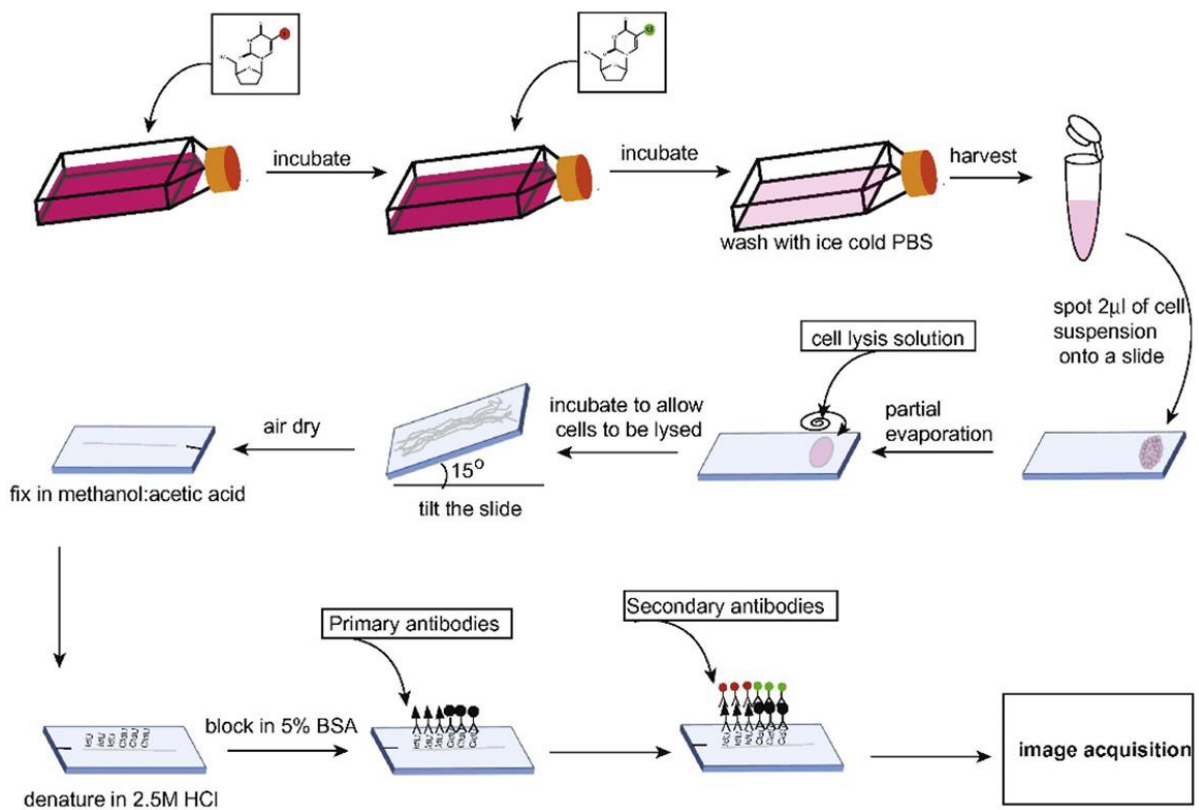


Figure 12: Schematic representation of the DNA Fiber Assay. DNA of exponentially growing cells was labelled with media containing CldU and IdU each for 20 min. Cells were washed with ice cold PBS and harvested. A drop of 2 µl was spotted on a slide and dried partial. Lysis buffer was added and slides were tilt slightly so that the drops could slowly run down the slide and chromatin fibers could be built. Fibers were dried, fixed and denatured. Incorporated IdU was stained with anti-mouse-BrdU and secondary fluorescence antibody Alexa 555 (red) and CldU was stained with anti-rabbit-BrdU and secondary fluorescence antibody Alexa 488 (green). Images of chromatin fibers were taken with fluorescence microscope using 63x magnification, length of fibers was measured and replication fork speed calculated. Adapted and taken from (Nieminuszczy et al., 2016).

4.2.2.2 ANALYSIS OF DNA REPLICATION IN LUMINAL BREAST CANCER CELL LINES

In order to assess whether the accumulation of DSBs seen in RAI2-depleted cells is caused by defects in replication, KPL-1 and MCF-7 cells were analysed using the DNA fiber assay. Exposition to nucleotide analogues was started seven days after RAI2 depletion induced by shRNA1. Fluorescence images in Figure 13 (upper part) show DNA fibers of KPL-1 and MCF-7 cells. Incorporated CldU was marked with red fluorescence antibody and IdU was visualised using green fluorescence antibody. Replication fork speeds were measured by converting the micrometer values of CldU and IdU length into kilobases (kb) and integrating the treatment time of 20 min to calculate the speed in kb/min. Both speeds (CldU and IdU incorporation) were summed up and replication speed of RAI2-depleted cells was compared to non-target control. No significant difference was observed in replication fork speed in both cell lines after RAI2 depletion (Figure 13a and b).

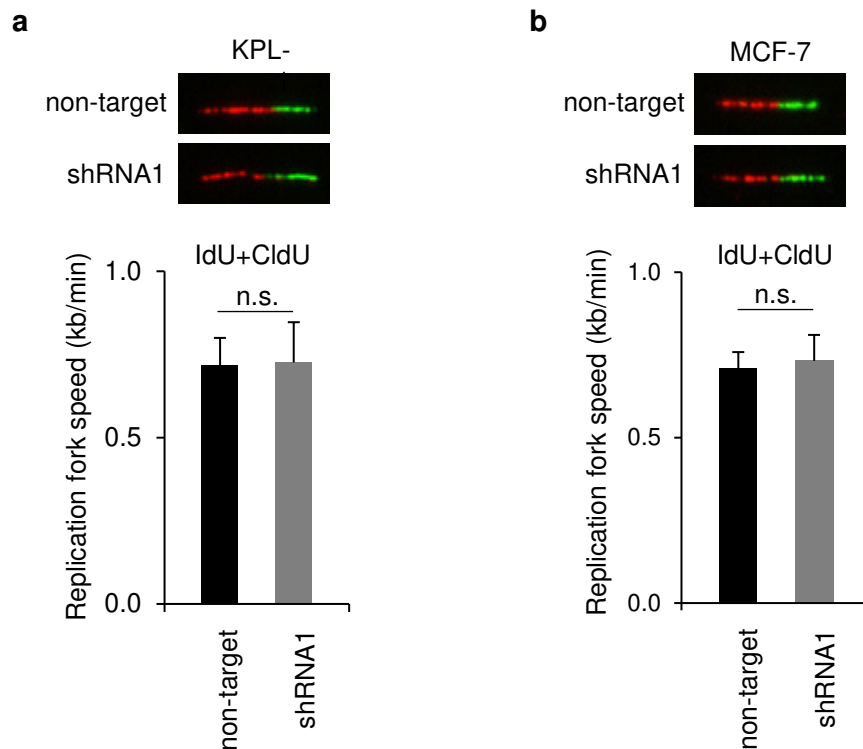


Figure 13: Replication fork speed was measured using DNA fiber assay. Images are showing exemplary DNA fibers of non-target and RAI2-depleted KPL-1 (a) and MCF-7 cells (b) that have incorporated CldU (red) and IdU (green) during replication. A minimum of 100 individual fibers were measured for each experiment and replication fork speed was calculated in kb/min. For p-values (student's *t*-test) a cut-off of 0.05 was applied.

4.2.2.3 ANALYSIS OF DNA REPLICATION IN CELLS WITH STALLED REPLICATION FORK

In order to test whether restart for replication forks is different in RAI2-depleted KPL-1 cells after stalling the replication forks, cells were treated with HU. HU is known to arrest the DNA synthesis by blocking the synthesis of deoxynucleotides (dNTPs) leading to stalled replication forks (Koc et al., 2004). In normal cells, replication forks are prone to stall when they pass unrepaired DNA damage, DNA-bound proteins or secondary structures and need to restart (Petermann and Helleday, 2010). Failure in replication restart can result in replication fork collapse and consequently in DSBs (Di Micco et al., 2006; Hanahan and Weinberg, 2011; Petermann et al., 2010). As RAI2 depletion leads to elevated DSBs, the capacity replication restart was analysed as possible reason for the increased DNA damage. Cells were treated with HU for 4h in between the incubation with medium containing CldU and medium containing IdU. Under these conditions, control and RAI2-depleted cells showed the same replication fork speed demonstrating that restart of the DNA replication after stalling was not affected through RAI2 depletion (Figure 14). Thus, RAI2 depletion has no influence on the replication process and elevated DNA damage does not result from defects in replication.

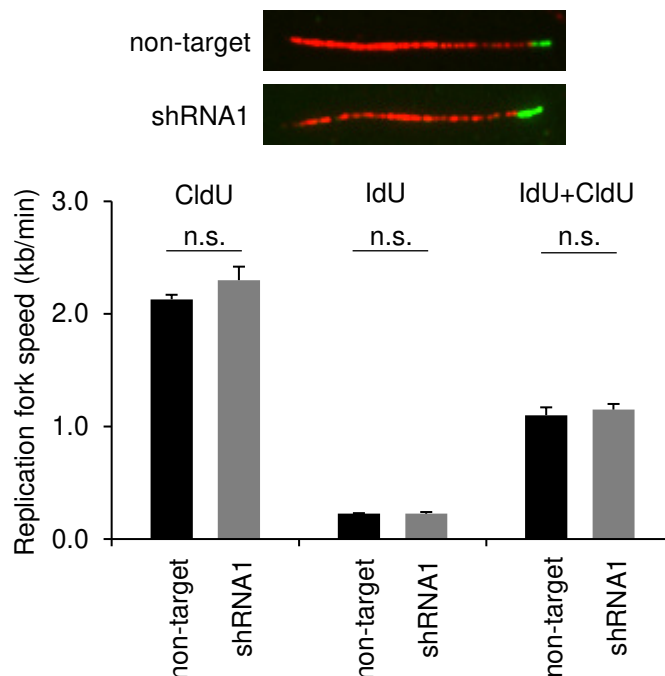


Figure 14: Analysis of replication restart in KPL-1 cells treated with hydroxyurea using DNA fiber assay. Images show DNA fibers of non-target and RAI2-depleted KPL-1 cells. Cells were incubated with medium containing IdU (red) for 20 min, afterwards treated with hydroxyurea for 4h to block the replication and finally incubated with medium containing CldU (green) for 20 min. A minimum of 100 individual fibers were measured for each experiment and replication fork speed was calculated in kb/min. For p-values (student's *t*-test) a cut-off of 0.05 was applied.

4.2.3 IMPACT OF RAI2 ON DNA DAMAGE RESPONSE

The repair of DNA damage is crucial to maintain chromosomal stability in the cell and to avoid formation of cancer (van Gent et al., 2001). To repair DNA damage like base modifications, DSBs and single-strand breaks, coordinated mechanisms are needed. As a first step in DSB repair, breaks are marked by γ H2AX foci (Rogakou et al., 1999). Foci give signals for downstream effector kinases, such as ataxia telangiectasia mutated (ATM) and ATM and Rad3-related (ATR) kinases, which regulate checkpoint proteins and trigger the DSB repair (Canman et al., 1998; Falck et al., 2001). The two main pathways to repair DSBs are the non-homologous end-joining (NHEJ) and the homologous recombination (HR) pathways. HR dominates the repair during S and G₂ phase, because a homologous sister chromatid, which is available due to replication of the DNA during S phase, is necessary for repair. NHEJ can occur throughout the cell cycle independently of a homologous sequence. During this faster but error-prone mechanism, blunt DNA ends are ligated to connect the DNA again (Ceccaldi et al., 2016). As depletion of RAI2 leads to an accumulation of DSBs, the function of DSB repair pathways was further investigated by analysing the two main DSB repair pathways NHEJ and HR in RAI2-depleted cells.

4.2.3.1 TRAFFIC LIGHT REPORTER ASSAY

What can be employed to investigate HR and NHEJ capacity in cell culture is the so-called Traffic Light Reporter (TLR) assay and it was established by Certo et al (Certo et al., 2011). This assay is plasmid-based and analyses the capacity of single cells to repair a DSB that is induced by a site-specific endonuclease. The TLR plasmid includes both a GFP- as well as a mCherry-disrupted cDNA, the former has a restriction site for the rare-cutting nuclease SceI. As a first step, the TLR plasmid is digested by SceI and transfected into cells together with another plasmid containing a homologous donor template for GFP gene. The present DSB can subsequently be repaired by NHEJ or by HR. In case the DSB is repaired by mutagenic NHEJ, the T2A sequence is shifted in frame and the cells show mCherry positivity. Performing HR, cells use the donor template as homologous sequence for the repair and appear green. The fluorescence signal of transfected cells is subsequently analysed by flow cytometry. To make sure that the transfection was successful, the TLR plasmid contains a BFP sequence under control of an EF-1 α promoter. The detailed workflow of the assay is described in Figure 15. In summary, the TLR assay allows the

measurement and quantification of NHEJ and HR repair capacity at single cell level (Certo et al., 2011).

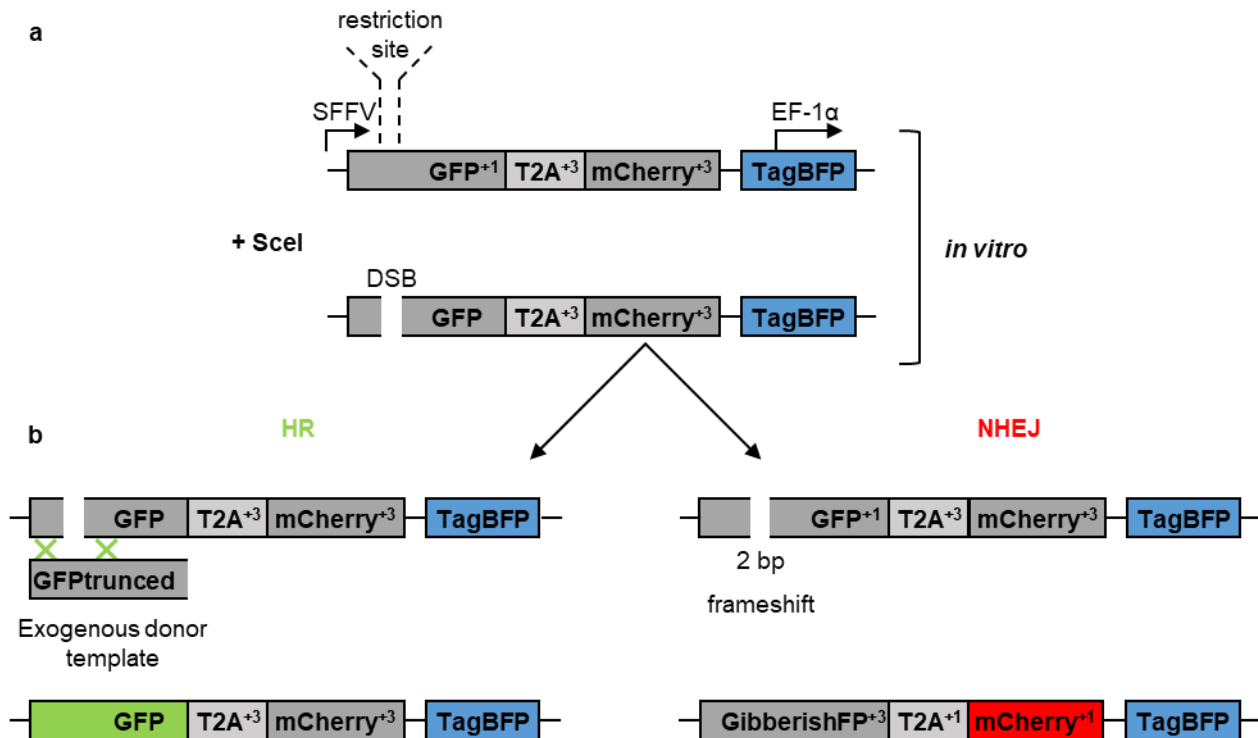


Figure 15: Schematic representation showing the principle behind the Traffic Light Reporter (TLR) system used to analyse DNA damage pathways. **a**, Reporter plasmid pCVL TLR BFP contains a BFP tag under control of a Ef-1 α promoter and a coding sequences for GFP, T2A and mCherry. A restriction site for the enzyme SclI is part of the GFP+1 sequence. First step in the workflow is the digestion of the reporter plasmid with SclI *in vitro* to induce a DNA DSB. **b**, As a second step, the same amount of digested reporter plasmid is transfected in non-target control and RAI2-depleted or in RAI2-overexpressing HEK293T cells using Lipofectamine2000 as transfection reagent. Additionally, a plasmid containing a truncated version of the GFP gene is transfected as an exogenous donor template for HR of GFP sequence. Cells can either repair the reporter plasmid by HR restoring a functional GFP open reading frame using the donor template. As a second option cells can also repair the DSB by mutagenic NHEJ. Here, a frameshift of 2 bp is generated during the repair process and the mCherry coding sequence will be in frame. The T2A linker enables mCherry to escape degradation of GibberishFP. Transfection for reporter plasmid is verified analysing BFP positivity of the cells. Fluorescence signal of the cells is measured by flow cytometry. Adapted and taken from (Certo et al., 2011).

4.2.3.2 ANALYSIS OF DNA DAMAGE PATHWAYS IN RAI2-DEPLETED HEK293T CELLS

As KPL-1 cells are challenging to transfect, the embryonic kidney cell line HEK293T were instead used to analyse potential effects of RAI2 on the two main DSB repair pathways HR and NHEJ. Using flow cytometry, the transfected cells were analysed and sorted due to their granularity to exclude cell duplets from analysis. BFP-positive cells were plotted against mCherry- and eGFP-fluorescence intensity. mCherry-positive cells indicated a repair event triggered by mutNHEJ and eGFP-positive cells represented cells with an HR repair event. Percentage of mCherry-positive

cells and eGFP-positive cells was calculated in RAI2-depleted samples and normalised to non-target control to determine the NHEJ or HR capacity. Analysis showed that RAI2 depletion results in a significantly reduced NHEJ capacity (Figure 16a), meaning that loss of RAI2 leads to impairments by repairing the DSB by NHEJ compared to non-target control. The HR pathway seemed unaffected by RAI2 depletion as the cells showed no significant difference in HR capacity (Figure 16b).

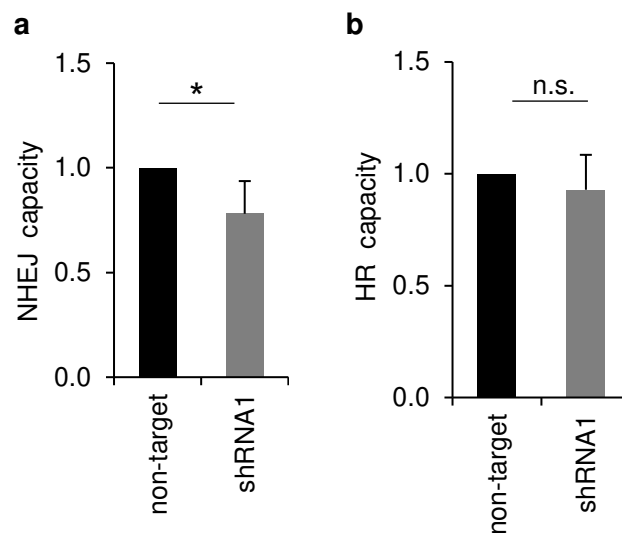


Figure 16: Analysis of the DNA damage pathways NHEJ and HR in RAI2-depleted HEK293T cells using the TLR assay. Non-target control and RAI2-depleted HEK293T cells were transfected with linearised pCVL TLR BFP and GFP donor plasmid. The percentage of mCherry-positive and GFP-positive cells was measured as an indication for HR and NHEJ events were assessed 48h post-transfection and the cells were analysed by flow cytometry. NHEJ (a) and HR capacity (b) was normalised to non-target control. For p-values (one sample *t*-test) a cut-off of 0.05 was applied.

4.2.3.3 ANALYSIS OF DNA DAMAGE PATHWAYS IN HEK293T CELLS OVEREXPRESSING RAI2

Next, it was analysed whether overexpression of RAI2 in HEK293T cells leads to differences in DNA damage response using the TLR Assay. In this case, parental cells were transfected additionally with a CMV plasmid containing a sequence to transient overexpress RAI2 or vector control. Analysis demonstrated that RAI2 overexpression leads to significantly higher HR capacity, whereas no significant changes in NHEJ capacity were observed in this setting (Figure 17a and b). In summary, RAI2 depletion leads to elevated DNA damage marked by increased γ H2AX signal and RAI2 modulates DNA repair capacity in general.

RESULTS

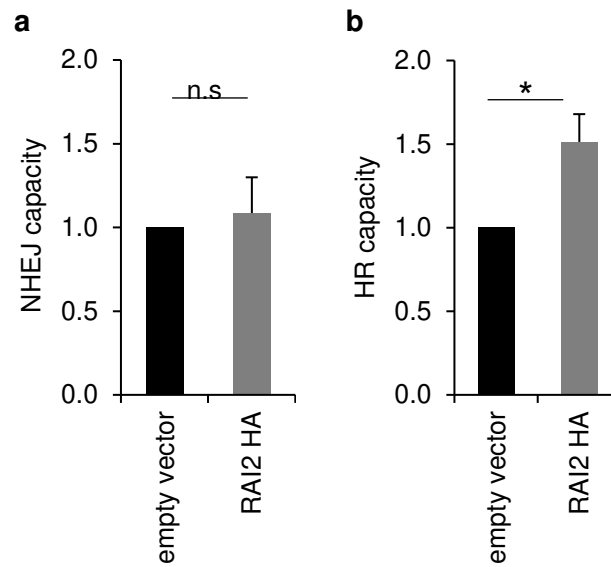


Figure 17: Analysis of the DNA damage pathways NHEJ and HR in RAI2-overexpressing HEK293T cells using the TLR assay. Empty vector and RAI2HA HEK293T cells were transfected with linearised pCVL TLR BFP and GFP donor plasmid. The percentage of mCherry-positive and GFP-positive cells was measured as an indication for HR and NHEJ events 48h post-transfection and cells were analysed by flow cytometry. NHEJ (a) and HR capacity (b) was normalised to empty vector control. For p-values (one sample *t*-test) a cut-off of 0.05 was applied.

4.3 ANALYSIS OF RAI2 EXPRESSION IN CELL CYCLE PHASES

Genes and proteins involved in cell cycle checkpoint regulation are tightly regulated during cell cycle and differentially expressed depending on their functional role (Gookin et al., 2017; Mjelle et al., 2015; Shaltiel et al., 2015). A host of different cell cycle checkpoints maintain normal cell function including the DNA damage checkpoint, the DNA replication checkpoint and the spindle assembly checkpoint (Elledge, 1996). As RAI2 is involved in DNA damage response, cell cycle-dependent expression of RAI2 was analysed.

4.3.1 ANALYSIS OF RAI2 EXPRESSION IN SYNCHRONISED BREAST CANCER CELLS

In order to test whether RAI2 expression is associated with a specific cell cycle phase parental MCF-7 cells were synchronised using a double thymidine block. Thymidine arrests cells at the G₁/S transition checkpoint of the cell cycle by inhibiting DNA synthesis (Schvartzman et al., 1984). Cells were seeded one day before treatment and exposed two times to thymidine overnight to optimise the number of cells that get arrested at the G₁/S boundary. In order to check the cell cycle distribution cells were fixed and DNA was stained with propidium iodide followed by flow cytometry analysis. Two-six hours after release from the second thymidine block, cells replicated their DNA and underwent S phase shown in the flow cytometry plots (Figure 18, below). After 8h cells reached G₂ phase followed by mitosis, which is shown in the FACS plots at time 10h and 12h after the blocking. At the end of measurement (time point 14h) cells reached G₁ phase (Figure 18, below).

Simultaneously, gene expression of *RAI2*, *CCNE2* and *CCND1* was measured in the synchronised MCF-7 cells using qRT-PCR, whereby the two latter genes were used as control for cell cycle distribution. *CCNE2* is the gene encoding for the protein Cyclin E2, which is a regulator of the cell cycle and normally expressed during G₁/S transition (Gookin et al., 2017). This gene had a peak in expression directly after releasing the cells from thymidine block, which confirmed that the cells were arrested in G₁/S phase before release (Figure 18). Additionally, the expression of *CCND1*, another cell cycle regulator encoding for the protein Cyclin D1, was expressed as expected during G₂/M transition (Figure 18) (Gookin et al., 2017). The expression pattern of *CCNE2* and *CCNB1* mirrored the cell cycle distribution analysed by flow cytometry. Analysis of *RAI2* gene expression in the synchronised MCF-7 cells revealed an induction of *RAI2* in S phase

RESULTS

followed by an increase of expression during S phase and a peak of expression in S/G₂ phase compared to unsynchronised cells (Figure 18).

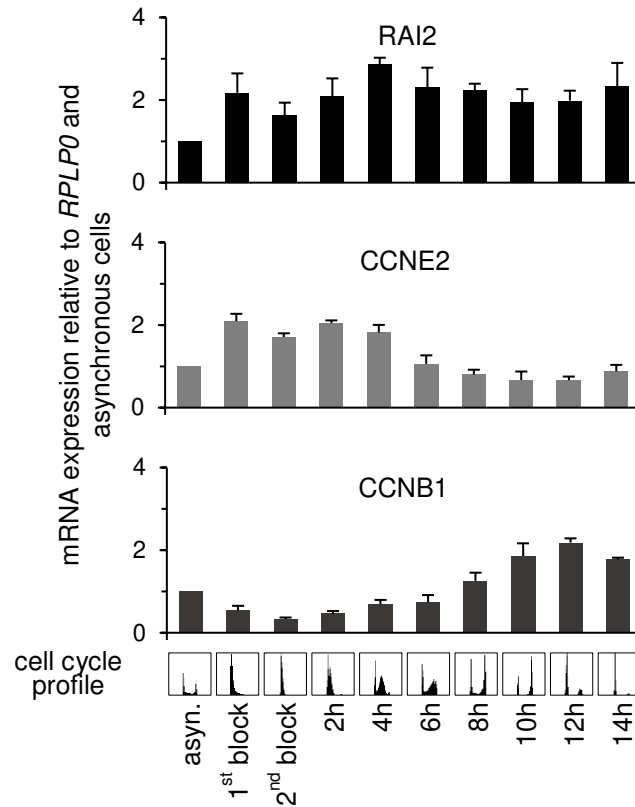


Figure 18: Analysis of *RAI2* gene expression in synchronised MCF-7 cells. Quantitative gene expression analysis was performed with synchronised parental MCF-7 cells to test cell cycle dependent expression of *RAI2* and the cell cycle specific markers *CCNE2* and *CCNB1* using qRT-PCR. Double thymidine block was used to block the cells in the S phase. Blocking time points and time points after release from thymidine (in h) as well as the cell cycle profiles belonging to each time point are shown. Gene expression is shown as average fold change normalised to *RPLP0* and unsynchronised cells. Indicated values are the mean of three replicates.

In order to test whether the protein expression pattern is same or different to *RAI2* gene expression pattern, total protein was isolated from MCF-7 cells blocked with thymidine and analysed by Western blot. Again, Cyclin E2 and Cyclin D1 were highly expressed in G₁/S phase and G₂/M phase, respectively (Figure 19). Moreover, total *RAI2* protein amount was higher in synchronised cells compared to asynchronous cells and showed the strongest expression during S/G₂ phase. Beyond that, *RAI2* protein expression correlated with the expression of γ H2AX, confirming that *RAI2* expression is associated with DNA damage (Figure 19). In conclusion, the

results revealed that RAI2 is prominently expressed in the S/G₂ phase indicating a possible functional role of RAI2 in the S/G₂ phase.

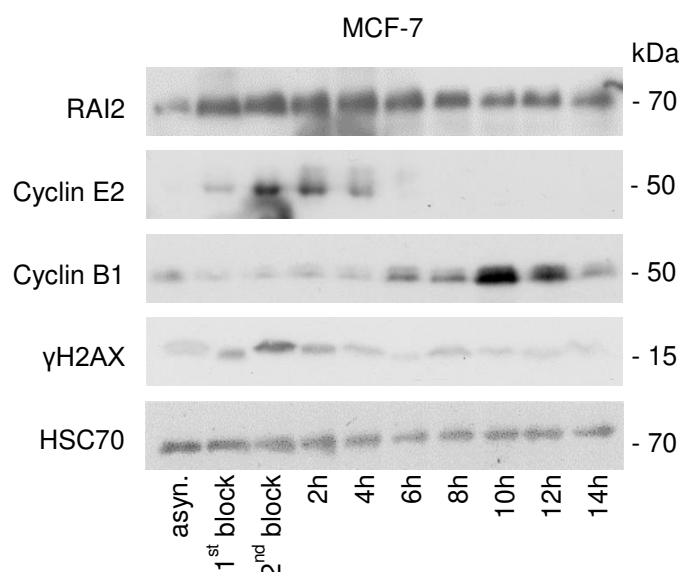


Figure 19: Analysis of RAI2 protein expression in synchronised MCF-7 cells. Western Blot analysis of RAI2, Cyclin E2, Cyclin B1 and DNA damage marker γ H2AX was performed with unsynchronised, blocked and synchronised MCF-7 cells. Double thymidine block was used to block the cells in the S-phase. HSC70 was used as loading control.

4.3.2 ANALYSIS OF RAI2 IN CELLS TREATED WITH CHEMOTHERAPEUTICS

In order to test whether RAI2 expression is affected by treatment with chemotherapeutic reagents that lead to cell cycle arrest in S/G₂ phase, KPL-1 and MCF-7 cells were treated with different cell cycle arresting reagents. RAI2 gene expression was analysed after treatment with etoposide, RO-3306 and paclitaxel using qRT-PCR. Etoposide inhibits the religation of the so-called topoisomerase II (TOPII) cleavage complexes, which normally reduces DNA tension. This results in a high level of enzyme-mediated breaks of the DNA and leads to an arrest of the cells in S phase (Fortune and Osheroff, 2000; Pommier et al., 2010). RO-3306 is a CDK1 inhibitor and arrests cells at the G₂/M border (Vassilev et al., 2006), whereas paclitaxel pauses the cell cycle in metaphase (Weaver, 2014). Treatment success was analysed by determining the cell cycle profile using flow cytometry and revealed an arrest of the cells in the predicted cell cycle phase in both cell lines (Figure 20, below). Analysis of qRT-PCR data showed that all treatments resulted in a significant upregulation of RAI2 gene expression at least more than 2.5 times ($p < 0.05$, Figure 20). For KPL-1 cells, RO-3306 and paclitaxel treatment led to the highest induction of RAI2 and for MCF-7 cells

the highest expression was observed after RO-3306 treatment. This shows that *RAI2* is mainly induced in cells that are arrested at the S/G₂ and the G₂/M border.

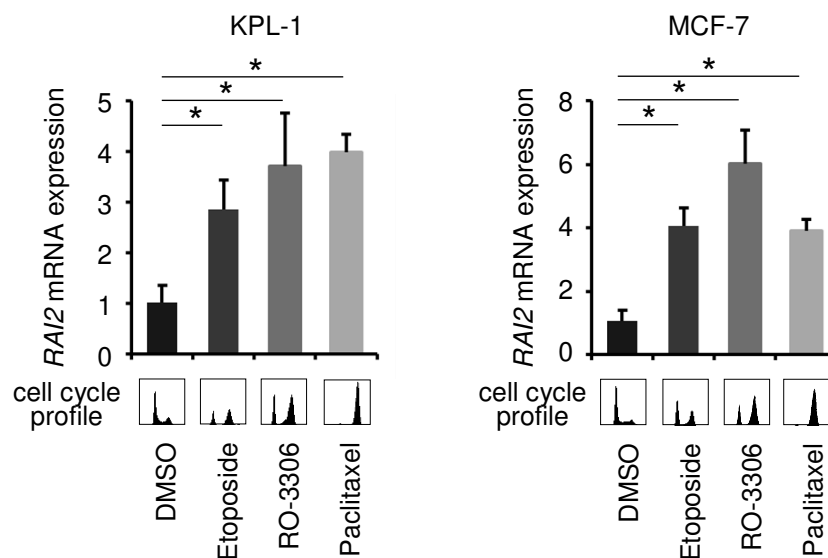


Figure 20: Analysis of *RAI2* gene expression in treated KPL-1 and MCF-7 cells. Parental cells were treated with 10 μ M etoposide, 10 μ M RO-3306 and 100 nM paclitaxel and quantitative gene expression analysis was performed using qRT-PCR. Cell cycle profiles analysed by flow cytometry are shown. Expression is shown as average fold change normalised to *RPLP0*. Error bars represent the standard deviation of the mean of three independent experiments. For p-values (Student's *t*-test) a cut-off of 0.05 was applied.

In order to test whether the induction of *RAI2* gene expression is also present on the protein level Western blot analysis was performed on KPL-1 and MCF-7 cells treated with the earlier used chemotherapeutic reagents (Figure 21). In KPL-1 cells, *RAI2* protein was highly elevated in all samples treated with genotoxic reagents compared to untreated samples. MCF-7 cells showed a strong, increased *RAI2* protein level only after etoposide treatment as well as a slight induction in the paclitaxel-treated sample. The increased *RAI2* protein expression after genotoxic treatment correlated with an increase of DNA damage as indicated by increased γ H2AX signal.

RESULTS

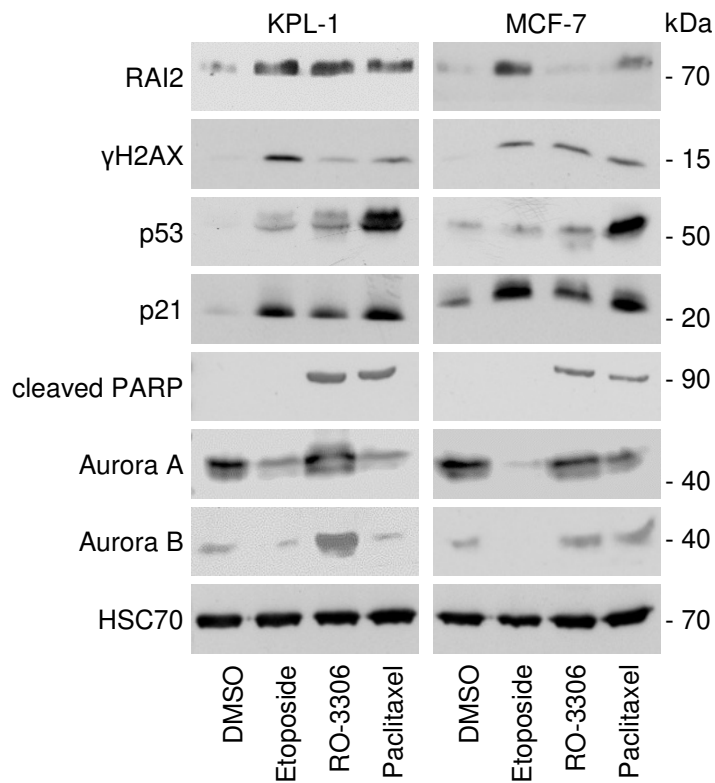


Figure 21: Analysis of protein expression in treated KPL-1 and MCF-7 cells. Cells were treated with 10 μ M Etoposide, 10 μ M RO-3306 and 100 nM Paclitaxel and Western blot analysis was performed. Protein expression of RAI2, γ H2AX, p53, p21, cleaved PARP and Aurora A and B were analysed. HSC70 serves as control.

Furthermore, a positive correlation was found with the protein expression of p53 and p21. Except for etoposide treatment, also a simultaneous increase of cleaved PARP, Aurora A and Aurora B protein expression was observed, which was indicative of induction of apoptosis and of G₂ arrest in the treated cells. In summary, RAI2 expression is induced during S/G₂ phase as well as in G₂-arrested cells and elevated after induction of DNA damage, which provides additional evidence for a functional role of RAI2 in response to DNA damage.

4.4 CLONOGENIC CAPACITY

In order to form a metastasis, tumour cells have to migrate to distant organs, arrest there and start to proliferate (Fidler, 2003). An *in vitro* assay to investigate the ability of single cells to proliferate and undergo unlimited cell division is the analysis of colony formation capacity. For this, low cell numbers are seeded to 6-well plates and capacity of clones to proliferate is measured after 12 days. The number of colonies or covered area with cells can be quantified and analysed. Measuring clonogenic capacity of cells treated with cytotoxic anti-cancer drugs provides information about the response of cells to treatment (Brown and Attardi, 2005; Puck and Marcus, 1956).

4.4.1 CLONOGENIC CAPACITY IN RAI2-DEPLETED KPL-1 AND MCF-7 CELL LINE

In order to determine possible differences in clonogenic capacity due to RAI2-depletion, KPL-1 and MCF-7 cells were analysed using the colony formation assay. For this, cells were transduced with shRNA1, grown for 12 days in a 6-well plate, fixed and the area covered with cells was analysed using an ImageJ tool (Guzman et al., 2014). Analysis revealed no difference in clonogenic capacity between non-target control and RAI2-depleted cells in both KPL-1 and MCF-7 cell line (Figures 18a and b).

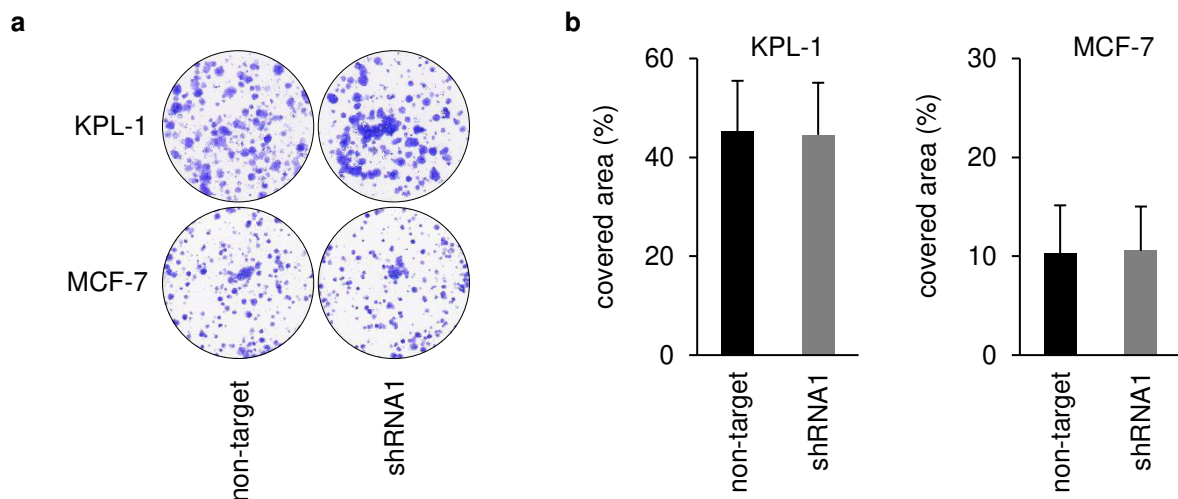


Figure 22: Clonogenic capacity in RAI2-depleted KPL-1 and MCF-7 cells. After induction of RAI2 depletion cells were cultured for 12 days. **a**, Representative images showing colony growth of control and RAI2-depleted KPL-1 and MCF-7 cells. **b**, Covered area was analysed using an Image J tool (Guzman et al., 2014). For p-values (Student's *t*-test) a cut-off of 0.05 was applied.

4.4.2 CLONOGENIC CAPACITY IN CELLS TREATED WITH CYTOTOXIC ANTI-CANCER DRUGS

As no difference in clonogenic capacity was observed between non-target and RAI2-depleted cells under standard condition, next, the colony formation assay was performed with cells treated with different cytotoxic anti-cancer drugs. The used drugs have effects on different cell cycle steps.

4.4.2.1 CLONOGENIC CAPACITY IN ARRESTED CELLS

In order to arrest cells in S phase a wide range of drugs are available that inhibit the enzyme topoisomerases (TOPs). Topoisomerases are regulating the torsional stress of DNA by inducing transient DNA breaks by either inducing single-strand breaks (TOP I) or DSBs (TOP II) (Banerji and Los, 2006). Targeting TOP I with camptothecin leads to a stabilisation of the DNA TOP I complex and this inhibits the religation of the DNA after uncoiling, leading to an arrest of the cells in S phase. As a consequence, cell death is triggered by generating replication-mediated DSB (Pommier, 2006; Pommier et al., 2003). The response to camptothecin was tested in KPL-1 and MCF-7 cells after RAI2-depletion using colony formation assay. As shown in Figure 23, clonogenic capacity after treatment was not different between non-target and RAI2-depleted samples in both cell lines.

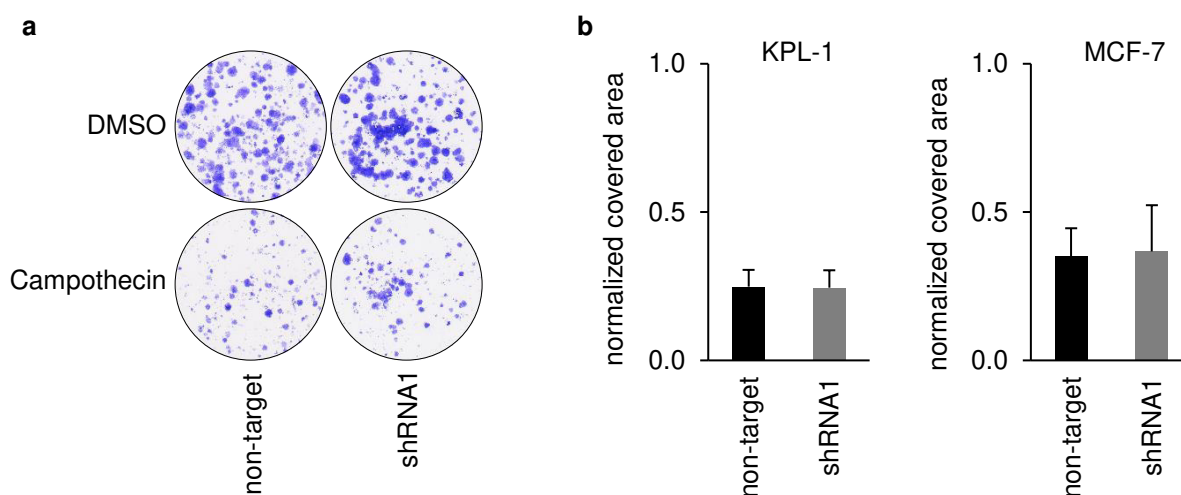


Figure 23: Clonogenic capacity in RAI2-depleted KPL-1 and MCF-7 cells after treatment with camptothecin. After induction of RAI2 depletion, cells were treated with 10 nM camptothecin for 4h and cultured for 12 days. a, Representative images showing colony growth of DMSO control and camptothecin-treated KPL-1 cells. b, Area percentage, which was covered by cells, was quantified using an Image J tool and normalised to DMSO control (Guzman et al., 2014). For p-values (Student's *t*-test) a cut-off of 0.05 was applied.

Cells were also treated with the TOP II inhibitor etoposide, which inhibits the religation of the TOP II cleavage complex from torsional-stressed DNA. Similar to camptothecin, etoposide leads to high levels of DSBs resulting in cell death (Fortune and Osheroff, 2000; Pommier et al., 2010). After treatment with etoposide, no significant difference in clonogenic capacity was observed between control and after RAI2 depletion in both cell lines KPL-1 and MCF-7 (Figure 24).

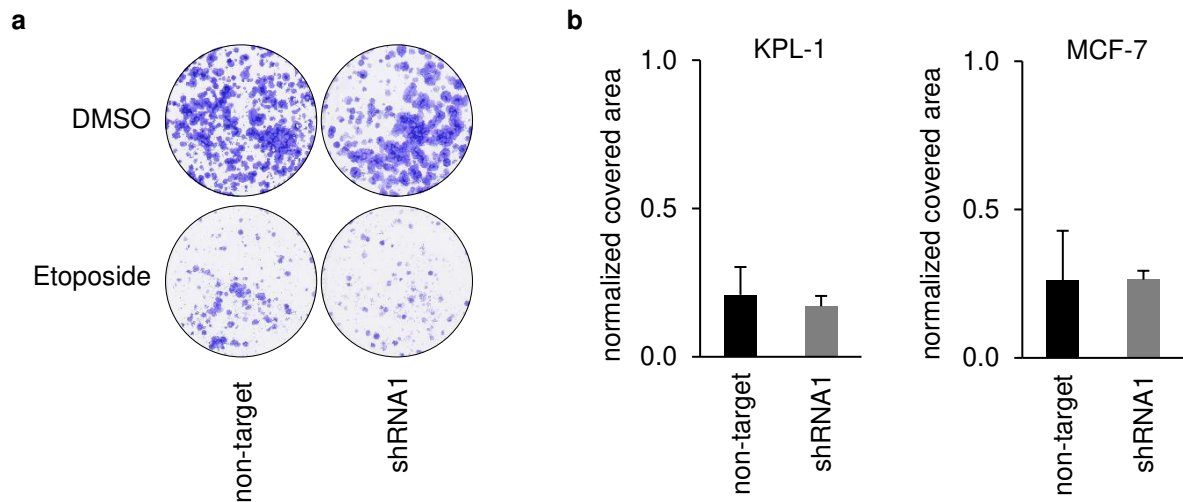


Figure 24: Clonogenic capacity in RAI2-depleted KPL-1 and MCF-7 cells after treatment with etoposide. After induction of RAI2 depletion, cells were treated with 10 μ M etoposide for 4h and cultured for 12 days. **a**, Representative images showing colony growth of DMSO control and etoposide-treated KPL-1 cells. **b**, Area percentage, which was covered by cells, was quantified using an Image J tool and normalised to DMSO control (Guzman et al., 2014). For p-values (Student's *t*-test) a cut-off of 0.05 was applied.

Inhibition of both TOPs using doxorubicin, which additionally intercalate into DNA, negatively affects the functioning of helicases and generates reactive oxygen species (Banerji and Los, 2006; Tacar et al., 2013), had no effect on clonogenic capacity in RAI2-depleted cell lines (Figure 25). Thus, targeting TOPs had no significant effect on clonogenic potential in RAI2-depleted cells compared to non-target control cells.

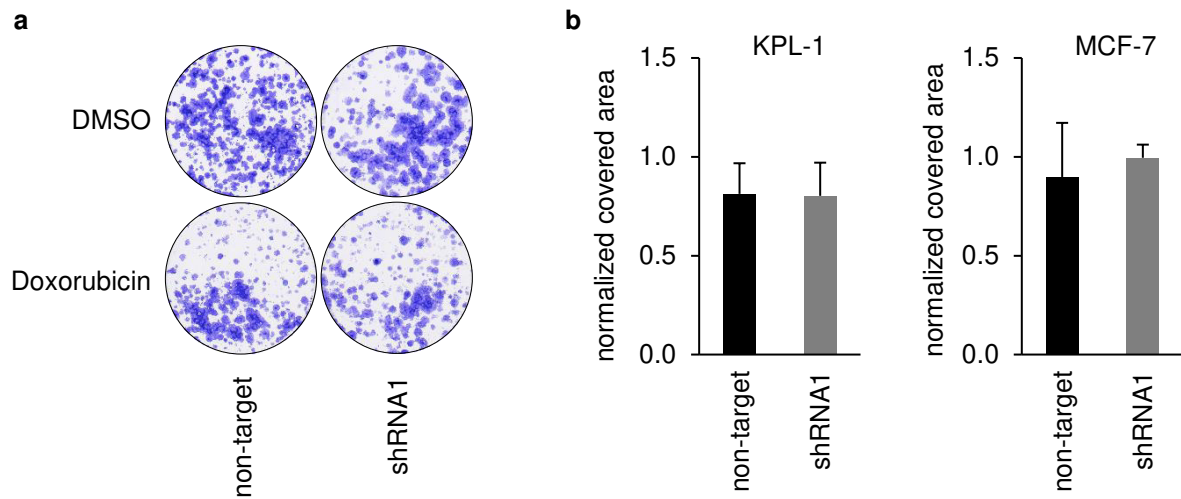


Figure 25: Clonogenic capacity in RAI2-depleted KPL-1 and MCF-7 cells after treatment with doxorubicin. After induction of RAI2 depletion cells were treated with 100 nM doxorubicin for 4h and cultured for 12 days. **a**, Representative images showing colony growth of DMSO control and doxorubicin-treated KPL-1 cells. **b**, Area percentage, which was covered by cells, was quantified using an Image J tool and normalised to DMSO control (Guzman et al., 2014). For p-values (Student's *t*-test) a cut-off of 0.05 was applied.

4.4.2.2 CLONOGENIC CAPACITY UPON OXIDATIVE STRESS

Oxidative stress is an imbalance in cell metabolism, where a high concentration of reactive oxygen species (ROS) is present in the cells that, among others, can lead to an oxidation of DNA bases. The most common product, a fallout of oxidative stress, is 8-oxoguanine, which is mended through base excision repair (David et al., 2007). H_2O_2 belongs to ROS and can be used for cell culture experiments to mimic oxidative stress. In order to analyse clonogenic capacity upon oxidative stress, cells were treated with H_2O_2 and colony formation was measured. RAI2-depleted cells showed no significant difference compared to non-target control when analysing clonogenic capacity (Figure 26).

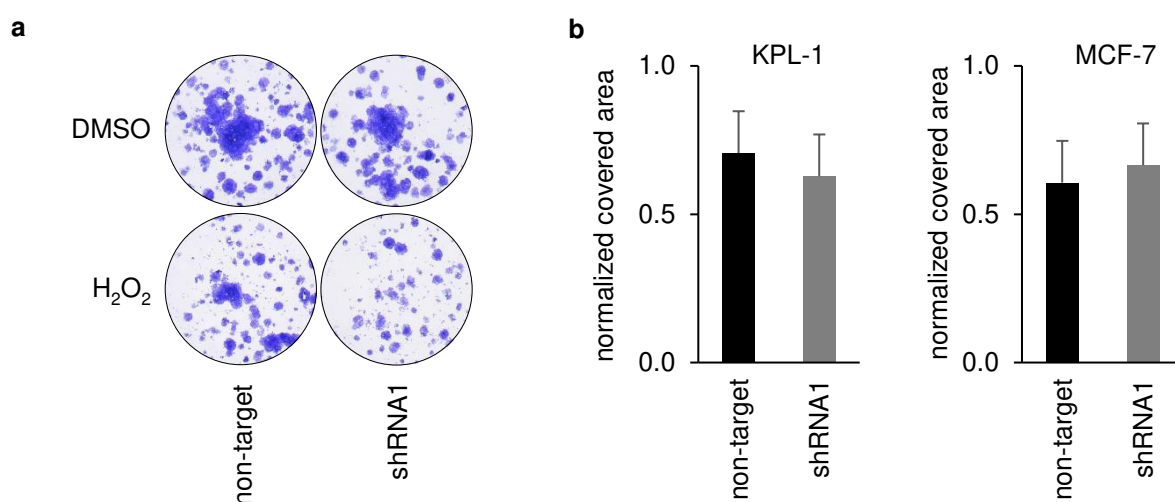


Figure 26: Clonogenic capacity in RAI2-depleted KPL-1 and MCF-7 cells after treatment with H_2O_2 . After induction of RAI2 depletion cells were treated with 30 μ M H_2O_2 for 4h and cultured for 12 days. **a**, Representative images showing colony growth of DMSO control H_2O_2 -treated KPL-1 cells. **b**, Area percentage, which was covered by cells, was quantified using an Image J tool and normalised to DMSO control (Guzman et al., 2014). For p-values (Student's *t*-test) a cut-off of 0.05 was applied.

4.4.2.3 CLONOGENIC CAPACITY UPON PARP INHIBITION

Inhibition of PARP is successful in treating patients with triple negative breast cancer that having germline mutation in *BRCA1* or *2* gene. When PARP is inhibited by olaparib, spontaneous single-strand breaks occur during S phase which leads to an accumulation of DSBs because of a replication fork collapse. Normally, these DSBs are repaired by HR including functional activity of *BRCA 1* and *2*. As *BRCA*-deficient cells show an HR defect irreparable toxic DSBs accumulate upon olaparib treatment and lead to cell death. This effect is called synthetic lethality and is utilised in patients with *BRCA* deficiency as treatment opportunity (Bryant et al., 2005; Sunada et

RESULTS

al., 2018). As RAI2 effects repair capacity, KPL-1 cells were treated with the PARP inhibitor olaparib and changes in clonogenic capacity upon RAI2 depletion was analysed. Again, even after this treatment, RAI2 depletion had no effect on colony formation (Figure 27).

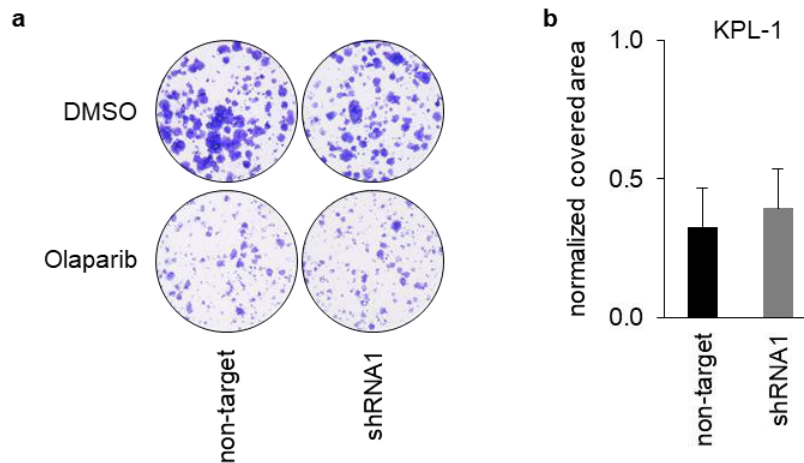


Figure 27: Clonogenic capacity in RAI2-depleted KPL-1 and MCF-7 cells after treatment with olaparib. After induction of RAI2 depletion cells were continuously treated with 100 nM olaparib and cultured for 12 days. **a**, Representative images showing colony growth of DMSO control and olaparib-treated KPL-1 cells. **b**, Area percentage, which was covered by cells, was quantified using an Image J tool and normalised to DMSO control (Guzman et al., 2014). For p-values (Student's *t*-test) a cut-off of 0.05 was applied.

4.5 LOCALISATION OF RAI2 AND CtBP1 IN CELLS OVEREXPRESSING RAI2 OR CtBP-BINDING MUTANT RAI2

In previous studies it was already shown that the RAI2 protein co-localises with CtBP1 and CtBP2 in nuclear speckles in RAI2 overexpressing MCF-7 cell line. Furthermore, it was demonstrated that the binding of RAI2 to CtBP2 depends on the non-consensus bipartite ALDLS binding domain of the RAI2 protein (Werner et al., 2015). As shown above (4.3.2, Figure 20 and Figure 21), RAI2 gene and protein expression is induced after treatment with etoposide and other chemotherapeutics. Therefore, the speckle formation was tested under chemotherapeutic condition by staining RAI2 and CtBP1 with KPL-1 and MCF-7 cells overexpressing RAI2 that were treated with etoposide before. Moreover, it was tested, if the formation of speckles is dependent on the binding to CtBP, analysing also the double-mutant cells of CtBP binding motive of RAI2 (4A mutant). To this purpose, the staining with RAI2 antibody was first established and conditions were optimised.

4.5.1 LOCALISATION AND FORMATION OF RAI2/CtBP1 SPECKLE AFTER TREATMENT WITH ETOPOSIDE

Figure 28a and b illustrate exemplary fluorescence images showing KPL-1 and MCF-7 cells overexpressing RAI2 and the CtBP-binding motive 4A mutant. The cells were treated with etoposide for 48h or with DMSO as control. RAI2 overexpressing cells showed RAI2 and CtBP1 positive staining in the nucleus and the proteins accumulated and formed speckles. These speckles were spread over the nucleus and the number of speckles per cell was ranged between 0 and 20 (Figure 28a and b). CtBP binding mutant cells had almost no speckles, indicating a dependence of RAI2 speckle formation on the binding to CtBP1. When treated with etoposide, the number of speckles increased in RAI2 overexpressing cells (Figure 28a) whereas in RAI2 mutant cells, only a few speckle were detected in treated cells (Figure 28a and b). Thus, treatment with etoposide may induce RAI2/CtBP1 speckle formation in KPL-1 and MCF-7 cells.

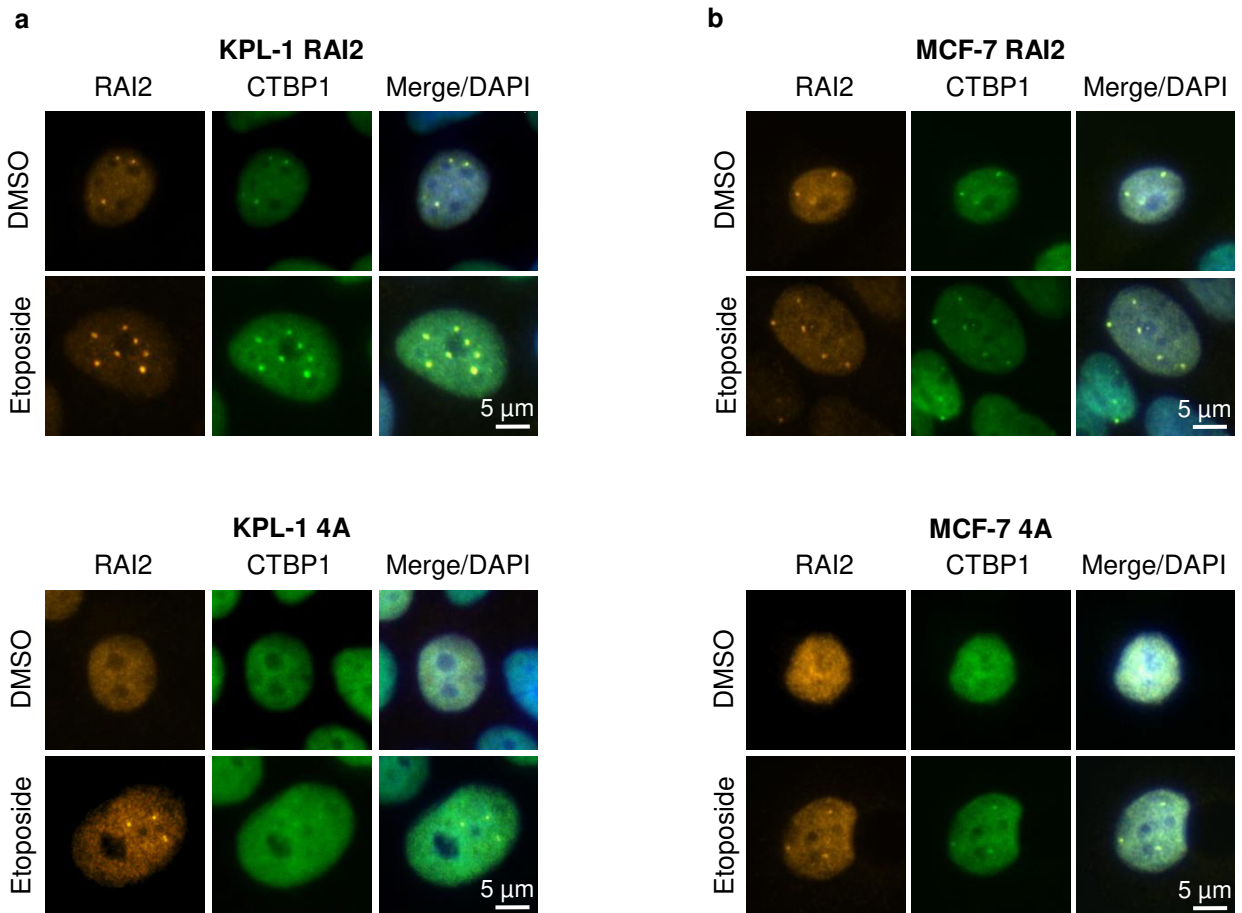


Figure 28: Immunofluorescence images taken from (a) KPL-1 and (b) MCF-7 RAI2 OE cells and 4A treated with etoposide. Cells were stained for RAI2, CtBP1 and DAPI and analysed with a fluorescence microscope at 40x magnification. Before staining, cells were treated with 10 µM etoposide for 48h.

4.5.2 QUANTIFICATION OF SPECKLE NUMBER AFTER TREATMENT WITH ETOPOSIDE

In order to quantify speckle formation in KPL-1 and MCF-7 cells overexpressing RAI2 and 4A mutant, images of cells were taken and the number of speckles counted per cell. Analysing the number of speckles in KPL-1 RAI2 overexpressing cells revealed a significant increase in speckle number after treatment with etoposide from 2 to 4 (median) ($p > 0.01$, Figure 29). In contrast, KPL-1 cells expressing 4A mutant RAI2 showed significantly smaller speckle numbers in control and etoposide-treated samples ($p < 0.01$, median = 0). However, also in these cells speckle formation is slightly increased after treatment with etoposide (Figure 29a). In MCF-7 cells overexpressing RAI2, a significantly elevated formation of speckles was observed from 2 to 3 (median) after treatment with etoposide ($p < 0.01$, Figure 29b). In contrast, MCF-7 RAI2 4A mutant cells show few to no

speckle formation (media=0) in both treatments (Figure 29). In summary, this demonstrates that the number of RAI2/CtBP1 speckles is elevated upon chemotherapeutic treatment and this effect is disrupted in cells overexpressing CtBP1 binding-deficient RAI2.

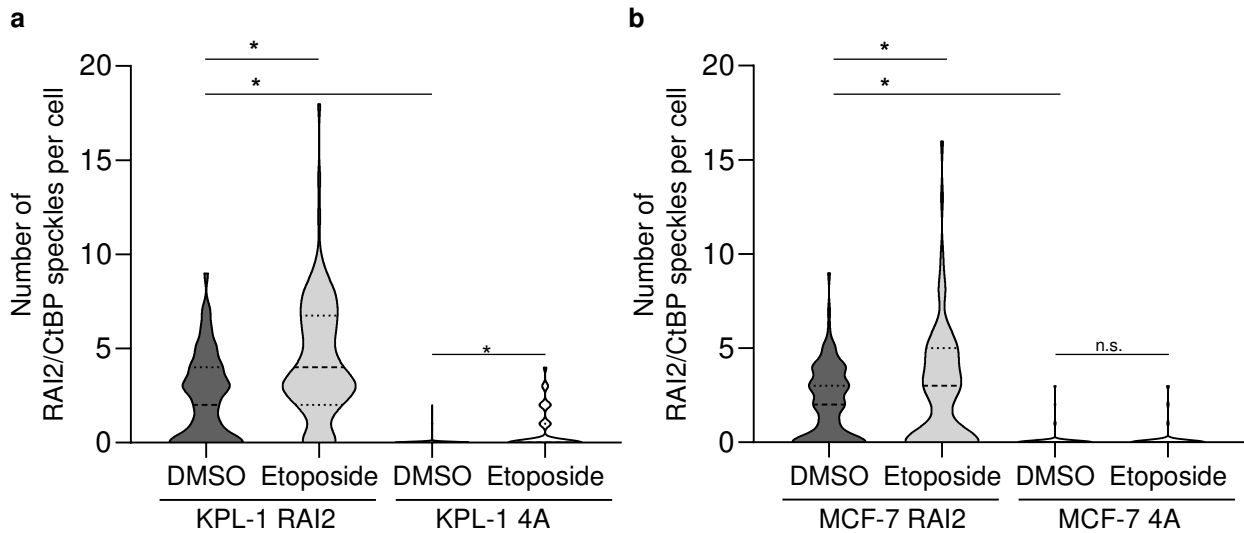


Figure 29: Quantification of speckle formation in (a) KPL-1 and (b) MCF-7 RAI2 OE and 4A cells treated with etoposide. Cells were treated with 10 μ M etoposide for 48h. Cells were stained for RAI2, CtBP1 and DAPI and analysed on images taken with a fluorescence microscope at 40 x magnification. At least 100 cells were counted per cell line and data are shown as violin blot with median. P-values were calculated by Poisson regression, * $p < 0.01$.

4.6 DEPENDENCE OF *RAI2* EXPRESSION ON THE CLINICAL OUTCOME OF PATIENTS WITH CIN TUMOURS

In patients with breast and other cancer types it was shown that increased CIN is associated with metastatic progression (Turajlic and Swanton, 2016). In order to analyse the effect of *RAI2* expression on patient's outcome, survival analyses of metastatic breast cancer patients with chromosomal unstable breast tumours were performed. Samples from METABRIC dataset were divided by the median of *RAI2* expression (high/low) and according to their CIN score (high/low). For each tumour the CIN70 score was calculated according to summation of expression values of all the CIN70 genes (Birkbak et al., 2011). Five-year overall survival was determined by Kaplan-Meier analysis.

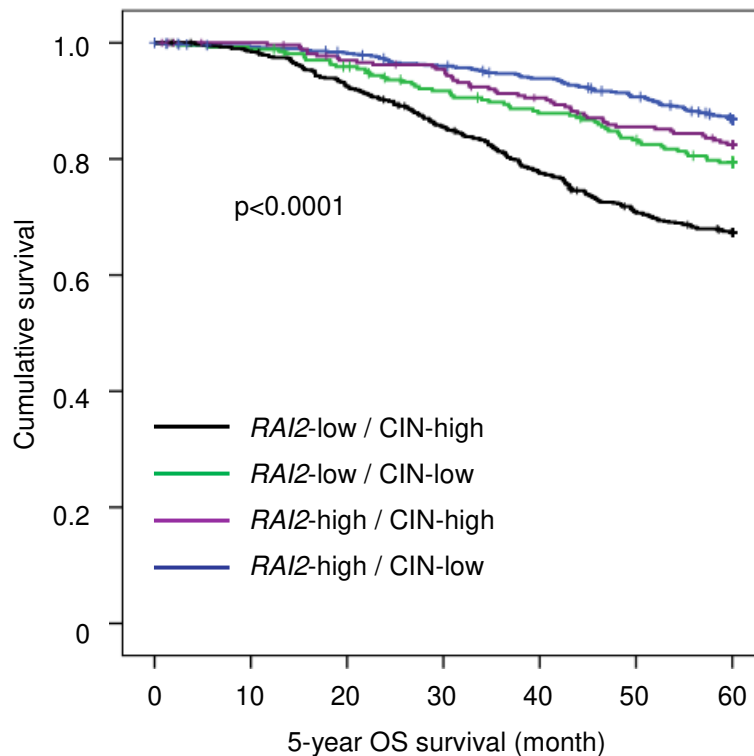


Figure 30: Five-year overall (OS) survival analysis of breast cancer patients. Overall survival analysis of *RAI2* gene expression stratified by median and CIN score in patients of the METABRIC dataset analysed by Kaplan-Meier estimations. A two-sided significance level below 0.05 was considered as significant.

After five years, the best survival rate with only 9.4% of deaths was shown for patients with high *RAI2* expression and low CIN score, followed by patients with mixed phenotype showing a five-year overall survival of 79.4% (*RAI2*-high/CIN-high) and 82.1% (*RAI2*-low/CIN-low). Interestingly, for patients with low *RAI2* levels and high CIN scores the five-year overall survival

rate was the lowest with 63.8%. Statistical analysis revealed that patients with low *RAI2* gene expression combined with high CIN score have a significantly worse prognosis compared to other patient groups ($p < 0.001$). Thus, low *RAI2* expression does not only result in a CIN phenotype in luminal breast cancer cells but has also prognostic relevance in breast cancer patients with a high CIN score.

5 DISCUSSION

A variety of checkpoint mechanisms and DNA repair pathways are active during cell division in order to avoid loss of genetic information (Aguilera and Gomez-Gonzalez, 2008). Disruption of these mechanisms results in loss of genetic information in the form of chromosomes/chromosome fragments or due to mutation and is known as genomic instability. Genomic instability is part of Hallmarks of Cancer which describe the characteristic of a cell leading to cancer progression and is an enable characteristics of tumours (Hanahan and Weinberg, 2011). The present study investigated the role of the putative metastasis suppressor retinoic acid-induced 2 (*RAI2*) gene in maintaining genomic integrity in breast cancer. The effect of modified *RAI2* expression in the response to DNA damage and the expression of *RAI2* under chemotherapeutic conditions were analysed in breast cancer cell lines. Furthermore, the localisation of *RAI2* and its binding partner CtBP was investigated. Finally, the impact of *RAI2* gene expression on survival in patients with chromosomal instability was analysed in a breast cancer data set.

5.1 MITOSIS IN *RAI2*-DEPLETED CELLS

Malfunction of mitosis due to defects in mitotic-related processes, like regulation of mitotic checkpoint, centromere formation or kinetochore-microtubule attachment can induce chromosomal instability (CIN) leading to cancer progression. Numerous genes involved in these processes are known to be commonly mutated in human cancer (Hanahan and Weinberg, 2011; Thompson et al., 2010). Previous analysis of luminal breast cancer cell lines performed at the ITB showed that loss of *RAI2* leads to a deregulation of cell cycle-associated genes, including those that play a role in the regulation of microtubule motor activity, mitosis and spindle apparatus (Werner et al., 2016).

The present study investigated the impact of *RAI2* on mitotic progression in individual breast cancer cells using live cell imaging. Analysis of mitosis in *RAI2*-depleted cells revealed a prolonged duration of mitosis. This increase resulted particularly from a significantly extended metaphase indicating that the mitotic checkpoint is activated arresting the cells in the metaphase. This arrest ensures that all kinetochores are correctly attached to the microtubules of the spindles (Musacchio and Salmon, 2007). It has been shown by others that cells with prolonged mitosis

exhibited elevated DNA damage and aneuploidy (Rajagopalan et al., 2004; Sotillo et al., 2007). Thus, cells with depleted RAI2 expression could exhibit an accumulation of DNA damage. Besides an extended metaphase, RAI2-depleted cells showed increased *de novo* micronuclei formation after telophase. These abnormal extra nuclear bodies are commonly occurring in human cancer and contain damaged chromosomal fragments and/or whole chromosomes thus representing a marker of chromosomal instability (Fenech et al., 2011). In the current study, analysis of live cell images of RAI2-depleted cells showed that chromosomal fragments or chromosomes which were not aligned in the metaphase plate and failed to get separated during anaphase, were incorporated into micronuclei. Over 30% of the RAI2-depleted cells analysed showed *de novo* micronuclei formation (compared to 10% non-target) indicating that loss of RAI2 leads to increased CIN.

As micronuclei can be a result of either loss of chromosomal fragments or whole chromosomes (Fenech et al., 2011), additional detailed immunofluorescence analysis were performed. By staining both DNA and centromeres it is possible to distinguish between chromosomes with a centromere region and acentric chromosomes which represent chromosomal fragments without centromeres. Interestingly, a significant increase of acentric chromosomes, which were not aligned to the metaphase plate or mis-segregated in anaphase, were observed in metaphases of RAI2-depleted cells. Loss of whole chromosomes and incidence of anaphase bridges, which are common mitotic defects arising from a connection of sister chromatids upon telomere dysfunction (Artandi and DePinho, 2010; Maser and DePinho, 2002; Murnane, 2012), was not altered by RAI2 depletion. Taken together, the results from live cell imaging and immunofluorescence staining showed that the prolonged duration of mitosis was due to the occurrence of acentric chromosomes in RAI2-depleted cells. These broken chromosomal fragments are consequently incorporated into micronuclei in the final step of the mitosis upon RAI2 depletion.

5.2 PREMITOTIC DEFECTS AFTER RAI2 DEPLETION

Occurrence of chromosomal fragments in mitotic cells can originate from premitotic double-strand breaks (DSBs) that are not repaired before the cell entering mitosis and are still present during chromosome segregation. They can be a result of dysfunctional DSB repair or replication stress (Burrell et al., 2013a; Gordon et al., 2012; Zeman and Cimprich, 2014). Here we analysed DSBs, replication and DSB repair pathways in order to determine whether deregulation

of one of these mechanisms was the main driving cause of the CIN phenotype in RAI2-depleted cells.

As one of the first steps for the following DNA repair cascade, DSBs are marked by phosphorylation of Histone H2 on Serine 139 (γ H2AX) in the form of foci which builds a platform for repair proteins (Rogakou et al., 1999). In order to find out if RAI2 depletion led to increased DSBs, cells were stained for the DSB marker γ H2AX. Interestingly, micronuclei of RAI2-depleted cells showed a very intensive γ H2AX signal, further confirming that fragmented chromosomes were incorporated into micronuclei after mitosis. The total γ H2AX foci signal was significantly increased after RAI2 depletion in the nuclei indicating elevated DSBs. The occurrence of DSBs was already described by others in cells with prolonged mitosis (Rajagopalan et al., 2004; Sotillo et al., 2007). Also, it has been shown that even the occurrence of prolonged mitosis in cancer cells can lead to increased γ H2AX signal (Dalton et al.). Within the cell population, a subpopulation of nuclei containing abundant small γ H2AX could be observed. This small type of γ H2AX foci is described as foci that are not associated with DNA damage repair proteins and do not show similarity to foci occurring at DSBs after irradiation (McManus and Hendzel, 2005). This steady-state γ H2AX phosphorylation is described to be dynamic during cell cycle progression with a peak of expression in mitosis (McManus and Hendzel, 2005) and is observed upon different stimuli, however, the function of the small γ H2AX foci is still unclear (Katsube et al., 2014; Revet et al., 2011). Analysis of cells with these small γ H2AX foci revealed a significantly increased number of cells upon RAI2 depletion. As RAI2 depletion alone results in acentric chromosomes, the chromosomal fragments are already present before mitotic entry. Thus, low RAI2 levels in breast cancer cells lead to elevated DSBs and a CIN phenotype at a premitotic cell cycle phase.

A common premitotic defect which is linked to DSBs and chromosomal instability, is replication stress (Burrell et al., 2013a; Zeman and Cimprich, 2014). A method to analyse DNA replication in cells is the so called DNA fiber assay that allows the analysis of ongoing replication and replication restart after replication fork stalling (Nieminuszczy et al., 2016). Analysis of fiber length as indicator of replication progression revealed that RAI2 had no impact on the replication progression. Additionally, dysfunction in replication restart, which could result in replication fork collapse and consequently lead to DSBs (Di Micco et al., 2006; Hanahan and Weinberg, 2011;

Petermann et al., 2010), was not observed in RAI2-depleted cells. This leads to the conclusion that replication stress is not the origin of increased incidence of DSBs and acentric chromosomes in RAI2-depleted cells.

Due to the fact, that RAI2 depletion results in elevated DSBs, the next step was to investigate the effect of RAI2 depletion on the two main DSB repair pathways – non-homologous end-joining (NHEJ) and homologous recombination (HR) – as their dysfunction can contribute to an accumulation of DSBs and premitotic defects. Interestingly, analysis of repair capacities in HEK293t using the Traffic Light Reporter Assay gave different results depending on whether RAI2 is depleted or overexpressed in the cells. On the one hand, RAI2 depletion led to a decreased NHEJ capacity with the HR capacity remaining unaffected in these cells, on the other hand, overexpression of RAI2 in HEK293t cells resulted in an elevated HR capacity and constant NHEJ capacity. This indicates, that RAI2 functions as a global player in the response to DNA damage rather than functioning specifically in one of the DSB repair pathways. As the DSBs are still marked by γ H2AX in RAI2-depleted cells, the initial recognition of DSBs, which is important for both DSB repair pathways, is not effected in absence of RAI2. Besides the accumulation of γ H2AX at DSBs (Rogakou et al., 1999), there are other factors that are related to both the NHEJ and HR pathways like ATM. In the S and G₂ phases of the cell cycle, ATM phosphorylates members of the MNR complex leading consequently to a phosphorylation and activation of other HR factors like BRCA1 and CtIP (Li et al., 2000; Matsuoka et al., 2007; Wang et al., 2013). Moreover, ATM was also shown to phosphorylate 53BP1 in G₁ phase contributing to an inhibition of DNA end resection by preventing binding of CtIP to DNA ends contributing NHEJ (Ceccaldi et al., 2016). The fact that there exist factors functioning in both HR and NHEJ underlines the global function of RAI2 in promoting DSB repair by possibly coordinating pathway choices. Thus, RAI2 avoids CIN in cells by maintaining global DSB repair capacity. Figure 31 summarises the characteristics of RAI2 overexpression and depleted cells preventing or contributing to CIN.

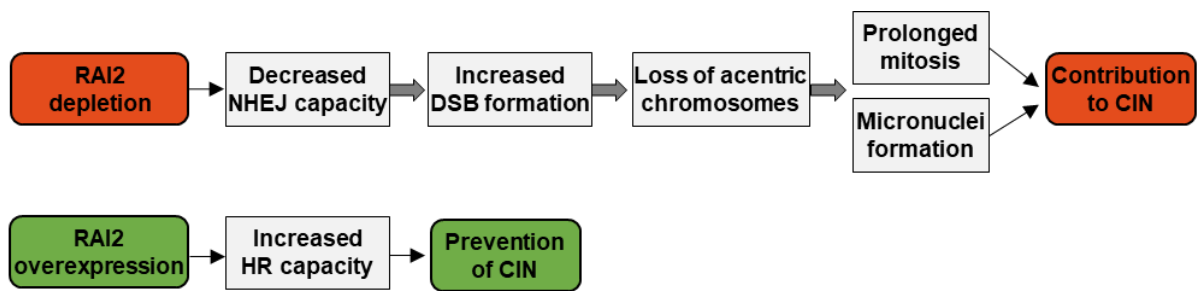


Figure 31: Consequences of RAI2 depletion and overexpression. Depletion of RAI2 leads to decreased non-homologous end-joining (NHEJ) capacity and DSB formation resulting in a loss of acentric chromosomes and consequently in prolonged mitosis and micronuclei formation. All these contribute to a CIN phenotype in luminal breast cancer cells lines upon RAI2 depletion. RAI2 overexpression results in increased capacity to repair double-strand breaks (DSBs) via the homologous recombination (HR) pathway preventing chromosomal instability (CIN).

5.3 IS THE RAI2 PROTEIN CELL CYCLE-DEPENDENT EXPRESSED?

Proteins involved in DNA damage repair response can be differentially expressed and regulated during cell cycle depending on which phase they actively promote the repair of DNA damage (Shaltiel et al., 2015). For instance, the CtIP protein, which plays a role in the 5' to 3' end resection during HR, shows low protein level during G₁ and is highly expressed during S/G₂ phase of the cell cycle in which HR is active to repair DSBs (Yu and Baer, 2000). In order to get an idea how the RAI2 gene and protein expression alters during cell cycle, RAI2 expression together with γ H2AX was studied in synchronised breast cancer cells. Analysis showed that RAI2 gene expression is induced in the S phase followed by a strong increase of expression during S/G₂ phase. RAI2 protein levels were elevated in S and S/G₂ phase too, indicating a possible functional role of RAI2 during S/G₂ phase. Moreover, the increase of RAI2 expression correlated with the expression of γ H2AX. It has been shown, however, by Kurose *et al* that synchronisation with thymidine induces DNA damage marked by increased γ H2AX (Kurose et al., 2006). Therefore, the expression data might also be based on the DSB induction upon thymidine treatment. This leads to the conclusion that RAI2 might be induced due to DNA damage in the synchronised cells and not in a cell cycle-dependent manner. Using a different method for synchronisation that avoids the induction of DNA damage like the method of mitotic shake-off (Jackman and O'Connor, 2001), would help to verify if RAI2 is induced due to the toxic effect of the thymidine for the DNA or in a cell cycle-dependent manner.

As RAI2 was induced in S/G₂ phase, RAI2 gene and protein expression was analysed in cells treated with different chemotherapeutics that block the cell cycle at different points. Induction of RAI2 was detected in cells treated with the topoisomerase II inhibitor etoposide, which leads to high level of enzyme-mediated breaks of the DNA and arrests cells in S phase (Fortune and Osheroff, 2000; Pommier et al., 2010). Moreover, treatment with the CdK-1 inhibitor RO-3306, which arrests the cells at the G₂/M border (Vassilev et al., 2006), also induces RAI2 expression. Further, the third tested inhibitor paclitaxel pausing the cell cycle in metaphase (Weaver, 2014) induces RAI2 expression. On the protein level, the induction of RAI2 correlated with the induction of γ H2AX under all three treatment conditions, further underlining that RAI2 is rather correlated to DNA damage than cell cycle-dependent regulated. Additionally, elevated levels of RAI2 protein correlated with an increase in p21 protein expression. This kinase regulates the cell cycle and when activated, arrests the cell cycle to promote repair of damaged DNA before cell division (Abbas and Dutta, 2009). Furthermore, RAI2 expression correlated with the expression of p53, “the guardian of the genome” (Lane, 1992) that triggers checkpoint activation to pause the cells upon DNA damage. Both the observed correlation of RAI2 expression with p21 and with p53 further led to the suggestion that RAI2 might be involved in regulating the response to DNA damage. As RAI2 is induced upon all tested inhibitors, and not specifically after arresting the cell in a specific cell cycle phase, the elevated RAI2 expression is more a response to increased DNA damage than being cell cycle-dependent regulated. The fact that RAI2 is not specifically cell cycle-regulated supports the observation, that depletion of RAI2 has no impact on proliferation (Werner et al., 2015). Thus, RAI2 possibly plays a super-ordinated role in response to DNA damage that is not restricted to one cell cycle phase. This is consistent with the results from DNA repair assay showing decreased NHEJ capacities in RAI2-depleted cells and elevated HR capacity in RAI2 overexpressing cells.

5.4 CLONOGENIC CAPACITY AFTER RAI2 DEPLETION

The current study showed that RAI2 depletion leads to CIN in luminal breast cancer cells. It has been shown by others that CIN can cause drug resistance against multiple chemotherapeutics by creating a higher level of genetic diversity which fosters the occurrence of drug resistant clones (Lee et al., 2016). Intratumoural heterogeneity is one of the key factors leading to ineffective

therapeutic response and drug resistance and remains a serious problem in cancer treatment (Greaves, 2015). Hypothetically, the CIN observed in RAI2-depleted breast cancer cells could drive genetic diversity leading to a growth advantage upon treatment. In order to find out if RAI2 expression has an impact on the ability of single tumour cells to proliferate and undergo unlimited cell division, control and RAI2-depleted cells were analysed by colony formation assay. Under standard conditions, the two analysed breast cancer cell lines showed the same clonogenic capacity in both control and the RAI2-depleted settings. Next, possible differences in the clonogenic capacity in response to various chemotherapeutic treatments were analysed, as the CIN phenotype in RAI2-depleted cells might influence the capacity of cells to proliferate. Surprisingly, no difference in clonogenic capacity was observed in any of the treatments that were used. A possible explanation is that RAI2-depleted cells compensate sensitivity to drugs by activating alternative signaling pathways thereby achieving drug-resistance. This is a common mechanism in cancer that reduces the effectiveness of current cancer therapies (Holohan et al., 2013; Sansregret et al., 2018). It would be beneficial to find the exact pathway, in which RAI2 is involved, and then screen pathways that are compensatively activated in RAI2-depleted cells, to overcome drug sensitivity.

5.5 RAI2 SPECKLE FORMATION

In 2015, it has been shown by the ITB that with C-terminal binding protein 1 (CtBP1) and CtBP2 are the main binding partner of RAI2 and that both proteins colocalise with RAI2 in form of nuclear speckles in MCF-7 cells. However the function and dynamics of these speckles were not further analysed (Werner et al., 2015). CtBP1 and 2 are oncogenic transcriptional corepressors that play a role in different cancer-related processes like promoting cell proliferation and migration (Chinnadurai, 2009). Importantly, CtBPs also ensure cell survival by avoiding mitotic chromosome segregation errors in breast cancer cell lines (Bergman et al., 2009). Consistent with effects of RAI2 depletion demonstrated in the current study, Bergman et al. have shown similar effects of CtBP loss in breast cancer including defective micronuclei formation and increased loss of chromosomes during mitosis (Bergman et al., 2009). However their finding lacks the analysis of premitotic processes upon CtBP depletion. In the present study, expression analysis showed that RAI2 gene and protein expression increased after treatment with different chemotherapeutic

agents. In order to investigate if this increase results in increased speckle formation, localisation and dynamics of RAI2 speckles were investigated upon etoposide treatment, a TOP2 inhibitor, using immunofluorescence staining. It was shown that not only MCF-7 cells overexpressing RAI2 showed RAI2/CtBP speckle but KPL-1 RAI2 overexpressing cells also did the same, demonstrating that these speckles were common in breast cancer cell lines overexpressing RAI2. Interestingly, treatment with etoposide further results in an increased number of speckles in the nuclei in both analysed cell lines. Such an accumulation of nuclear factors is described for many proteins with different functions in compartments called paraspeckles, nucleoli, cajal bodies or repair foci (Lamond and Earnshaw, 1998; Platani and Lamond, 2004; Rothkamm et al., 2015). For instance, paraspeckles are compartments of proteins with functions in several RNA metabolic pathways, including pre-mRNA processing and RNA stability and proteins of these compartments are also known to promote DNA damage response (Jaafar et al., 2017; Knott et al., 2016). Also DNA damage response proteins and post-transcriptional modifications accumulate at the site of DNA breaks, known as DNA damage foci, and give rise to downstream signalling DNA damage repair pathway (Polo and Jackson, 2011; Rothkamm et al., 2015). In the current study, the elevated RAI2 speckle number in cells treated with DNA damaging reagent indicates that the RAI2 protein accumulates after DNA damage and facilitates DNA damage response to maintain chromosomal integrity. However, the exact compartment in which RAI2 is localised and active still has to be investigated.

In order to investigate the dependence of RAI2 to bind to CtBP in this process, speckle formation was analysed in cells overexpressing RAI2 containing a mutant binding site to CtBP. Interestingly, when the binding sites to CtBP were mutated, almost no RAI2/CtBP speckles were observed. Thus, binding to CtBP is necessary for RAI2 speckle formation and/or inversely. CtBPs are known to have oncogene potential by repressing promoters of tumour suppressors and are upregulated in metastatic cancer types (Barroilhet et al., 2013; Chinnadurai, 2009; Wang et al., 2012). Potentially, the presence of RAI2 leads to storage of CtBP proteins in the form of nuclear speckles, avoiding the function of CtBP as corepressor. Tumour suppressor genes like E-cadherin and p16LnK4a would be transcribed leading to a non-tumourigenic phenotype (Chinnadurai, 2009). Interestingly, CtBP1 transcriptionally downregulates BRCA1 (Deng et al., 2012), which plays an important role in the DNA end resection in the HR pathway (Li and Heyer, 2008). Moreover, CtIP, which is also a factor involved in end resection, is cofactor for the CtBP (Schaeper et al., 1998),

linking CtBP to the DNA damage response and HR. Thus, RAI2/CtBP speckles are dynamic structures, as their number is increased after treatment with DNA damage inducing agent. These might link the RAI2/CtBP speckles to function in DNA damage response by maintaining a non-invasive phenotype and chromosomal stability.

5.6 IMPACT OF RAI2 ON CHROMOSOMAL UNSTABLE BREAST CANCER PATIENTS

Functional analysis demonstrated that RAI2 was important for the maintenance of chromosomal integrity in luminal breast cancer cells. Depletion of RAI2 leads to an induction of DSBs and results in loss of acentric chromosomes and CIN. In patients, CIN can contribute to clonal diversity within the tumour mass, which can predict patient's outcome and therapeutic strategies (Burrell et al., 2013b; Dagogo-Jack and Shaw, 2018). Recently, it has been demonstrated that massive CIN directly causes intratumoural heterogeneity in non-small-cell lung cancer (Jamal-Hanjani et al., 2017). Moreover, in breast cancer patients, it has been shown that the onset of CIN contributes to metastasis (Turajlic and Swanton, 2016). In order to investigate, if low RAI2 expression has also an impact on patient's outcome, breast cancer samples from the large Metabric dataset were analysed by Kaplan-Meier analysis. Samples were grouped by CIN score (low and high) as well as according to the mRNA expression of RAI2 (low and high). Matching to the biological data, patients with low RAI2 and a high CIN score showed the lowest five-year overall survival rate compared to the other three groups. Interestingly, the two groups with the best survival showed high RAI2 expression, which further points out the importance of RAI2 for patient's outcome also independently of the CIN status. Thus, a lack of RAI2 might drive early metastatic progression in breast cancer by contributing intertumoural heterogeneity through an induction of CIN. This fits together with the earlier finding that RAI2 acts as metastasis suppressor gene for early hematogenous dissemination (Werner et al., 2015).

5.7 CONCLUSION AND OUTLOOK

Genomic instability is part of Hallmarks of Cancer which describe the characteristics of a cell leading to cancer progression and is an enable characteristics of tumours (Hanahan and Weinberg, 2011). Genomic instability especially on the chromosome level, which is described as chromosomal instability (CIN), can create high levels of intratumoural heterogeneity, the main reason for ineffective therapeutic response and drug resistance in cancer treatment (Bakhoun et al., 2018; Turajlic and Swanton, 2016; Turajlic et al., 2018). A variety of checkpoint mechanisms and DNA repair pathways are active during cell division in order to avoid loss of genetic information. Disruption of these mechanisms results in loss of genetic information in the form of chromosomes/chromosome fragments or due to mutations (Aguilera and Gomez-Gonzalez, 2008).

The current study provides first experimental evidence that RAI2 protein is important to maintain chromosomal integrity in luminal breast cancer cells. Breast cancer cell lines with low RAI2 expression showed decreased DNA damage response resulting in elevated number of DSBs and loss of chromosomal fragments that are incorporated into micronuclei after mitosis. The analysis of mitotic defects was performed with breast cancer cell lines that were classified as luminal cell lines derived from patients with metastatic breast cancer (Kurebayashi et al., 1995; Soule et al., 1973). Although the percentage of micronuclei and the incidence of acentric chromosomes was significantly increased in RAI2-depleted cells, mitotic defects were already observed in the control cells. It has been described published that MCF-7 cells have an intrinsic capacity to clonal heterogeneity as different subclones showed genetic plasticity (Nugoli et al., 2003). Thus, the breast cancer cell lines used for the RAI2 knockdown experiments are per se instable because of their metastatic origin which already influence the response to DNA damage upon RAI2 depletion. Therefore, the impact of RAI2 depletion should be additionally tested in cells derived from non-tumoural tissue for example using MCF-10 cells that show characteristics of normal breast epithelium (Soule et al., 1990). Using this cells for analysis would give information about the function of RAI2 in a normal, chromosomal stable cell environment. Thereby, it could be verified if RAI2 just functions in cells with metastatic background and in general in response to DNA damage induced by chemotherapeutic or if it plays a role in response to endogenous DNA damage that occurs normally during cell division (Tubbs and Nussenzweig, 2017).

Moreover, it should be considered to analyse the DNA damage response function of RAI2 in other tumour entities as RAI2 was also shown to be prognostically relevant also in lung, colon and ovarian cancer patients (Werner et al., 2015). Besides that, the potentially multiple function of RAI2 in cancer should not be forgotten, as the function of RAI2 might be dependent on the metabolic background of the different cell or cancer types. This includes the role of RAI2 as corepressor of steroid regulated genes in prostate and breast cancer cells (Besler et al., 2018) and its role in migration and invasion in colon cancer (Yan et al., 2018).

Normally cells with damaged DNA are held before entering the mitotic phase to ensure DNA repair and intact chromosomes before cell division. Otherwise the non-repairable cells are forced into apoptosis to avoid the continuous existence of mutations in the daughter cells (Zhou and Elledge, 2000). It might be possible that this checkpoint is also deactivated upon RAI2 depletion because acentric chromosomes are occurring in RAI2-depleted cells during mitosis. Therefore, additionally to the DNA damage response pathways a possible deregulation of the G₂/M transition pathway should be further analysed using protein-based analysis in a RAI2-depleted setting.

This thesis showed for the first time that RAI2 plays a role in maintaining chromosomal integrity by facilitating DNA damage response in breast cancer cells. However, the exact pathway, in which RAI2 plays a role still have to be elucidated. Analysis of a deregulation of DNA damage pathway protein is necessary to look for the exact step in the DNA damage response where RAI2 functions. Additionally, also the RAI2/CtBP speckles should be further analysed precisely, to find the link of the speckles to DNA damage. It is already known that CtBP is linked to DNA damage over the interaction with HR proteins CtIP and BRCA1 (Chinnadurai, 2009; Deng et al., 2012; Li et al., 2000; Schaeper et al., 1998). Internal ongoing interaction studies using a SILAC-immunoprecipitation quantitative proteomic analysis approach revealed that RAI2 interacts, in addition to CtBP1, with PARP (Werner et al., 2018). As PARP is the key protein in the activation of single-strand break and base excision repair pathway (Pilie et al., 2019), RAI2 might also be linked to the repair of single-strand breaks through the interaction with PARP1 and not just to DSB repair. Possibly, RAI2/CtBP speckles are platforms for DNA damage proteins of different pathways that dynamically build up upon all types of DNA breaks.

It has been shown previously that low *RAI2* expression is associated with shortened overall survival in breast, lung, ovarian and colon cancer and that *RAI2* acts as metastasis suppressor for early hematogenous dissemination in breast cancer (Werner et al., 2015). The current data indicate that the tumour suppressive function of *RAI2* arise from its role in maintaining chromosomal stability. By this, *RAI2* might limit the development of intratumoural heterogeneity which would otherwise promote cells to acquire metastatic traits. This correlates with the finding that high *RAI2* mRNA expression in breast cancer patients results in a better five-year overall survival compared to patients with low *RAI2* expression levels.

Determining the exact biological mechanism by which *RAI2* prevents CIN might be critical to optimise existing therapies or set up new therapeutic approaches for cancer treatment in the future. Potentially, activation of the *RAI2* protein in cancer cells could arrest the cells in a state of genomic stability thereby avoiding the activation of metastatic traits. Contrary, low *RAI2* expression could exploit to develop a newly therapeutic approach based on the synthetic lethality concept. This concept makes use of the fact that the perturbation of one gene alone is viable for the cell but the depletion of a second gene simultaneously by using specific inhibitors results in the loss of viability in the tumour cells (O'Neil et al., 2017). The concept is already implemented in the clinics by giving PARP inhibitors to breast cancer patients with *BRCA1* germline mutations (Mavaddat et al., 2012; Robson et al., 2017). During this study, the clonogenic capacity of *RAI2* depleted cells was already tested under different chemotherapeutic conditions. However, these analysis revealed no differences. One could think about to induce *RAI2* depletion in triple-negative breast cancer cell lines which are innately more aggressive compared to luminal breast cancer cell lines (Dai et al., 2017). Possibly, these cell lines cannot compensate the response to DNA damage via compensatory pathways, because this pathways are already mutated. Induction of CIN by *RAI2* depletion in these cells might lead to a better response to DNA damage reagents and chemotherapeutics than in the luminal cells forcing them into apoptosis. Determining the exact mechanism by which *RAI2* promotes DNA damage response and avoids CIN together with looking for inhibitors that deactivate second compensatory repair pathways, would be beneficial for development of new synthetic lethality-based treatment options for metastatic breast cancer patients.

6 LITERATURE

Abbas, T., and Dutta, A. (2009). p21 in cancer: intricate networks and multiple activities. *Nature reviews Cancer* *9*, 400-414.

Aguilera, A., and Garcia-Muse, T. (2012). R loops: from transcription byproducts to threats to genome stability. *Molecular cell* *46*, 115-124.

Aguilera, A., and Gomez-Gonzalez, B. (2008). Genome instability: a mechanistic view of its causes and consequences. *Nature reviews Genetics* *9*, 204-217.

Artandi, S.E., and DePinho, R.A. (2010). Telomeres and telomerase in cancer. *Carcinogenesis* *31*, 9-18.

Bailey, S.M., and Murnane, J.P. (2006). Telomeres, chromosome instability and cancer. *Nucleic acids research* *34*, 2408-2417.

Bakhoun, S.F., Ngo, B., Laughney, A.M., Cavallo, J.A., Murphy, C.J., Ly, P., Shah, P., Sriram, R.K., Watkins, T.B.K., Taunk, N.K., *et al.* (2018). Chromosomal instability drives metastasis through a cytosolic DNA response. *Nature* *553*, 467-472.

Banerji, S., and Los, M. (2006). Important differences between topoisomerase-I and -II targeting agents. *Cancer biology & therapy* *5*, 965-966.

Barber, T.D., McManus, K., Yuen, K.W., Reis, M., Parmigiani, G., Shen, D., Barrett, I., Nouhi, Y., Spencer, F., Markowitz, S., *et al.* (2008). Chromatid cohesion defects may underlie chromosome instability in human colorectal cancers. *Proceedings of the National Academy of Sciences of the United States of America* *105*, 3443-3448.

Barlow, J.H., Faryabi, R.B., Callen, E., Wong, N., Malhowski, A., Chen, H.T., Gutierrez-Cruz, G., Sun, H.W., McKinnon, P., Wright, G., *et al.* (2013). Identification of early replicating fragile sites that contribute to genome instability. *Cell* *152*, 620-632.

Barroilhet, L., Yang, J., Hasselblatt, K., Paranal, R.M., Ng, S.K., Rauh-Hain, J.A., Welch, W.R., Bradner, J.E., Berkowitz, R.S., and Ng, S.W. (2013). C-terminal binding protein-2 regulates response of epithelial ovarian cancer cells to histone deacetylase inhibitors. *Oncogene* *32*, 3896-3903.

Bennett, C.B., Snipe, J.R., and Resnick, M.A. (1997). A persistent double-strand break destabilizes human DNA in yeast and can lead to G2 arrest and lethality. *Cancer research* *57*, 1970-1980.

Bergman, L.M., Birts, C.N., Darley, M., Gabrielli, B., and Blaydes, J.P. (2009). CtBPs promote cell survival through the maintenance of mitotic fidelity. *Molecular and cellular biology* *29*, 4539-4551.

Berman, A.T., Thukral, A.D., Hwang, W.T., Solin, L.J., and Vapiwala, N. (2013). Incidence and patterns of distant metastases for patients with early-stage breast cancer after breast conservation treatment. *Clinical breast cancer* *13*, 88-94.

Besler, K., Weglarz, A., Zill, C., Jensen, J., Wikman, H., Pantel, K., and Werner, S. (2018). Role of RAI2 protein in progression of breast and prostate cancer to hormone independent disease (AACR).

- Birkbak, N.J., Eklund, A.C., Li, Q., McClelland, S.E., Endesfelder, D., Tan, P., Tan, I.B., Richardson, A.L., Szallasi, Z., and Swanton, C. (2011). Paradoxical relationship between chromosomal instability and survival outcome in cancer. *Cancer research* *71*, 3447-3452.
- Bishop, A.J., and Schiestl, R.H. (2001). Homologous recombination as a mechanism of carcinogenesis. *Biochimica et biophysica acta* *1471*, M109-121.
- Blevins, M.A., Huang, M., and Zhao, R. (2017). The Role of CtBP1 in Oncogenic Processes and Its Potential as a Therapeutic Target. *Molecular cancer therapeutics* *16*, 981-990.
- Bloom, H.J., and Richardson, W.W. (1957). Histological grading and prognosis in breast cancer; a study of 1409 cases of which 359 have been followed for 15 years. *British journal of cancer* *11*, 359-377.
- Boettcher, B., and Barral, Y. (2013). The cell biology of open and closed mitosis. *Nucleus (Austin, Tex)* *4*, 160-165.
- Boveri, T. (1914). Zur Frage der Entstehung maligner Tumoren.
- Branzei, D., and Foiani, M. (2010). Maintaining genome stability at the replication fork. *Nature reviews Molecular cell biology* *11*, 208-219.
- Bray, F., Ferlay, J., Soerjomataram, I., Siegel, R.L., Torre, L.A., and Jemal, A. (2018). Global cancer statistics 2018: GLOBOCAN estimates of incidence and mortality worldwide for 36 cancers in 185 countries. *CA: a cancer journal for clinicians* *68*, 394-424.
- Brookes, P., and Lawley, P.D. (1964). Evidence for the binding of polynuclear aromatic hydrocarbons to the nucleic acid of mouse skin: Relation between carcinogenic power of hydrocarbons and their binding to deoxyribonucleic acid. *Nature* *202*, 781-784.
- Brown, J.M., and Attardi, L.D. (2005). The role of apoptosis in cancer development and treatment response. *Nature reviews Cancer* *5*, 231-237.
- Bryant, H.E., Schultz, N., Thomas, H.D., Parker, K.M., Flower, D., Lopez, E., Kyle, S., Meuth, M., Curtin, N.J., and Helleday, T. (2005). Specific killing of BRCA2-deficient tumours with inhibitors of poly(ADP-ribose) polymerase. *Nature* *434*, 913-917.
- Burdette, W.J. (1955). The significance of mutation in relation to the origin of tumors: a review. *Cancer research* *15*, 201-226.
- Burrell, R.A., McClelland, S.E., Endesfelder, D., Groth, P., Weller, M.C., Shaikh, N., Domingo, E., Kanu, N., Dewhurst, S.M., Gronroos, E., *et al.* (2013a). Replication stress links structural and numerical cancer chromosomal instability. *Nature* *494*, 492-496.
- Burrell, R.A., McGranahan, N., Bartek, J., and Swanton, C. (2013b). The causes and consequences of genetic heterogeneity in cancer evolution. *Nature* *501*, 338-345.
- Byun, J.S., and Gardner, K. (2013). C-Terminal Binding Protein: A Molecular Link between Metabolic Imbalance and Epigenetic Regulation in Breast Cancer. *International journal of cell biology* *2013*, 647975.
- Caldecott, K.W. (2008). Single-strand break repair and genetic disease. *Nature reviews Genetics* *9*, 619-631.

- Callahan, R., and Hurvitz, S. (2011). Human epidermal growth factor receptor-2-positive breast cancer: Current management of early, advanced, and recurrent disease. *Current opinion in obstetrics & gynecology* 23, 37-43.
- Cameron, D., Piccart-Gebhart, M.J., Gelber, R.D., Procter, M., Goldhirsch, A., de Azambuja, E., Castro, G., Jr., Untch, M., Smith, I., Gianni, L., *et al.* (2017). 11 years' follow-up of trastuzumab after adjuvant chemotherapy in HER2-positive early breast cancer: final analysis of the HERceptin Adjuvant (HERA) trial. *Lancet (London, England)* 389, 1195-1205.
- Canman, C.E., Lim, D.S., Cimprich, K.A., Taya, Y., Tamai, K., Sakaguchi, K., Appella, E., Kastan, M.B., and Siliciano, J.D. (1998). Activation of the ATM kinase by ionizing radiation and phosphorylation of p53. *Science (New York, NY)* 281, 1677-1679.
- Cardoso, F., Costa, A., Norton, L., Cameron, D., Cufer, T., Fallowfield, L., Francis, P., Gligorov, J., Kyriakides, S., Lin, N., *et al.* (2012). 1st International consensus guidelines for advanced breast cancer (ABC 1). *Breast (Edinburgh, Scotland)* 21, 242-252.
- Carter, S.L., Eklund, A.C., Kohane, I.S., Harris, L.N., and Szallasi, Z. (2006). A signature of chromosomal instability inferred from gene expression profiles predicts clinical outcome in multiple human cancers. *Nature genetics* 38, 1043-1048.
- Ceccaldi, R., Rondinelli, B., and D'Andrea, A.D. (2016). Repair Pathway Choices and Consequences at the Double-Strand Break. *Trends in cell biology* 26, 52-64.
- Certo, M.T., Ryu, B.Y., Annis, J.E., Garibov, M., Jarjour, J., Rawlings, D.J., and Scharenberg, A.M. (2011). Tracking genome engineering outcome at individual DNA breakpoints. *Nature methods* 8, 671-676.
- Chaffer, C.L., and Weinberg, R.A. (2011). A perspective on cancer cell metastasis. *Science (New York, NY)* 331, 1559-1564.
- Chinnadurai, G. (2009). The transcriptional corepressor CtBP: a foe of multiple tumor suppressors. *Cancer research* 69, 731-734.
- Cserni, G., Chmielik, E., Cserni, B., and Tot, T. (2018). The new TNM-based staging of breast cancer. *Virchows Archiv : an international journal of pathology* 472, 697-703.
- d'Adda di Fagagna, F., Reaper, P.M., Clay-Farrace, L., Fiegler, H., Carr, P., Von Zglinicki, T., Saretzki, G., Carter, N.P., and Jackson, S.P. (2003). A DNA damage checkpoint response in telomere-initiated senescence. *Nature* 426, 194-198.
- Dagogo-Jack, I., and Shaw, A.T. (2018). Tumour heterogeneity and resistance to cancer therapies. *Nature reviews Clinical oncology* 15, 81-94.
- Dai, X., Cheng, H., Bai, Z., and Li, J. (2017). Breast Cancer Cell Line Classification and Its Relevance with Breast Tumor Subtyping. *Journal of Cancer* 8, 3131-3141.
- Dalton, W.B., Nandan, M.O., Moore, R.T., and Yang, V.W. (2007). Human cancer cells commonly acquire DNA damage during mitotic arrest. *Cancer research* 67, 11487-11492.
- David, S.S., O'Shea, V.L., and Kundu, S. (2007). Base-excision repair of oxidative DNA damage. *Nature* 447, 941-950.

- De Angelis, R., Sant, M., Coleman, M.P., Francisci, S., Baili, P., Pierannunzio, D., Trama, A., Visser, O., Brenner, H., Ardanaz, E., *et al.* (2014). Cancer survival in Europe 1999-2007 by country and age: results of EURO CARE--5 a population-based study. *The Lancet Oncology* *15*, 23-34.
- de Lange, T. (2009). How telomeres solve the end-protection problem. *Science (New York, NY)* *326*, 948-952.
- Deckbar, D., Birraux, J., Krempler, A., Tchouandong, L., Beucher, A., Walker, S., Stiff, T., Jeggo, P., and Lobrich, M. (2007). Chromosome breakage after G2 checkpoint release. *The Journal of cell biology* *176*, 749-755.
- Deng, Y., Deng, H., Liu, J., Han, G., Malkoski, S., Liu, B., Zhao, R., Wang, X.J., and Zhang, Q. (2012). Transcriptional down-regulation of Brca1 and E-cadherin by CtBP1 in breast cancer. *Molecular carcinogenesis* *51*, 500-507.
- Dereli-Oz, A., Versini, G., and Halazonetis, T.D. (2011). Studies of genomic copy number changes in human cancers reveal signatures of DNA replication stress. *Molecular oncology* *5*, 308-314.
- Di, L.J., Byun, J.S., Wong, M.M., Wakano, C., Taylor, T., Bilke, S., Baek, S., Hunter, K., Yang, H., Lee, M., *et al.* (2013). Genome-wide profiles of CtBP link metabolism with genome stability and epithelial reprogramming in breast cancer. *Nature communications* *4*, 1449.
- Di, L.J., Fernandez, A.G., De Siervi, A., Longo, D.L., and Gardner, K. (2010). Transcriptional regulation of BRCA1 expression by a metabolic switch. *Nature structural & molecular biology* *17*, 1406-1413.
- Di Micco, R., Fumagalli, M., Cicalese, A., Piccinin, S., Gasparini, P., Luise, C., Schurra, C., Garre, M., Nuciforo, P.G., Bensimon, A., *et al.* (2006). Oncogene-induced senescence is a DNA damage response triggered by DNA hyper-replication. *Nature* *444*, 638-642.
- Difilippantonio, M.J., Zhu, J., Chen, H.T., Meffre, E., Nussenzweig, M.C., Max, E.E., Ried, T., and Nussenzweig, A. (2000). DNA repair protein Ku80 suppresses chromosomal aberrations and malignant transformation. *Nature* *404*, 510-514.
- Elledge, S.J. (1996). Cell cycle checkpoints: preventing an identity crisis. *Science (New York, NY)* *274*, 1664-1672.
- England (2002-2006). Breast cancer survival statistics by stage 2002-2006 (<https://www.cancerresearchuk.org/health-professional/cancer-statistics/statistics-by-cancer-type/breast-cancer/survival#ref-3>: Former Anglia Cancer Network). 26.04.2019
- Falck, J., Mailand, N., Syljuasen, R.G., Bartek, J., and Lukas, J. (2001). The ATM-Chk2-Cdc25A checkpoint pathway guards against radioresistant DNA synthesis. *Nature* *410*, 842-847.
- Faraoni, I., and Graziani, G. (2018). Role of BRCA Mutations in Cancer Treatment with Poly(ADP-ribose) Polymerase (PARP) Inhibitors. *Cancers* *10*.
- Fenech, M. (2007). Cytokinesis-block micronucleus cytome assay. *Nature protocols* *2*, 1084-1104.
- Fenech, M., Kirsch-Volders, M., Natarajan, A.T., Surralles, J., Crott, J.W., Parry, J., Norppa, H., Eastmond, D.A., Tucker, J.D., and Thomas, P. (2011). Molecular mechanisms of micronucleus,

nucleoplasmic bridge and nuclear bud formation in mammalian and human cells. *Mutagenesis* *26*, 125-132.

Ferlay, J., Colombet, M., Soerjomataram, I., Dyba, T., Randi, G., Bettio, M., Gavin, A., Visser, O., and Bray, F. (2018). Cancer incidence and mortality patterns in Europe: Estimates for 40 countries and 25 major cancers in 2018. *European journal of cancer (Oxford, England : 1990)* *103*, 356-387.

Fidler, I.J. (2003). The pathogenesis of cancer metastasis: the 'seed and soil' hypothesis revisited. *Nature reviews Cancer* *3*, 453-458.

Fisher, B., Dignam, J., Bryant, J., DeCillis, A., Wickerham, D.L., Wolmark, N., Costantino, J., Redmond, C., Fisher, E.R., Bowman, D.M., *et al.* (1996). Five versus more than five years of tamoxifen therapy for breast cancer patients with negative lymph nodes and estrogen receptor-positive tumors. *Journal of the National Cancer Institute* *88*, 1529-1542.

Fortune, J.M., and Osheroff, N. (2000). Topoisomerase II as a target for anticancer drugs: when enzymes stop being nice. *Progress in nucleic acid research and molecular biology* *64*, 221-253.

Geyer, C.E., Forster, J., Lindquist, D., Chan, S., Romieu, C.G., Pienkowski, T., Jagiello-Gruszfeld, A., Crown, J., Chan, A., Kaufman, B., *et al.* (2006). Lapatinib plus capecitabine for HER2-positive advanced breast cancer. *The New England journal of medicine* *355*, 2733-2743.

Glover, T.W., Wilson, T.E., and Arlt, M.F. (2017). Fragile sites in cancer: more than meets the eye. *Nature reviews Cancer* *17*, 489-501.

Gookin, S., Min, M., Phadke, H., Chung, M., Moser, J., Miller, I., Carter, D., and Spencer, S.L. (2017). A map of protein dynamics during cell-cycle progression and cell-cycle exit. *PLoS biology* *15*, e2003268.

Gordon, D.J., Resio, B., and Pellman, D. (2012). Causes and consequences of aneuploidy in cancer. *Nature reviews Genetics* *13*, 189-203.

Greaves, M. (2015). Evolutionary determinants of cancer. *Cancer Discov* *5*, 806-820.

Grooteclaes, M., Deveraux, Q., Hildebrand, J., Zhang, Q., Goodman, R.H., and Frisch, S.M. (2003). C-terminal-binding protein corepresses epithelial and proapoptotic gene expression programs. *Proceedings of the National Academy of Sciences of the United States of America* *100*, 4568-4573.

Guzman, C., Bagga, M., Kaur, A., Westermarck, J., and Abankwa, D. (2014). ColonyArea: an ImageJ plugin to automatically quantify colony formation in clonogenic assays. *PloS one* *9*, e92444.

Hanahan, D., and Weinberg, R.A. (2000). The hallmarks of cancer. *Cell* *100*, 57-70.

Hanahan, D., and Weinberg, R.A. (2011). Hallmarks of cancer: the next generation. *Cell* *144*, 646-674.

Hansemann, D. (1890). Ueber asymmetrische Zelltheilung in Epithelkrebsen und deren biologische Bedeutung. *Virchows Arch Pathol Anat Physiol Klin Medicin Band* *119*, 299-326.

Hansemann, D. (1892). Ueber die Anaplasie der Geschwulstzellen und die asymmetrische Mitose. *Arch Pathol Anat Physiol Klin Medicin Band* *129*, 436-449.

- Holohan, C., Van Schaeybroeck, S., Longley, D.B., and Johnston, P.G. (2013). Cancer drug resistance: an evolving paradigm. *Nature reviews Cancer* *13*, 714-726.
- Ichijima, Y., Yoshioka, K., Yoshioka, Y., Shinohe, K., Fujimori, H., Unno, J., Takagi, M., Goto, H., Inagaki, M., Mizutani, S., *et al.* (2010). DNA lesions induced by replication stress trigger mitotic aberration and tetraploidy development. *PloS one* *5*, e8821.
- Jaafar, L., Li, Z., Li, S., and Dynan, W.S. (2017). SFPQ*NONO and XLF function separately and together to promote DNA double-strand break repair via canonical nonhomologous end joining. *Nucleic acids research* *45*, 1848-1859.
- Jackman, J., and O'Connor, P.M. (2001). Methods for synchronizing cells at specific stages of the cell cycle. *Current protocols in cell biology Chapter 8*, Unit 8.3.
- Jacobs, J.J., and de Lange, T. (2004). Significant role for p16INK4a in p53-independent telomere-directed senescence. *Current biology : CB* *14*, 2302-2308.
- Jamal-Hanjani, M., Wilson, G.A., McGranahan, N., Birkbak, N.J., Watkins, T.B.K., Veeriah, S., Shafi, S., Johnson, D.H., Mitter, R., Rosenthal, R., *et al.* (2017). Tracking the Evolution of Non-Small-Cell Lung Cancer. *The New England journal of medicine* *376*, 2109-2121.
- Jonk, L.J., de Jonge, M.E., Vervaart, J.M., Wissink, S., and Kruijer, W. (1994). Isolation and developmental expression of retinoic-acid-induced genes. *Developmental biology* *161*, 604-614.
- Joose, S.A., Gorges, T.M., and Pantel, K. (2015). Biology, detection, and clinical implications of circulating tumor cells. *EMBO molecular medicine* *7*, 1-11.
- Katsube, T., Mori, M., Tsuji, H., Shiomi, T., Wang, B., Liu, Q., Neno, M., and Onoda, M. (2014). Most hydrogen peroxide-induced histone H2AX phosphorylation is mediated by ATR and is not dependent on DNA double-strand breaks. *Journal of biochemistry* *156*, 85-95.
- Kennecke, H., Yerushalmi, R., Woods, R., Cheang, M.C., Voduc, D., Speers, C.H., Nielsen, T.O., and Gelmon, K. (2010). Metastatic behavior of breast cancer subtypes. *Journal of clinical oncology : official journal of the American Society of Clinical Oncology* *28*, 3271-3277.
- Knijnenburg, T.A., Wang, L., Zimmermann, M.T., Chambwe, N., Gao, G.F., Cherniack, A.D., Fan, H., Shen, H., Way, G.P., Greene, C.S., *et al.* (2018). Genomic and Molecular Landscape of DNA Damage Repair Deficiency across The Cancer Genome Atlas. *Cell reports* *23*, 239-254.e236.
- Knott, G.J., Bond, C.S., and Fox, A.H. (2016). The DBHS proteins SFPQ, NONO and PSPC1: a multipurpose molecular scaffold. *Nucleic acids research* *44*, 3989-4004.
- Koc, A., Wheeler, L.J., Mathews, C.K., and Merrill, G.F. (2004). Hydroxyurea arrests DNA replication by a mechanism that preserves basal dNTP pools. *The Journal of biological chemistry* *279*, 223-230.
- Kurebayashi, J., Kurosumi, M., and Sonoo, H. (1995). A new human breast cancer cell line, KPL-1 secretes tumour-associated antigens and grows rapidly in female athymic nude mice. *British journal of cancer* *71*, 845-853.

- Kurose, A., Tanaka, T., Huang, X., Traganos, F., and Darzynkiewicz, Z. (2006). Synchronization in the cell cycle by inhibitors of DNA replication induces histone H2AX phosphorylation: an indication of DNA damage. *Cell proliferation* *39*, 231-240.
- Lamond, A.I., and Earnshaw, W.C. (1998). Structure and function in the nucleus. *Science (New York, NY)* *280*, 547-553.
- Lane, D.P. (1992). Cancer. p53, guardian of the genome. *Nature* *358*, 15-16.
- Langlands, F.E., Horgan, K., Dodwell, D.D., and Smith, L. (2013). Breast cancer subtypes: response to radiotherapy and potential radiosensitisation. *The British journal of radiology* *86*, 20120601.
- Lee, J.K., Choi, Y.L., Kwon, M., and Park, P.J. (2016). Mechanisms and Consequences of Cancer Genome Instability: Lessons from Genome Sequencing Studies. *Annual review of pathology* *11*, 283-312.
- Lefebvre, C., Bachelot, T., Filleron, T., Pedrero, M., Campone, M., Soria, J.C., Massard, C., Levy, C., Arnedos, M., Lacroix-Triki, M., *et al.* (2016). Mutational Profile of Metastatic Breast Cancers: A Retrospective Analysis. *PLoS medicine* *13*, e1002201.
- Lengauer, C., Kinzler, K.W., and Vogelstein, B. (1998). Genetic instabilities in human cancers. *Nature* *396*, 643-649.
- Li, C.I., Uribe, D.J., and Daling, J.R. (2005). Clinical characteristics of different histologic types of breast cancer. *British journal of cancer* *93*, 1046-1052.
- Li, S., Ting, N.S., Zheng, L., Chen, P.L., Ziv, Y., Shiloh, Y., Lee, E.Y., and Lee, W.H. (2000). Functional link of BRCA1 and ataxia telangiectasia gene product in DNA damage response. *Nature* *406*, 210-215.
- Li, X., and Heyer, W.D. (2008). Homologous recombination in DNA repair and DNA damage tolerance. *Cell research* *18*, 99-113.
- Lingle, W.L., Barrett, S.L., Negron, V.C., D'Assoro, A.B., Boeneman, K., Liu, W., Whitehead, C.M., Reynolds, C., and Salisbury, J.L. (2002). Centrosome amplification drives chromosomal instability in breast tumor development. *Proceedings of the National Academy of Sciences of the United States of America* *99*, 1978-1983.
- Maser, R.S., and DePinho, R.A. (2002). Connecting chromosomes, crisis, and cancer. *Science (New York, NY)* *297*, 565-569.
- Mateuca, R., Lombaert, N., Aka, P.V., Decordier, I., and Kirsch-Volders, M. (2006). Chromosomal changes: induction, detection methods and applicability in human biomonitoring. *Biochimie* *88*, 1515-1531.
- Matsuoka, S., Ballif, B.A., Smogorzewska, A., McDonald, E.R., 3rd, Hurov, K.E., Luo, J., Bakalarski, C.E., Zhao, Z., Solimini, N., Lerenthal, Y., *et al.* (2007). ATM and ATR substrate analysis reveals extensive protein networks responsive to DNA damage. *Science (New York, NY)* *316*, 1160-1166.
- Mavaddat, N., Barrowdale, D., Andrulis, I.L., Domchek, S.M., Eccles, D., Nevanlinna, H., Ramus, S.J., Spurdle, A., Robson, M., Sherman, M., *et al.* (2012). Pathology of breast and ovarian cancers among BRCA1 and BRCA2 mutation carriers: results from the Consortium of Investigators of

Modifiers of BRCA1/2 (CIMBA). *Cancer epidemiology, biomarkers & prevention : a publication of the American Association for Cancer Research, cosponsored by the American Society of Preventive Oncology* 21, 134-147.

McGranahan, N., Furness, A.J., Rosenthal, R., Ramskov, S., Lyngaa, R., Saini, S.K., Jamal-Hanjani, M., Wilson, G.A., Birkbak, N.J., Hiley, C.T., *et al.* (2016). Clonal neoantigens elicit T cell immunoreactivity and sensitivity to immune checkpoint blockade. *Science (New York, NY)* 351, 1463-1469.

McKinnon, P.J. (2004). ATM and ataxia telangiectasia. *EMBO reports* 5, 772-776.

McManus, K.J., and Hendzel, M.J. (2005). ATM-dependent DNA damage-independent mitotic phosphorylation of H2AX in normally growing mammalian cells. *Molecular biology of the cell* 16, 5013-5025.

Mjelle, R., Hegre, S.A., Aas, P.A., Slupphaug, G., Drablos, F., Saetrom, P., and Krokan, H.E. (2015). Cell cycle regulation of human DNA repair and chromatin remodeling genes. *DNA repair* 30, 53-67.

Murnane, J.P. (2012). Telomere dysfunction and chromosome instability. *Mutation research* 730, 28-36.

Musacchio, A., and Salmon, E.D. (2007). The spindle-assembly checkpoint in space and time. *Nature reviews Molecular cell biology* 8, 379-393.

Nam, H.J., Naylor, R.M., and van Deursen, J.M. (2015). Centrosome dynamics as a source of chromosomal instability. *Trends in cell biology* 25, 65-73.

NCCN (2018). NCCN Clinical Practice Guidelines for Breast Cancer (https://www.nccn.org/professionals/physician_gls/#site: National Comprehensive Cancer Network). 26.04.2019

Nieminuszczy, J., Schwab, R.A., and Niedzwiedz, W. (2016). The DNA fibre technique - tracking helicases at work. *Methods (San Diego, Calif)* 108, 92-98.

Nugoli, M., Chuchana, P., Vendrell, J., Orsetti, B., Ursule, L., Nguyen, C., Birnbaum, D., Douzery, E.J., Cohen, P., and Theillet, C. (2003). Genetic variability in MCF-7 sublines: evidence of rapid genomic and RNA expression profile modifications. *BMC cancer* 3, 13.

O'Sullivan, R.J., and Karlseder, J. (2010). Telomeres: protecting chromosomes against genome instability. *Nature reviews Molecular cell biology* 11, 171-181.

Olivier, M., Hollstein, M., and Hainaut, P. (2010). TP53 mutations in human cancers: origins, consequences, and clinical use. *Cold Spring Harbor perspectives in biology* 2, a001008.

Ozer, O., and Hickson, I.D. (2018). Pathways for maintenance of telomeres and common fragile sites during DNA replication stress. *Open biology* 8.

Pan, H., Gray, R., Braybrooke, J., Davies, C., Taylor, C., McGale, P., Peto, R., Pritchard, K.I., Bergh, J., Dowsett, M., *et al.* (2017). 20-Year Risks of Breast-Cancer Recurrence after Stopping Endocrine Therapy at 5 Years. *The New England journal of medicine* 377, 1836-1846.

Perez de Castro, I., de Carcer, G., and Malumbres, M. (2007). A census of mitotic cancer genes: new insights into tumor cell biology and cancer therapy. *Carcinogenesis* 28, 899-912.

- Perou, C.M., Sorlie, T., Eisen, M.B., van de Rijn, M., Jeffrey, S.S., Rees, C.A., Pollack, J.R., Ross, D.T., Johnsen, H., Akslen, L.A., *et al.* (2000). Molecular portraits of human breast tumours. *Nature* *406*, 747-752.
- Petermann, E., and Helleday, T. (2010). Pathways of mammalian replication fork restart. *Nature reviews Molecular cell biology* *11*, 683-687.
- Petermann, E., Orta, M.L., Issaeva, N., Schultz, N., and Helleday, T. (2010). Hydroxyurea-stalled replication forks become progressively inactivated and require two different RAD51-mediated pathways for restart and repair. *Molecular cell* *37*, 492-502.
- Pilie, P.G., Tang, C., Mills, G.B., and Yap, T.A. (2019). State-of-the-art strategies for targeting the DNA damage response in cancer. *Nature reviews Clinical oncology* *16*, 81-104.
- Platani, M., and Lamond, A.I. (2004). Nuclear organisation and subnuclear bodies. *Progress in molecular and subcellular biology* *35*, 1-22.
- Polo, S.E., and Jackson, S.P. (2011). Dynamics of DNA damage response proteins at DNA breaks: a focus on protein modifications. *Genes & development* *25*, 409-433.
- Pommier, Y. (2006). Topoisomerase I inhibitors: camptothecins and beyond. *Nature reviews Cancer* *6*, 789-802.
- Pommier, Y., Leo, E., Zhang, H., and Marchand, C. (2010). DNA topoisomerases and their poisoning by anticancer and antibacterial drugs. *Chemistry & biology* *17*, 421-433.
- Pommier, Y., Redon, C., Rao, V.A., Seiler, J.A., Sordet, O., Takemura, H., Antony, S., Meng, L., Liao, Z., Kohlhagen, G., *et al.* (2003). Repair of and checkpoint response to topoisomerase I-mediated DNA damage. *Mutation research* *532*, 173-203.
- Preston, B.D., Albertson, T.M., and Herr, A.J. (2010). DNA replication fidelity and cancer. *Seminars in cancer biology* *20*, 281-293.
- Puck, T.T., and Marcus, P.I. (1956). Action of x-rays on mammalian cells. *The Journal of experimental medicine* *103*, 653-666.
- Rajagopalan, H., Jallepalli, P.V., Rago, C., Velculescu, V.E., Kinzler, K.W., Vogelstein, B., and Lengauer, C. (2004). Inactivation of hCDC4 can cause chromosomal instability. *Nature* *428*, 77-81.
- Revet, I., Feeney, L., Bruguera, S., Wilson, W., Dong, T.K., Oh, D.H., Dankort, D., and Cleaver, J.E. (2011). Functional relevance of the histone gammaH2Ax in the response to DNA damaging agents. *Proceedings of the National Academy of Sciences of the United States of America* *108*, 8663-8667.
- Riballo, E., Critchlow, S.E., Teo, S.H., Doherty, A.J., Priestley, A., Broughton, B., Kysela, B., Beamish, H., Plowman, N., Arlett, C.F., *et al.* (1999). Identification of a defect in DNA ligase IV in a radiosensitive leukaemia patient. *Current biology : CB* *9*, 699-702.
- Rizvi, N.A., Hellmann, M.D., Snyder, A., Kvistborg, P., Makarov, V., Havel, J.J., Lee, W., Yuan, J., Wong, P., Ho, T.S., *et al.* (2015). Cancer immunology. Mutational landscape determines sensitivity to PD-1 blockade in non-small cell lung cancer. *Science (New York, NY)* *348*, 124-128.

- Robles, A.I., and Harris, C.C. (2010). Clinical outcomes and correlates of TP53 mutations and cancer. *Cold Spring Harbor perspectives in biology* 2, a001016.
- Robson, M., Im, S.A., Senkus, E., Xu, B., Domchek, S.M., Masuda, N., Delaloge, S., Li, W., Tung, N., Armstrong, A., *et al.* (2017). Olaparib for Metastatic Breast Cancer in Patients with a Germline BRCA Mutation. *The New England journal of medicine* 377, 523-533.
- Rocquain, J., Gelsi-Boyer, V., Adelaide, J., Murati, A., Carbuccia, N., Vey, N., Birnbaum, D., Mozziconacci, M.J., and Chaffanet, M. (2010). Alteration of cohesin genes in myeloid diseases. *American journal of hematology* 85, 717-719.
- Rogakou, E.P., Boon, C., Redon, C., and Bonner, W.M. (1999). Megabase chromatin domains involved in DNA double-strand breaks in vivo. *The Journal of cell biology* 146, 905-916.
- Romond, E.H., Perez, E.A., Bryant, J., Suman, V.J., Geyer, C.E., Jr., Davidson, N.E., Tan-Chiu, E., Martino, S., Paik, S., Kaufman, P.A., *et al.* (2005). Trastuzumab plus adjuvant chemotherapy for operable HER2-positive breast cancer. *The New England journal of medicine* 353, 1673-1684.
- Ross, J.S., and Fletcher, J.A. (1998). The HER-2/neu oncogene in breast cancer: prognostic factor, predictive factor, and target for therapy. *Stem cells (Dayton, Ohio)* 16, 413-428.
- Rothkamm, K., Barnard, S., Moquet, J., Ellender, M., Rana, Z., and Burdak-Rothkamm, S. (2015). DNA damage foci: Meaning and significance. *Environmental and molecular mutagenesis* 56, 491-504.
- Rothkamm, K., Kuhne, M., Jeggo, P.A., and Lobrich, M. (2001). Radiation-induced genomic rearrangements formed by nonhomologous end-joining of DNA double-strand breaks. *Cancer research* 61, 3886-3893.
- Sansregret, L., Vanhaesebroeck, B., and Swanton, C. (2018). Determinants and clinical implications of chromosomal instability in cancer. *Nature reviews Clinical oncology* 15, 139-150.
- Savage, J.R. (1988). A comment on the quantitative relationship between micronuclei and chromosomal aberrations. *Mutation research* 207, 33-36.
- Schaeper, U., Subramanian, T., Lim, L., Boyd, J.M., and Chinnadurai, G. (1998). Interaction between a cellular protein that binds to the C-terminal region of adenovirus E1A (CtBP) and a novel cellular protein is disrupted by E1A through a conserved PLDLS motif. *The Journal of biological chemistry* 273, 8549-8552.
- Schindelin, J., Arganda-Carreras, I., Frise, E., Kaynig, V., Longair, M., Pietzsch, T., Preibisch, S., Rueden, C., Saalfeld, S., Schmid, B., *et al.* (2012). Fiji: an open-source platform for biological-image analysis. *Nature methods* 9, 676-682.
- Schneeweiss, A., Ruckhaberle, E., and Huober, J. (2015). Chemotherapy for Metastatic Breast Cancer - An Anachronism in the Era of Personalised and Targeted Oncological Therapy? *Geburtshilfe und Frauenheilkunde* 75, 574-583.
- Schvartzman, J.B., Krimer, D.B., and Van't Hof, J. (1984). The effects of different thymidine concentrations on DNA replication in pea-root cells synchronized by a protracted 5-fluorodeoxyuridine treatment. *Experimental cell research* 150, 379-389.

- Schvartzman, J.M., Sotillo, R., and Benezra, R. (2010). Mitotic chromosomal instability and cancer: mouse modelling of the human disease. *Nature reviews Cancer* *10*, 102-115.
- Scully, R., and Livingston, D.M. (2000). In search of the tumour-suppressor functions of BRCA1 and BRCA2. *Nature* *408*, 429-432.
- Shaltiel, I.A., Krenning, L., Bruinsma, W., and Medema, R.H. (2015). The same, only different - DNA damage checkpoints and their reversal throughout the cell cycle. *Journal of cell science* *128*, 607-620.
- Silkworth, W.T., Nardi, I.K., Paul, R., Mogilner, A., and Cimini, D. (2012). Timing of centrosome separation is important for accurate chromosome segregation. *Molecular biology of the cell* *23*, 401-411.
- Sishc, B.J., and Davis, A.J. (2017). The Role of the Core Non-Homologous End Joining Factors in Carcinogenesis and Cancer. *Cancers* *9*.
- Solomon, D.A., Kim, T., Diaz-Martinez, L.A., Fair, J., Elkahloun, A.G., Harris, B.T., Toretsky, J.A., Rosenberg, S.A., Shukla, N., Ladanyi, M., *et al.* (2011). Mutational inactivation of STAG2 causes aneuploidy in human cancer. *Science (New York, NY)* *333*, 1039-1043.
- Someya, M., Sakata, K., Matsumoto, Y., Yamamoto, H., Monobe, M., Ikeda, H., Ando, K., Hosoi, Y., Suzuki, N., and Hareyama, M. (2006). The association of DNA-dependent protein kinase activity with chromosomal instability and risk of cancer. *Carcinogenesis* *27*, 117-122.
- Sotillo, R., Hernando, E., Diaz-Rodriguez, E., Teruya-Feldstein, J., Cordon-Cardo, C., Lowe, S.W., and Benezra, R. (2007). Mad2 overexpression promotes aneuploidy and tumorigenesis in mice. *Cancer cell* *11*, 9-23.
- Sotiriou, C., and Pusztai, L. (2009). Gene-expression signatures in breast cancer. *The New England journal of medicine* *360*, 790-800.
- Soule, H.D., Maloney, T.M., Wolman, S.R., Peterson, W.D., Jr., Brenz, R., McGrath, C.M., Russo, J., Pauley, R.J., Jones, R.F., and Brooks, S.C. (1990). Isolation and characterization of a spontaneously immortalized human breast epithelial cell line, MCF-10. *Cancer research* *50*, 6075-6086.
- Soule, H.D., Vazquez, J., Long, A., Albert, S., and Brennan, M. (1973). A human cell line from a pleural effusion derived from a breast carcinoma. *Journal of the National Cancer Institute* *51*, 1409-1416.
- Sunada, S., Nakanishi, A., and Miki, Y. (2018). Crosstalk of DNA double-strand break repair pathways in poly(ADP-ribose) polymerase inhibitor treatment of breast cancer susceptibility gene 1/2-mutated cancer. *Cancer science* *109*, 893-899.
- Tacar, O., Sriamornsak, P., and Dass, C.R. (2013). Doxorubicin: an update on anticancer molecular action, toxicity and novel drug delivery systems. *The Journal of pharmacy and pharmacology* *65*, 157-170.
- Thompson, S.L., Bakhoun, S.F., and Compton, D.A. (2010). Mechanisms of chromosomal instability. *Current biology : CB* *20*, R285-295.

- Tubbs, A., and Nussenzweig, A. (2017). Endogenous DNA Damage as a Source of Genomic Instability in Cancer. *Cell* *168*, 644-656.
- Turajlic, S., and Swanton, C. (2016). Metastasis as an evolutionary process. *Science (New York, NY)* *352*, 169-175.
- Turajlic, S., Xu, H., Litchfield, K., Rowan, A., Chambers, T., Lopez, J.I., Nicol, D., O'Brien, T., Larkin, J., Horswell, S., *et al.* (2018). Tracking Cancer Evolution Reveals Constrained Routes to Metastases: TRACERx Renal. *Cell* *173*, 581-594.e512.
- van Gent, D.C., Hoeijmakers, J.H., and Kanaar, R. (2001). Chromosomal stability and the DNA double-stranded break connection. *Nature reviews Genetics* *2*, 196-206.
- Vassilev, L.T., Tovar, C., Chen, S., Knezevic, D., Zhao, X., Sun, H., Heimbrook, D.C., and Chen, L. (2006). Selective small-molecule inhibitor reveals critical mitotic functions of human CDK1. *Proceedings of the National Academy of Sciences of the United States of America* *103*, 10660-10665.
- Vogelstein, B., Lane, D., and Levine, A.J. (2000). Surfing the p53 network. *Nature* *408*, 307-310.
- Walczak, C.E., Cai, S., and Khodjakov, A. (2010). Mechanisms of chromosome behaviour during mitosis. *Nature reviews Molecular cell biology* *11*, 91-102.
- Walpole, S.M., Hiriyana, K.T., Nicolaou, A., Bingham, E.L., Durham, J., Vaudin, M., Ross, M.T., Yates, J.R., Sieving, P.A., and Trump, D. (1999). Identification and characterization of the human homologue (RAI2) of a mouse retinoic acid-induced gene in Xp22. *Genomics* *55*, 275-283.
- Wang, H., Shi, L.Z., Wong, C.C., Han, X., Hwang, P.Y., Truong, L.N., Zhu, Q., Shao, Z., Chen, D.J., Berns, M.W., *et al.* (2013). The interaction of CtIP and Nbs1 connects CDK and ATM to regulate HR-mediated double-strand break repair. *PLoS genetics* *9*, e1003277.
- Wang, R., Asangani, I.A., Chakravarthi, B.V., Ateeq, B., Lonigro, R.J., Cao, Q., Mani, R.S., Camacho, D.F., McGregor, N., Schumann, T.E., *et al.* (2012). Role of transcriptional corepressor CtBP1 in prostate cancer progression. *Neoplasia (New York, NY)* *14*, 905-914.
- Wang, Y., Xu, H., Liu, T., Huang, M., Butter, P.P., Li, C., Zhang, L., Kao, G.D., Gong, Y., Maity, A., *et al.* (2018). Temporal DNA-PK activation drives genomic instability and therapy resistance in glioma stem cells. *JCI insight* *3*.
- Watson, J.D., and Crick, F.H. (1953). Molecular structure of nucleic acids; a structure for deoxyribose nucleic acid. *Nature* *171*, 737-738.
- Weaver, B.A. (2014). How Taxol/paclitaxel kills cancer cells. *Molecular biology of the cell* *25*, 2677-2681.
- Weigelt, B., Peterse, J.L., and van 't Veer, L.J. (2005). Breast cancer metastasis: markers and models. *Nature reviews Cancer* *5*, 591-602.
- Werner, S., Bartkowiak, K., Steffen, P., Besler, K., Böttcher, L., Schlüter, H., Pantel, K., and Wikman, H. (2018). Deciphering the interactome of the metastasis-suppressor protein RAI2 (AACR).
- Werner, S., Borgmann, K., Pantel, K., and Wikman, H. (2016). Novel function of the RAI2 protein in genomic integrity of breast cancer cells (AACR).

- Werner, S., Brors, B., Eick, J., Marques, E., Pogenberg, V., Parret, A., Kemming, D., Wood, A.W., Edgren, H., Neubauer, H., *et al.* (2015). Suppression of early hematogenous dissemination of human breast cancer cells to bone marrow by retinoic Acid-induced 2. *Cancer Discov* *5*, 506-519.
- Yan, W., Wu, K., Herman, J.G., Xu, X., Yang, Y., Dai, G., and Guo, M. (2018). Retinoic acid-induced 2 (RAI2) is a novel tumor suppressor, and promoter region methylation of RAI2 is a poor prognostic marker in colorectal cancer. *Clinical epigenetics* *10*, 69.
- Yarden, Y., and Sliwkowski, M.X. (2001). Untangling the ErbB signalling network. *Nature reviews Molecular cell biology* *2*, 127-137.
- Yu, X., and Baer, R. (2000). Nuclear localization and cell cycle-specific expression of CtIP, a protein that associates with the BRCA1 tumor suppressor. *The Journal of biological chemistry* *275*, 18541-18549.
- Zeman, M.K., and Cimprich, K.A. (2014). Causes and consequences of replication stress. *Nature cell biology* *16*, 2-9.
- Zhou, B.B., and Elledge, S.J. (2000). The DNA damage response: putting checkpoints in perspective. *Nature* *408*, 433-439.

LIST OF ABBREVIATIONS

ACA	Anti-centromere antibody
APS	Ammonium persulfate
ATM	Ataxia telangiectasia mutated
ATR	ATM and Rad3-related
BRCA	Breast cancer type susceptibility protein
BSA	Bovine serum albumin
cDNA	Complementary DNA
Chk	Checkpoint kinase
CIN	Chromosomal instability
CldU	5-Chloro-20-deoxyuridine
CtBP	C-terminal binding protein
DAPI	4',6-Diamidino-2-phenylindole
DMEM	Dulbecco's modified eagle's medium
DMSO	Dimethyl sulfoxide
DNA	Deoxyribonucleic acid
dNTPs	Desoxyribonucleoside triphosphate set
DSB	Double-strand break
DTT	Dithiothreitol
ECL	Electrochemoluminescence
ECL	Enhanced Chemoluminescence
EDTA	Ethylenediaminetetraacetic acid
ER	Oestrogen receptor
FACS	Fluorescence-activated cell sorting)
FCS	Fetal calf serum
FCS	Fetal calf serum
h	Hour/s
H ₂ O ₂	Peroxide
HER2	<i>Human epidermal growth factor 2</i>
HR	Homologous recombination
HRP	Horseradish peroxidase
HU	Hydroxy Urea
IdU	5-Iodo-20-deoxyuridine
ITB	Institute of Tumor Biology
kDa	kDa
min	Minutes
MMR	DNA mismatch repair
MRN	Mre11-Rad50-Nbs1

LIST OF ABBREVIATION

NCCN	National comprehensive cancer network
NHEJ	Non homologous end-joining
OE	Overexpression
P53	Cellular tumor antigen p53
PAGE	Polyacrylamide Gel Electrophoresis
PARP	Poly(ADP-ribose) polymerase
PBS	Phosphate buffered saline
PCR	Polymerase chain reaction
PFA	Paraformaldehyde
p-H3 Ser10	Phosphorylation of Histone H3 on Serine 10
PR	Progesterone receptor
qRT-PCR	Quantitative real-time PCR
RAI2	Retinoic acid-induced 2
RNA	Ribonucleic acid
ROS	Reactive oxygen species
RT	Room temperature
SDS	Sodium dodecyl sulfate
SEM	Standard error of the mean
shRNA	Small hairpin RNA
SSB	Single-strand break
TAE	Tris-acetate-EDTA
TBS-T	Tris-Buffered Saline/Tween20
TE	Tris-EDTA
TEMED	Tetramethylethylenediamine
TLR	Traffic Light Reporter
T _m	Melting temperature
TOP	Topoisomerase
Wt	Wild type
γH2AX	Phosphorylation of Histone H2AX on Serine 139

DANKSAGUNG

An erster Stelle möchte ich mich bei meinen Betreuern Stefan Werner und Haiju Wikman bedanken, die mir durch ihre Ideen erst ermöglicht haben, an diesem spannenden Projekt zu arbeiten und zu promovieren. Die wissenschaftliche Unterstützung, kritischen Fragen und anregenden Gesprächen haben das Projekt sehr vorangebracht. Danke, dass Ihr mich immer wieder daran erinnert habt, das große Ganze nicht zu vergessen!

Danke sagen möchte ich Prof. Pantel, dass ich die Möglichkeit hatte am Institut für Tumorbologie meine Doktorarbeit zu verfassen. Während der Fertigstellung des Manuskripts konnte ich auf Ihren wissenschaftlichen Input zählen und Sie hatten immer Anregungen parat, wie man den Aufbau des Papers immer noch spannenden gestalten konnte. Danke dafür!

Ich bedanke mich herzlich bei Herrn Prof. Wim Walter für die Begutachtung meiner Dissertation. Ebenso ein Dank geht an Herrn Prof. Tim Gilberger für die Zusage, als Teil meiner Prüfungskommission zu fungieren.

Sehr hervorheben möchte ich meinen Dank an das Team der AG Wikman, an Katharina, Svenja, Jolanthe, Desiree, Jana, Yassine, Elke, Simon und Martin. Ohne eure tatkräftige Unterstützung und Hilfe wäre gar nichts gelaufen! Vielen Dank an Desiree für das Korrekturlesen meiner Arbeit und die vielen hilfreichen Kommentare. Besonderen Dank zukommen lassen möchte ich an dieser Stelle Katharina und Svenja, die mich die gesamte Doktorandenzeit begleitet haben und mir immer zur Seite gestanden und ausgeholfen haben, wenn Not am Mann war. Wir haben viel zusammen erlebt, motivierende und nicht so motivierende Tage im Labor, einen beeindruckenden Kongress in Chicago und haben, egal was war, immer wieder zur guten Laune zurückgefunden. Auf euch konnte ich immer zählen!

Ein großen Dank möchte ich an die ITB Girls (Johanna, Sonja, Pari, Ines, Leonie, Yang) und dem Boy (Sebastian) sagen, zu denen ich immer kommen konnte mit Problemen oder nur zum Quatschen, die ich bitten konnte, die Zellkulturzeit zu schieben und die mit mir in der Mensa um Sitzplätze gekämpft haben. Ich habe die Zeit mit euch sehr genossen und hoffe, wir bleiben auch nach meiner Doktorandenzeit weiter in Kontakt.

DANKSAGUNG

Bedanken möchte ich mich beim gesamten Tumorbioogie-Team für Unterstützung bei allen technischen und wissenschaftlichen Fragen. Vielen Dank an euch alle!

Ich bedanke mich herzlich bei Alexandra Zielinski und Prof. Kerstin Borgmann für die Einführung in die Welt des DNA Fiber Assays und das Beantworten aller Fragen rund um DNA Schäden.

Ebenfalls bedanke ich mich bei der UKE Microcopy Imaging Facility, insbesondere bei Bernd Zobiak, für die Durchführung der Live Cell Imaging Experimente. Desweiteren gilt mein Dank der UKE FACS Core Facility für die Unterstützung bei technischen Fragen.

Mein besonderer Dank gebührt meiner Familie, besonders meinen Eltern und Großeltern, die mich schon von klein an für die Natur und Biologie begeistert haben.

Zuletzt möchte ich meinem Freund Vincent von ganzem Herzen danken. Ich bedanke mich bei Dir für deine Unterstützung und Zuneigung und dafür, dass du mich mit deiner ruhigen und sachlichen Art immer wieder auf den Boden der Tatsachen zurückgeholt hast.

EIDENSSTATTLICHE VERSICHERUNG

Hiermit erkläre ich an Eides statt, dass ich die vorliegende Dissertationsschrift selbst verfasst und keine anderen als die angegebenen Quellen und Hilfsmittel benutzt habe.

Hamburg, der

Lena Böttcher

ENGLISH CERTIFICATE



Universitätsklinikum Hamburg-Eppendorf | Martinistraße 52 | 20246 Hamburg
Institut für Tumorbologie

Universitätsklinikum Hamburg-Eppendorf
Institut für Tumorbologie
Martinistraße 52, 20246 Hamburg

Dr. Linda Scarrott
Visiting Scientist at UKE
Boehringer Ingelheim Pharma GmbH & Co. KG
Transl. Medicine and Clin. Pharmacology
Tel: +49 (7351)54-187716
E-Mail: linda.scarrott@boehringer-ingelheim.com

Hamburg, 28.05.2019
Seite 1/1

Subject: English Language Thesis Certification for Lena Böttcher

To whom it may concern,

Lena Böttcher, who was born on 09.07.1990 in Hamburg, Germany, is submitting her doctoral dissertation in English. The title of the thesis is "The Role of RAI2 in maintenance of genomic stability".

I hereby certify, as a native English speaker and molecular biologist, that I have read the thesis and that the English language used in this thesis is sufficiently correct for submission.

Yours Sincerely,

Dr. Linda Scarrott

Universitätsklinikum Hamburg Eppendorf
Zentrum für Experimentelle Medizin
Institut für Tumorbologie
Martinistraße 52, 20246 Hamburg, Germany
Tel. +49 40-74105-3556, Fax: +49 40-74105-6546